



CE-QUAL-W2: A Two-Dimensional, Laterally Averaged, Hydrodynamic and Water Quality Model, Version 4.5

User Manual: Part 4 – Model Examples

Edited by

Scott A. Wells
Professor
Department of Civil and Environmental Engineering
Portland State University
Portland, OR 97207-0751

Department of Civil and Environmental Engineering
Portland State University
Portland, OR 97207-0751

June 2022

CONTENTS

Contents

Contents	ii
List of Figures	iii
List of Tables.....	vii
Preface.....	viii
1. Introduction	1
2. Model Examples Distributed with the Model Release	1
Columbia Slough Estuary.....	2
DeGray Reservoir with Sediment Diagenesis and Vertical Algae Migration.....	6
Detroit Lake	8
Long Lake or Spokane Lake.....	12
Multiple Water Body Cascade	20
Particle Tracking.....	23
Sediment Diagenesis Example	25
Spokane River	26
SysTDG Columbia River – Bonneville Reservoir	30
3. Examples of Model Applications – Tom Cole.....	31
Model Preparation.....	31
Calibration	31
Lake/Reservoir.....	34
Water budget.....	34
Hydrodynamics and Temperature.....	36
Water Quality.....	48
Estuary	68
Boundary conditions.....	68
Water surface elevations and flows.....	69
Time of Travel	71
Temperature and Salinity	71
Water Quality.....	74
River	75
Channel Slope.....	75
Channel bottom.....	76
Hydrodynamics and Temperature.....	81
Water Quality.....	85
Summary	93
4. References.....	94

List of Figures

Figure 1. Model examples distributed with model release version.....	1
Figure 2. USGS model examples illustrating using the auto-port selection feature.	1
Figure 3. Lower Columbia Slough system.	2
Figure 4. Columbia Slough, Portland, Oregon (City of Portland, BES).	3
Figure 5. Grid layout for Columbia Slough Branch 1.....	5
Figure 6. Segment layout for Columbia Slough.....	6
Figure 7. DeGray Reservoir (Bing Maps, 2019).....	7
Figure 8. DeGray Reservoir computational grid.....	8
Figure 9. Detroit Reservoir model grid.....	9
Figure 10. Branch and inflow layout for Detroit Reservoir.	9
Figure 11. Predicted evaporation losses from Detroit Reservoir in 2002.....	10
Figure 12. Percent of reservoir volume optimal habitat for striped bass for Detroit Reservoir	11
Figure 13. Reservoir temperature on Julian day 168.2 in the year 2002. for Branch 1 for Detroit Lake.....	12
Figure 14: Upper Spokane River in Washington.....	13
Figure 15: Long Lake located west of the City of Spokane.....	13
Figure 16: Long Lake bathymetric contours.....	14
Figure 17: Long Lake Dam and Powerhouse	14
Figure 18: Long Lake Segment and Layers.....	15
Figure 19: Long Lake segment layout.	16
Figure 20. Long Lake 2000 upstream inflow.....	16
Figure 21. 2000 Long Lake upstream inflow temperatures	17
Figure 22. Little Spokane River flow 2000	17
Figure 23. Little Spokane River temperature, 2000	18
Figure 24. Long Lake outflows, 2000.....	18
Figure 25. Chehalis River study area from near Doty, through Centralia to Aberdeen in southwestern Washington State (Google earth, 2017).	21
Figure 26. Longitudinal profile of the Chehalis River thalweg (vertical lines show model branch breaks). Only the first 3 branches were modeled in this example.	22
Figure 27. Particle tracking reservoir grid example.	23
Figure 28. Side view of model grid for branch 1 in particle release example.	24
Figure 29. Branch temperature, velocity and particles in Tecplot frame.	24
Figure 30. Sediment diagenesis model grid example.	25
Figure 31. Side view of Branch 1 of sediment diagenesis example.....	25
Figure 32. Typical output files from the sediment diagenesis example.....	26
Figure 33. Spokane River between Upper Falls Dam and Nine Mile Dam.	27
Figure 34. Model segment layout.	28
Figure 35. Model vertical layers for Spokane River model.	28
Figure 36. Bonneville pool CE-QUAL-W2 model.	30
Figure 37. Side view of Bonneville pool in the Columbia River.	30

LIST OF FIGURES

Figure 38. Allatoona Reservoir computed (lines) vs. observed (symbols) water surface elevations for 1992, 1993, 1996, and 1997.....	36
Figure 39. 1989 Pineflat Reservoir computed versus observed temperatures.	40
Figure 40. 1993 Pineflat Reservoir computed versus observed temperatures.	41
Figure 41. 1981 Bluestone Reservoir computed versus observed temperatures.....	41
Figure 42. 1983 Bluestone Reservoir computed versus observed temperatures.....	42
Figure 43. 1988 Richard B. Russell computed versus observed temperatures.....	43
Figure 44. 1994 Richard B. Russell computed versus observed temperatures.....	43
Figure 45. 1996 Richard B. Russell computed versus observed temperatures.....	44
Figure 46. Paintsville Reservoir computed versus observed temperatures.	45
Figure 47. 1992 Brownlee Reservoir computed versus observed temperatures.	46
Figure 48. 1995 Brownlee Reservoir computed versus observed temperatures.	46
Figure 49. C.J. Strike Reservoir computed versus observed temperatures.	47
Figure 50. Allatoona Reservoir computed vs. observed DO.....	49
Figure 51. Brownlee Reservoir computed vs. observed DO.....	50
Figure 52. C.J. Strike Reservoir computed vs. observed DO.	50
Figure 53. DeGray Reservoir computed vs. observed DO.....	51
Figure 54. Richard B. Russell Reservoir computed vs. observed DO, March through June, 1988.....	51
Figure 55. Richard B. Russell Reservoir computed vs. observed DO, June through October, 1988.	52
Figure 56. 1996 Richard B. Russell computed vs. observed DO.	52
Figure 57. Neely Henry Reservoir computed vs. observed DO.....	53
Figure 58. J. Strom Thurmond Reservoir computed vs. observed DO.	53
Figure 59. Monroe Reservoir computed vs. observed DO.	54
Figure 60. Rimov Reservoir computed vs. observed DO.	54
Figure 61. Shepaug Reservoir computed vs. observed DO.....	55
Figure 62. Shepaug Reservoir computed vs. observed DO.....	55
Figure 63. Weiss Reservoir computed vs. observed DO.....	56
Figure 64. West Point Reservoir computed vs. observed DO.	56
Figure 65. Walter F. George Reservoir computed vs. observed DO.	57
Figure 66. Rimov Reservoir computed vs. observed phytoplankton biomass.....	58
Figure 67. Rimov Reservoir computed vs. observed phytoplankton biomass.....	59
Figure 68. Rimov Reservoir computed vs. observed phytoplankton biomass.....	59
Figure 69. Rimov Reservoir computed vs. observed phytoplankton biomass.....	60
Figure 70. Rimov Reservoir computed vs. observed phytoplankton biomass.....	60
Figure 71. Rimov Reservoir computed vs. observed phytoplankton biomass.....	61
Figure 72. Rimov Reservoir computed vs. observed phytoplankton with wind rotated 90°.	62
Figure 73. Rimov Reservoir computed vs. observed phytoplankton with wind rotated 90°	62
Figure 74. Rimov Reservoir computed vs. observed phytoplankton with wind rotated 90°.	63
Figure 75. Rimov Reservoir computed vs. observed phytoplankton with wind rotated 90°.	63

LIST OF FIGURES

Figure 76. Rimov Reservoir computed vs. observed phytoplankton with wind rotated 90°.....	64
Figure 77. Rimov Reservoir computed vs. observed phytoplankton with wind rotated 90°.....	64
Figure 78. Rimov Reservoir computed vs. observed phytoplankton with no inflowing phytoplankton.....	65
Figure 79. Rimov Reservoir computed vs. observed phytoplankton with no inflowing phytoplankton.....	66
Figure 80. Rimov Reservoir computed vs. observed phytoplankton with no inflowing phytoplankton.....	66
Figure 81. Rimov Reservoir computed vs. observed phytoplankton with no inflowing phytoplankton.....	67
Figure 82. Rimov Reservoir computed vs. observed phytoplankton with no inflowing phytoplankton.....	67
Figure 83. Rimov Reservoir computed vs. observed phytoplankton with no inflowing phytoplankton.....	68
Figure 84. Water level data versus model predictions for Longview, WA during a 20-day period in 1993.....	70
Figure 85. Model flow predictions versus data for a 20-day period during 1998 at Beaver Army Terminal near Quincy, OR.....	71
Figure 86. Patuxent River computed versus observed vertical salinity distributions.....	72
Figure 87. Patuxent River computed versus observed vertical temperature distributions.....	73
Figure 88. Patuxent River computed versus observed nutrient, dissolved oxygen, and chl a time series.....	74
Figure 89. Snake River water level comparison between CE-QUAL-W2 V3 and USGS field data.....	76
Figure 90. Channel vertical grid where every slope change is a new branch.....	76
Figure 91. Snake River channel slope determination.....	77
Figure 92. Channel slope for the Bull Run system.....	78
Figure 93. Vertical grid for W2 model of Bull Run Lower River.....	79
Figure 94. Bull Run River computed versus observed tracer at three stations progressing downstream.....	81
Figure 95. Spokane River computed versus observed water surface elevations at Spokane.....	82
Figure 96. Spokane River computed versus observed flows at the city of Spokane.....	82
Figure 97. Snake River computed versus observed temperature at six stations.....	83
Figure 98. Computed versus observed temperatures for the Spokane River at Stateline Bridge (upstream boundary), City of Spokane, Fort Wright Bridge, and Riverside State Park.....	84
Figure 99. Spokane River computed versus observed conductivity below Nine Mile Dam.....	85
Figure 100. Snake River computed versus observed dissolved oxygen at six stations.	86
Figure 101. Snake River computed versus observed orthophosphorus at six stations.	87
Figure 102. Snake River computed versus observed nitrate-nitrite at six stations.....	88
Figure 103. Snake River computed versus observed chlorophyll a at six stations.....	89
Figure 104. Snake River computed versus total organic carbon.....	90

LIST OF FIGURES

Figure 105. Spokane River computed versus observed dissolved oxygen at Riverside State Park.....	90
Figure 106. Spokane River computed versus observed dissolved oxygen below Nine Mile Dam.....	91
Figure 107. Spokane River computed versus observed pH upstream of Nine Mile Dam.....	91
Figure 108. Spokane River computed versus observed nitrate-nitrite at Riverside State Park.....	92
Figure 109. Spokane River computed versus observed soluble reactive phosphorus below Nine Mile Dam.....	92
Figure 110. Spokane River computed versus observed total nitrogen below Nine Mile Dam.....	93

List of Tables

Table 1. Model branch characteristics for the Columbia Slough model.....	3
Table 2. Listing of point source tributary inflows to the Lower Columbia Slough model....	3
Table 3. DeGray Reservoir Physical Characteristics.....	7
Table 4. Branch and segment layout for DeGray Lake.....	8
Table 5. Long Lake Dam and Reservoir Specifications.....	15
Table 6. Computational Grid Setup.....	16
Table 7. Long Lake model input and output files	19
Table 8. Summary of waterbody and branch segments and layers for the 3 waterbodies in this example.....	22
Table 9. Model files for the Spokane River example.....	29
Table 11. Coefficients affecting thermal calibration.....	37
Table 12. Reservoir thermal simulations with error statistics for station closest to dam.	39

Preface

This manual documents the two-dimensional, laterally averaged, hydrodynamic and water quality model CE-QUAL-W2. As in all complex models, there have been many contributors. This re-write of the User Manual was based on prior User Manuals: Environmental and Hydraulic Laboratories (1986), Cole and Buchak (1995) Version 2, and Cole and Wells (2000) Version 3.0 through Cole and Wells (2019) Version 4.1. Hence, one can think of the primary author as merely an editor of past documents, rather than reflecting one person's sole authorship. This updated User Manual contains numerous corrections, new figures, new sections, additional documentation, and improvements in organization and presentation of information compared to Cole and Wells (2019).

This section of the User Manual Part 4 documents the examples provided in the model download and goes over typical applications for reservoirs, lakes, rivers, and estuaries.

The other sections of the User Manual are divided into multiple sections for ease of updating and editing:

- User Manual Part 1: Introduction to CE-QUAL-W2, Model download package, how to run the model, model versions, changes between model versions
- User Manual Part 2: Theoretical basis for CE-QUAL-W2: hydrodynamics and water quality, particle transport and numerical scheme
- User Manual Part 3: Model input and output file descriptions and input/output file examples
- User Manual Part 4: Model examples
- User Manual Part 5: Release notes, bug fixes, differences in model versions, history of bug fixes, and other user manuals such as for the GUI interface, the water balance algorithm, and other external codes.

This report should be cited as follows:

Wells, S. A. (2022) "CE-QUAL-W2: A two-dimensional, laterally averaged, hydrodynamic and water quality model, version 4.5, user manual part 4, model examples," Department of Civil and Environmental Engineering, Portland State University, Portland, OR.

or for referencing an author of a section,

Cole, T. (2022) "Examples of Model Applications," in "CE-QUAL-W2: A two-dimensional, laterally averaged, hydrodynamic and water quality model, version 4.5, user manual part 4, model examples," ed. by S. Wells, Department of Civil and Environmental Engineering, Portland State University, Portland, OR.

1. Introduction

This section of the User’s Manual describes the example problems distributed with the model release and provides examples of other CE-QUAL-W2 applications. This section of the User Manual also includes an updated section from the Cole and Wells (2019) User Manual written primarily by Tom Cole on application of the model to reservoirs, estuaries, and rivers.

2. Model Examples Distributed with the Model Release

The examples problems released with the code are shown in Figure 1. A description of each of these models is discussed in this part of the User Manual.

- 📁 Columbia Slough Estuary_ExcelControlFile
- 📁 DeGray Reservoir_ExcelControlFile
- 📁 Detroit Reservoir
- 📁 LongLake_ExcelControlFile
- 📁 MultipleWaterBodyCascade
- 📁 Particle tracking
- 📁 Sediment diagenesis example
- 📁 Spokane River
- 📁 Spokane River csv input format_ExcelControlFile
- 📁 SysTDG Columbia River

Figure 1. Model examples distributed with model release version.

Also released with the model download are two other examples – one for the USGS Auto Port Selection and one for using W2Post for plotting calibration profiles. The USGS Auto Port Selection examples are in the directory, “USGS Examples for using USGS Auto Port Selection Algorithm” and include the examples shown in Figure 2. A description of these examples is provided in the README.txt file provided by Stewart Rounds of the USGS.

📁 det_multigate_example3	6/26/2019 11:26 AM	File folder
📁 det_multigate_example4	6/26/2019 11:26 AM	File folder
📁 det_normal_uro-float_400fmin	6/26/2019 11:26 AM	File folder
📁 lop-dex_lopFloat_20ppmin	6/26/2019 11:26 AM	File folder
📄 README.txt	7/6/2019 8:11 PM	Text Document

Figure 2. USGS model examples illustrating using the auto-port selection feature.

The W2Post example is included in the download directory: "W2tools post-processor integrated with W2control preprocessor". This includes the DeGray Reservoir example with computed temperature calibration data and statistics.

Columbia Slough Estuary

The Upper and Lower Columbia Slough are each long (about 9 miles) and narrow (from 50 ft to 200 ft wide) water bodies in the Portland metropolitan area in Multnomah County. The Lower Columbia Slough, as shown in , is connected to the Willamette River near its mouth with the Columbia River where it experiences a tidal fluctuation of its water surface of between 1 to 3 ft. Inflows to the Lower Columbia Slough included in the past combined-sewer-overflows (CSOs), storm water (from storm water pipes and from pump stations on the Northern side of the Lower Slough), water from Smith and Bybee Lakes, leachate from the St. John's Landfill, and inflows (both pumped and gravity inflows) from the Upper Columbia Slough at MCDD1 (Multnomah County Drainage District #1). The example problem is set up for a 2-branch model of the Lower Columbia Slough.

The Upper Columbia Slough, shown in Figure 4 and termed the "Middle" and "Upper" Slough, was historically maintained to provide irrigation water to agricultural and commercial users in the summer months. The Upper Slough is connected by pipes and an overflow weir during the fall, winter, and spring to Fairview Lake. During the summer, Fairview Lake is connected to the Upper Slough only by flow over and leakage through the weir. Water is also pumped from the Upper Slough to the Lower Columbia Slough at a pump station at MCDD1 and from the Upper Slough to the Columbia River at MCDD4 (Multnomah County Drainage District #4). At MCDD1, pipes also allow gravity flow from the Upper Slough to the Lower Slough. Other inflows to the Upper Columbia Slough include ground-water and storm water from the Portland International Airport and other industrial, commercial, and residential neighborhoods in the area.

The model has 2 branches as shown in comprising the main arm of the Lower Slough and the branch named North Slough. Details of the bathymetry are shown in Table 1. The model grid is shown in Figure 5 and Figure 6. The vertical grid spacing is 0.305 to 0.61 m or 1 to 2 ft.

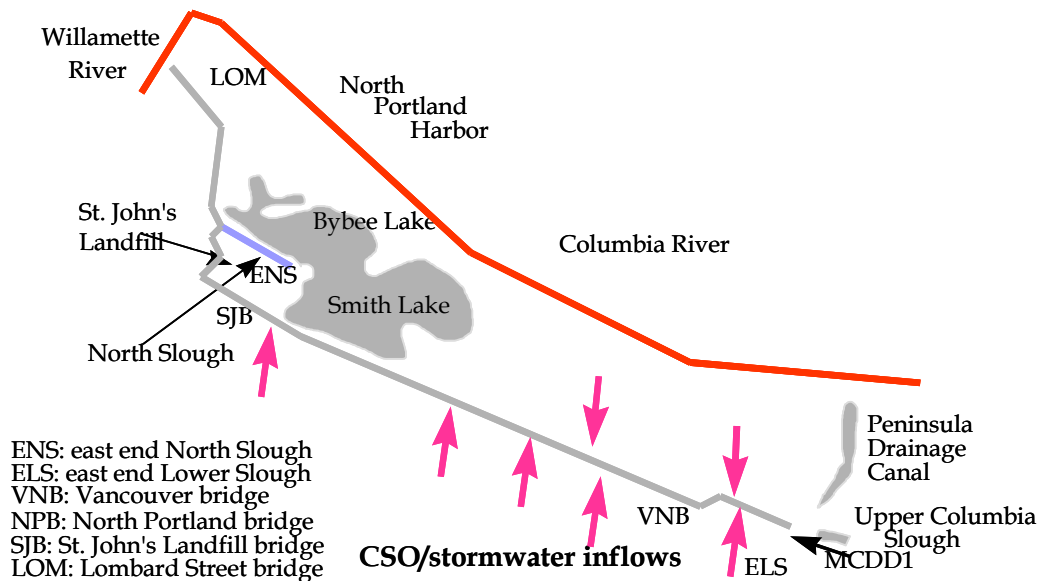


Figure 3. Lower Columbia Slough system.

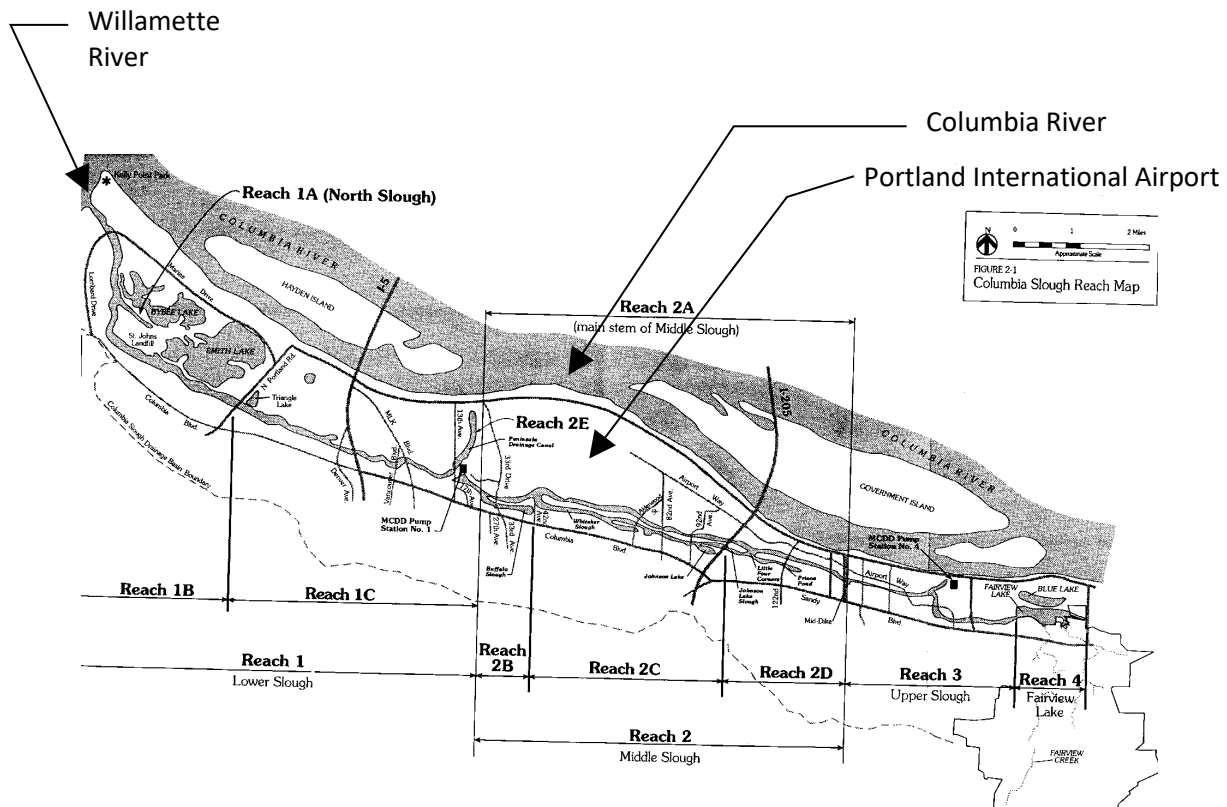


Figure 4. Columbia Slough, Portland, Oregon (City of Portland, BES).

Table 1. Model branch characteristics for the Columbia Slough model.

Branch	Length (ft)	Length (m)	Segment spacing, ft	Segment spacing, m	Number of Segments	Segment number upstream end	Segment number downstream end
1 (Lower Slough)	43640	13302	502-1003	152.9-305.8	44	2	45
2 (North Slough)	4503	1373	1500	457.5	3	48	50

The model has 17 tributary inputs (CSOs and storm water inputs) and 1 upstream flow input from the Upper Slough. Cell numbers of storm water inflows, CSOs and the Upper Slough are shown in Table 2. Note that the cell number 45 is a head boundary condition and that the model calculates the flow rate in and out of the Slough based on head elevations.

Table 2. Listing of point source tributary inflows to the Lower Columbia Slough model.

ID	Internal trib #	Inflow branch	Inflow cell #	Outfall Location	Flow file	Temp. File	Conc. file
13 th Street, CSO# 65, 64	1	1	3	755' downstream from ELS**	Qtr_tr1.npt	Ttr_tr1.npt	Ctr_tr1.npt

CALIBRATION

ID	Internal trib #	Inflow branch	Inflow cell #	Outfall Location	Flow file	Temp. File	Conc. file
PENN. P2-2	2	1	4	2433' downstream from ELS**	Qtr_tr2.npt	Ttr_tr2.npt	Ctr_tr2.npt
Vancouver, CSO# 63	3	1	8	5814' downstream from ELS**	Qtr_tr3.npt	Ttr_tr3.npt	Ctr_tr3.npt
Albina, CSO# 62	4	1	9	7098' downstream from ELS**	Qtr_tr4.npt	Ttr_tr4.npt	Ctr_tr4.npt
PENN. P2-1	5	1	12	9723' downstream from ELS**	Qtr_tr5.npt	Ttr_tr5.npt	Ctr_tr5.npt
Fenwick, CSO# 61	6	1	12	10290' downstream from ELS**	Qtr_tr6.npt	Ttr_tr6.npt	Ctr_tr6.npt
Kenton, CSO #60	7	1	14	12448' downstream from ELS**	Qtr_tr7.npt	Ttr_tr7.npt	Ctr_tr7.npt
Bayard, CSO #59	8	1	17	14998' downstream from ELS**	Qtr_tr8.npt	Ttr_tr8.npt	Ctr_tr8.npt
PENN P1-1	9	1	18	16328' downstream from ELS**	Qtr_tr9.npt	Ttr_tr9.npt	Ctr_tr9.npt
Chautauqua, CSO #58	10	1	19	17491' downstream from ELS**	Qtr_tr10.npt	Ttr_tr10.npt	Ctr_tr10.npt
Fiske, CSO #57	11	1	22	19777' downstream from ELS**	Qtr_tr11.npt	Ttr_tr11.npt	Ctr_tr11.npt
Oregonian, CSO #56	12	1	26	24389' downstream from ELS**	Qtr_tr12.npt	Ttr_tr12.npt	Ctr_tr12.npt
Oswego, CSO #55, 55A, 54A	13	1	29	27577' downstream from ELS**	Qtr_tr13.npt	Ttr_tr13.npt	Ctr_tr13.npt
RG-1	14	1	33	31450' downstream from ELS**	Qtr_tr14.npt	Ttr_tr14.npt	Ctr_tr14.npt
St. Johns, CSO #54	15	1	33	30924' downstream from ELS**	Qtr_tr15.npt	Ttr_tr15.npt	Ctr_tr15.npt

ID	Internal trib #	Inflow branch	Inflow cell #	Outfall Location	Flow file	Temp. File	Conc. file
RG-2	16	1	37	35212' downstream from ELS**	Qtr_tr16.npt	Ttr_tr16.npt	Ctr_tr16.npt
RG-3	17	1	45	43076' downstream from ELS**	Qtr_tr17.npt	Ttr_tr17.npt	Ctr_tr17.npt

** East end of Lower Slough

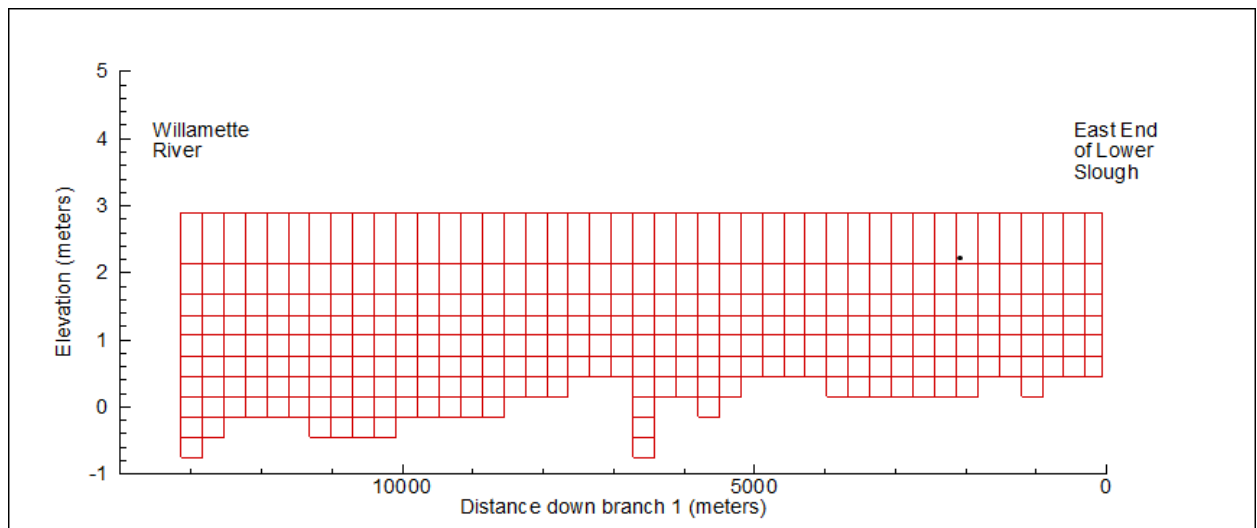


Figure 5. Grid layout for Columbia Slough Branch 1.

CALIBRATION

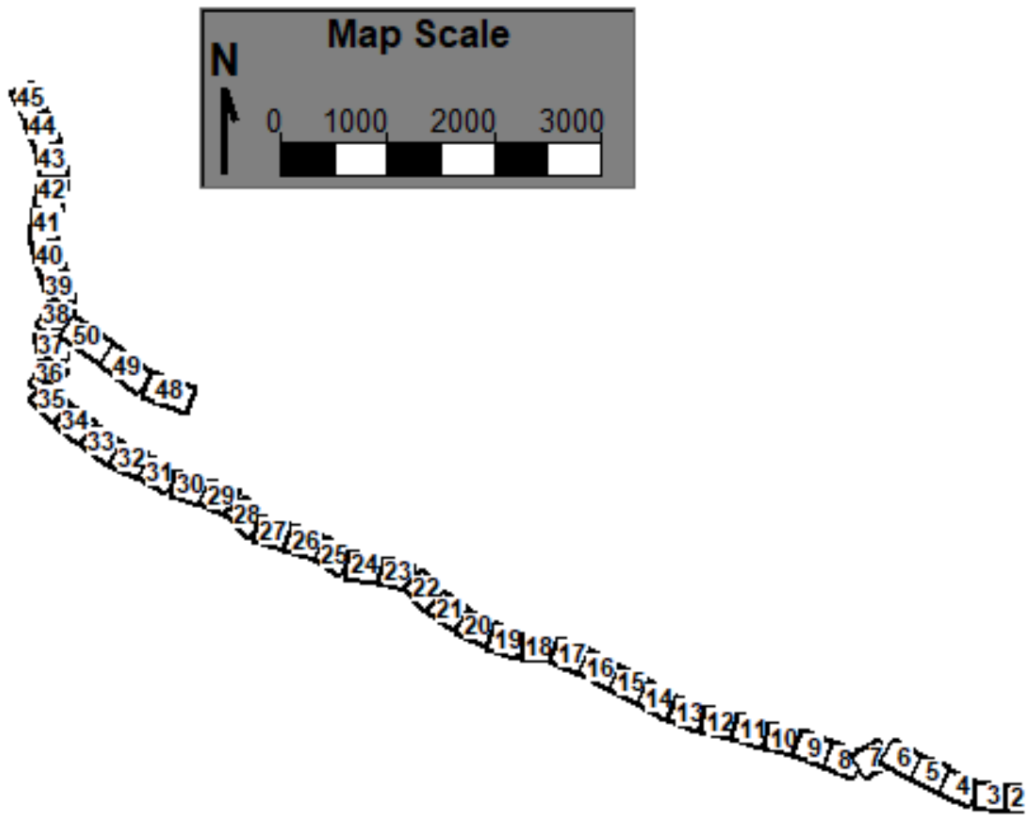


Figure 6. Segment layout for Columbia Slough.

This example shows how to use an external head boundary condition and set up files for that external head. Note though that this is an old example using the old input format for head boundary conditions. The User Manual Part 3 shows how many of these files can be developed in a much simpler format, especially if there is no stratification in the Willamette River, the location of the external head condition.

For example, the model uses the file "tdh_br1.npt" for the temperature downstream head external boundary condition. An updated, much simpler format file is also included in this example, "tdh_br1.csv". A similar csv file could be developed for the cdh_br1.npt file following guidelines in the User Manual Part 3. Also, the control file for this example is from the Excel file, **w2_con_ColSlough.xls**, which is used to produce the file **w2_con.csv**.

DeGray Reservoir with Sediment Diagenesis and Vertical Algae Migration

This example demonstrates many features of the CE-QUAI-W2 model that are described in the User manual Part 3, such as

- Sediment diagenesis

- Vertical migration of algae
- Contour plotting for temperature using
- Environmental performance
- Fish habitat

DeGray Reservoir is located on the Caddo River in south central Arkansas and is the site of the first water quality test application of CE-QUAL-W2. Impounded in 1969, the reservoir is used for power generation, flood control, and recreation. DeGray is classified as a monomictic, deep storage reservoir. Figure 7 shows a map of the system with sampling locations and Table 3 gives the important physical characteristics for the reservoir.

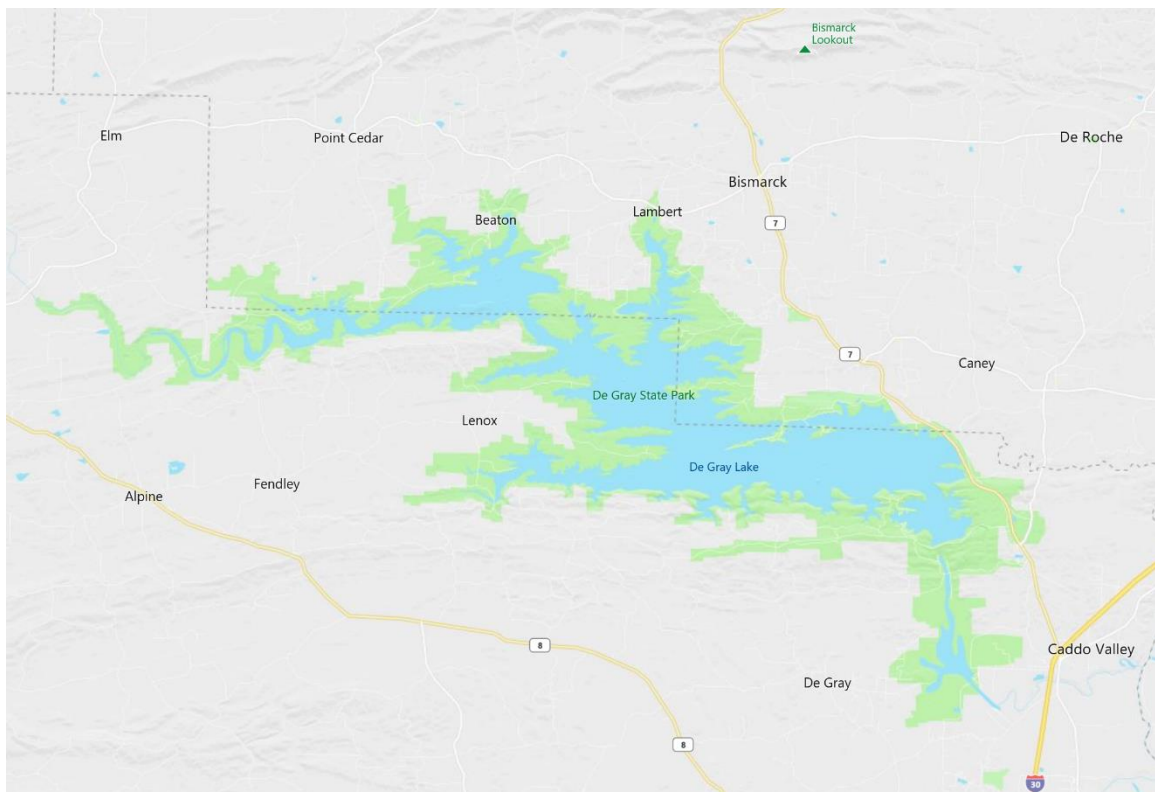


Figure 7. DeGray Reservoir (Bing Maps, 2019).

Table 3. DeGray Reservoir Physical Characteristics

Area	Volume	Depth		Residence Time
		Average	Maximum	
5,092 ha	613,692 acre-ft	14.9 m	56 m	560 days

DeGray Reservoir was originally modeled as a one-branch system with no tributary inflows. The grid layout is shown in Figure 8. The outlet location is in layer 13. Details of the bathymetry setup are given in Table

CALIBRATION

4. The grid only has one orientation angle for the entire grid. Under typical modeling situations, the orientation angle would vary by segment. Also, this grid should have several model side branches rather than just one. The model vertical grid is 2 m which is a bit coarse since typically we use 1 m or less grid spacing.

Table 4. Branch and segment layout for DeGray Lake.

Branch	Branch length	Segment lengths	Maximum width	Layer height	Upstream segment	Downstream segment
1	30 km	1000 m	5530 m	2 m	2	31

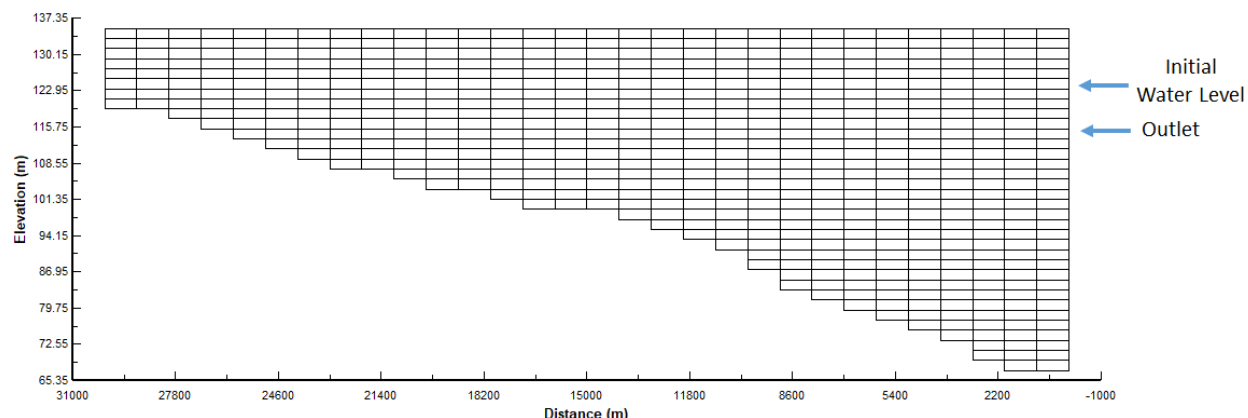


Figure 8. DeGray Reservoir computational grid

This example shows how to set up and use the fish habitat (output file `habitat.csv`) and the environmental performance (note the output files, such as `envrprf_t_1.csv` for temperature and `envrprf_c_1.csv` for concentration of state variables) to evaluate a model simulation. These are set-up using the input files `w2_habitat.npt` and `w2_envirprf.npt`. Also, output files are written for the W2 Post post-processor and for contour plotting of depth vs time and temperature (input file `w2_lake_river_contour.csv`). Descriptions of these files are shown in the User Manual Part 3. Also, the control file for this example is from the Excel file, `w2_con_DeGray.xlsx`, which is used to produce the file `w2_con.csv`.

This example also has sediment diagenesis turned ON (input file `w2_diagenesis.npt`) and vertical migration of algae (input file `w2_AlgaeMigration.csv`) turned ON.

See the model User manual in Part 3 how to use these features. All these auxiliary input files are tabs in the Excel file: `w2_con_DeGray.xlsx`.

Detroit Lake

The following example is meant to explore running the model, examining fish habitat, and travel time of particles released at the upper end of the reservoir. This is a model of Detroit Reservoir in Oregon, USA. The original model was developed by the USGS (Sullivan et al, 2007) and has been simplified for this example.

The model has 4 branches and 31 segments as shown in Figure 9. The vertical layer height is about 2 meters. The spatial layout of the branches and inflows is shown below in Figure 10.

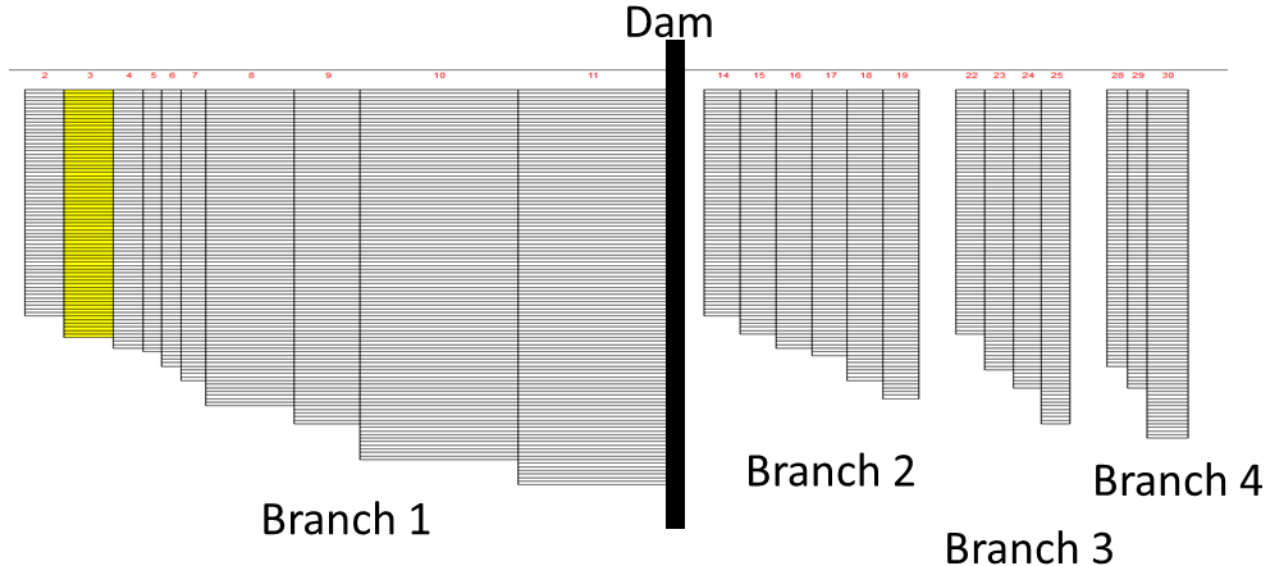


Figure 9. Detroit Reservoir model grid.

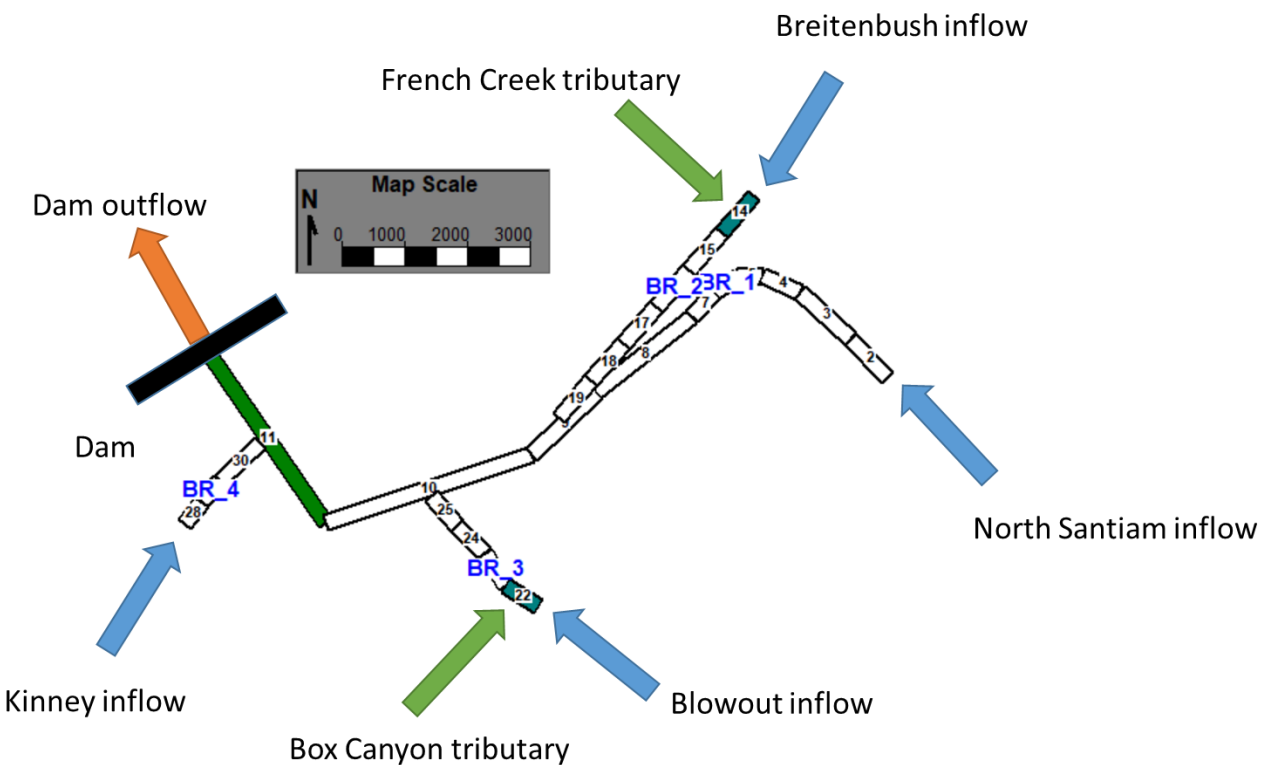


Figure 10. Branch and inflow layout for Detroit Reservoir.

CALIBRATION

The model files are organized in a zipped file that organizes many of the input files in a subdirectory called "InputFiles". All output files will be written to the directory where the model executables are located even though these too could be written to a separate directory using guidelines in the User Manual for directing output to separate file directories.

For this example, after running the preprocessor and model executable, we will look at just 2 aspects of the model predictions:

- (1) Flow balance summary
- (2) Fish habitat volume.

The output file for overall flow balance is a file called "flowbal.csv". This shows the flow in and out as well as evaporation losses over the 2002 year. This file opens in Excel and one can see the model predicted evaporation losses over the year as shown in Figure 11. One can also see the model predicted mass balance errors (very, very small) and inflow and outflow volumes.

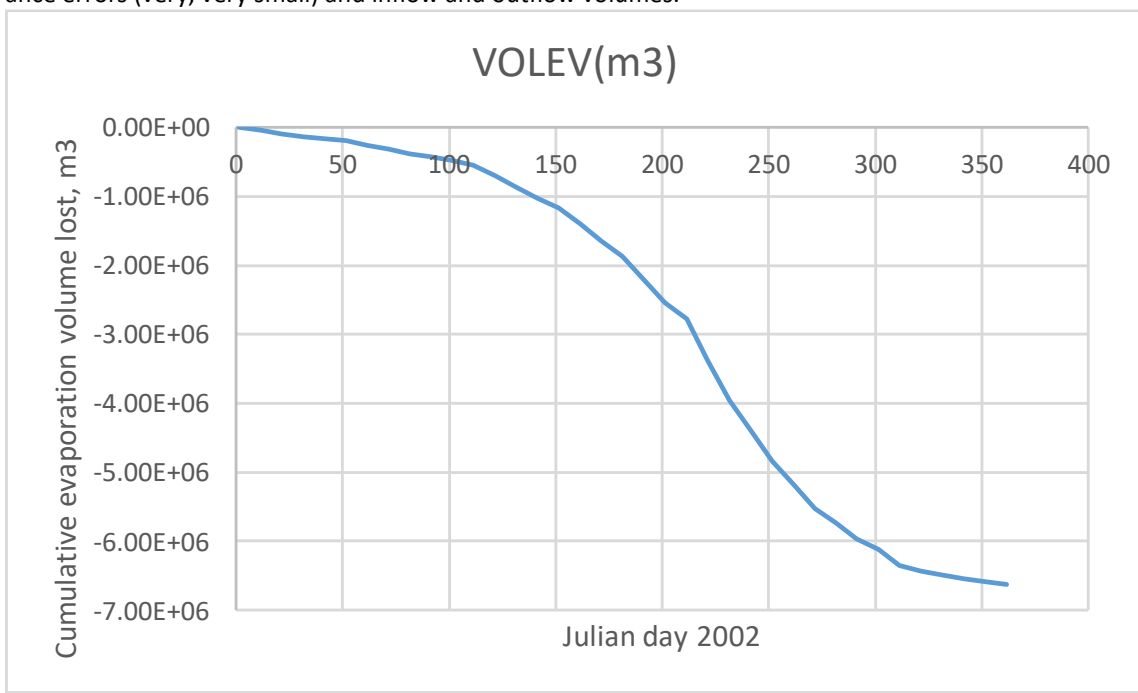


Figure 11. Predicted evaporation losses from Detroit Reservoir in 2002.

The output file for the fish habitat volumes is a file called "habitat.csv". This file shows the habitat volumes and % volumes for each of the species shown in the beginning of the file. This file opens easily in Excel, and one can see the model predicted fish habitat for striped bass in % of the reservoir volume over the year in Figure 12. Of course, this reservoir is too cold in the winter months for this species.

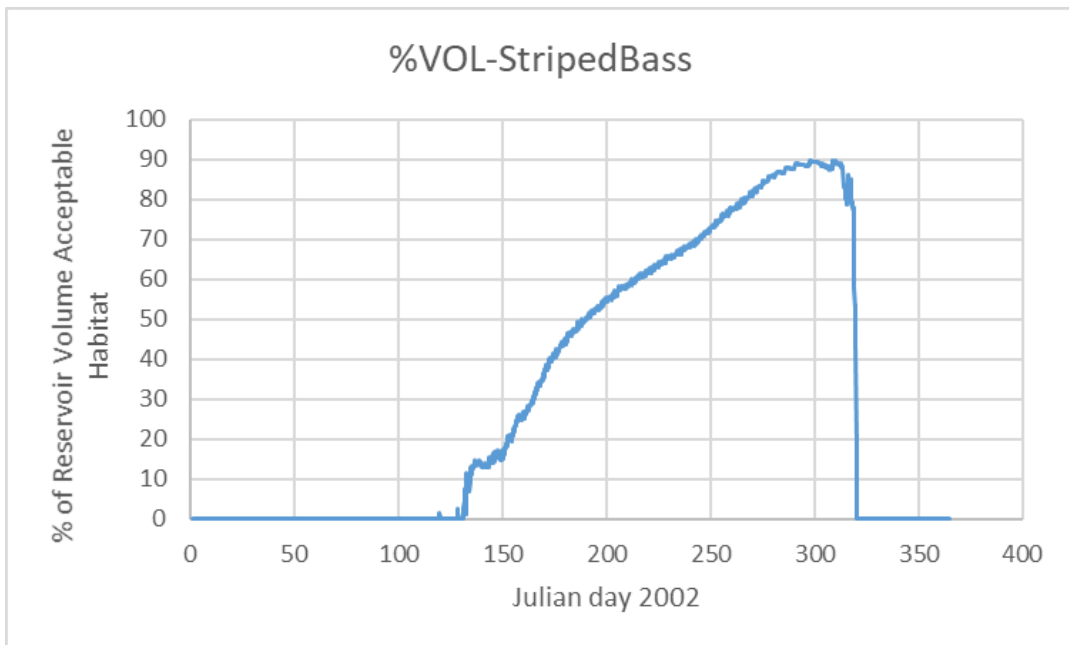


Figure 12. Percent of reservoir volume optimal habitat for striped bass for Detroit Reservoir

There are many other aspects of the model to explore and the documentation will assist you in exploring other aspects of this model example such as the suspended solids distributions in the reservoir and stratification dynamics.

By installing the “w2post” GUI post-processor, many aspects of the model can be examined – such as contour plots of temperature stratification, time series plots, profile plots. One example is shown in Figure 13 which is a contour plot for Julian day 167 for the year 2002 using the w2post GUI.

CALIBRATION

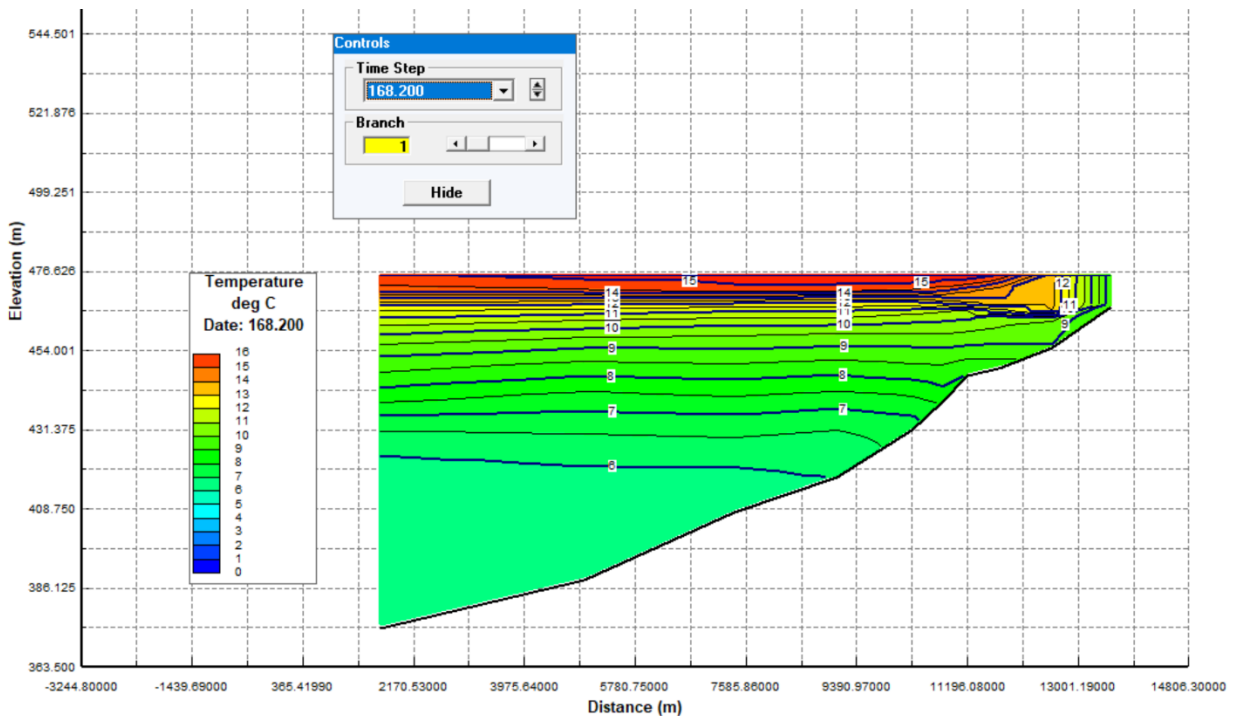


Figure 13. Reservoir temperature on Julian day 168.2 in the year 2002. for Branch 1 for Detroit Lake.

Long Lake or Spokane Lake

This example was provided to test the new Excel based control file, **w2_con.xls**, which writes out a csv file names **w2_con.csv** which is used in lieu of the files **w2_con.npt** and **graph.npt**. This is described in the User Manual Section 3.

Long Lake is part of the Spokane River that flows from Idaho to the Columbia River. Characteristics of the lake are described below. Figure 14 shows the location of the Upper Spokane River system. Figure 15 shows a close-up of the Spokane River from the WA-ID State line to the Long Lake Dam.

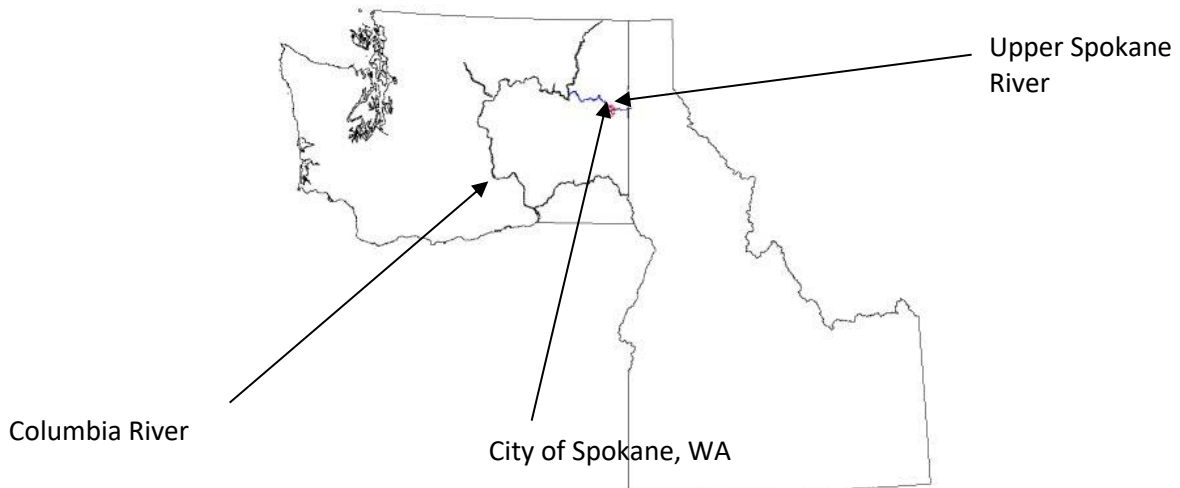


Figure 14: Upper Spokane River in Washington

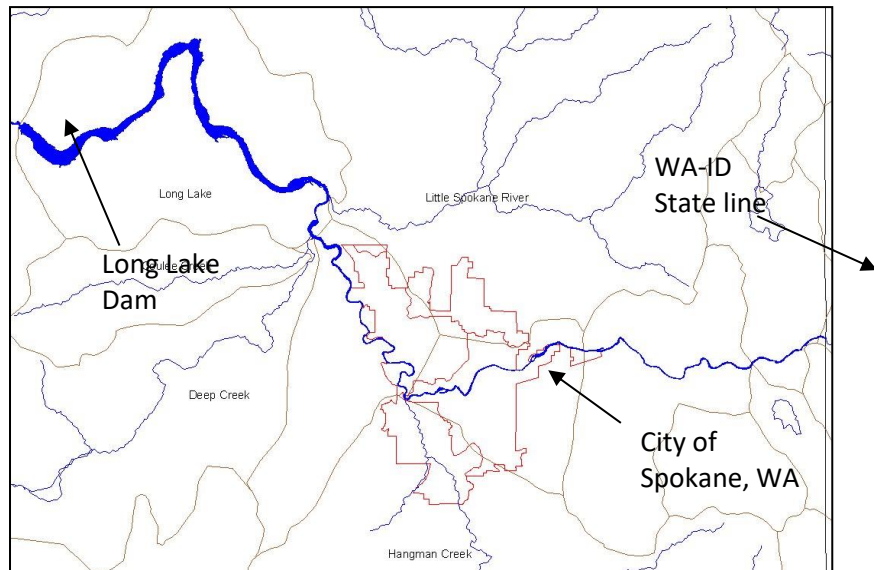


Figure 15: Long Lake located west of the City of Spokane.

Long Lake Bathymetry

The Long Lake bathymetry was originally developed by the WA Department of Ecology and was based on bathymetric contour maps provided by AVISTA Corporation. Figure 16 shows an image of the reservoir contours used to develop the lake bathymetry.

CALIBRATION

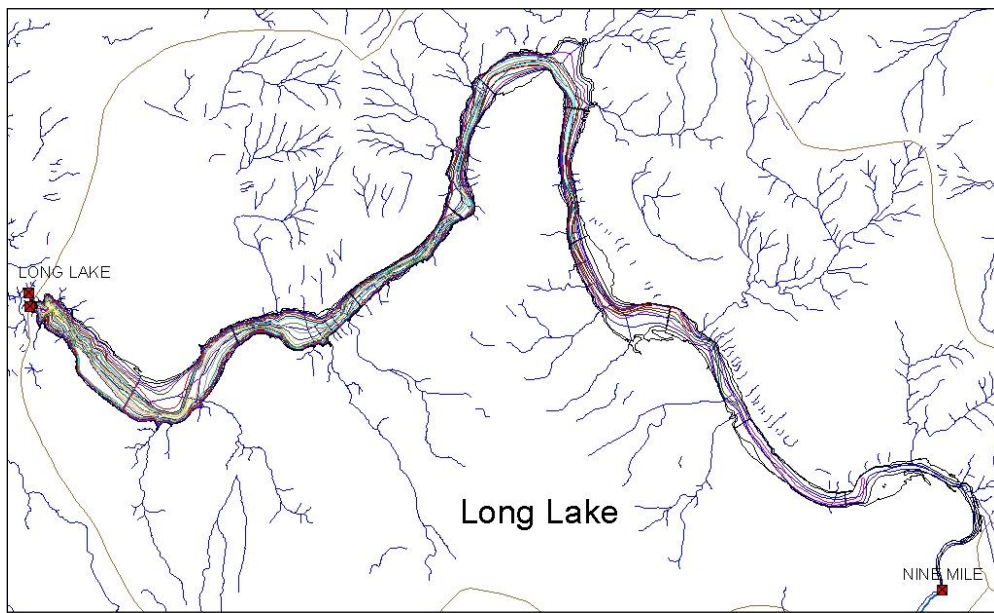


Figure 16: Long Lake bathymetric contours

Long Lake Dam and Reservoir

The dam facilities are located at RM 32.5 and the lake backs up to one mile below Nine Mile Dam at RM 57.8. The Long Lake section of the model includes from Nine Mile Dam to Long Lake Dam, depending on water level the upper most segments of the model may act like a river or lake. The lake has a maximum depth of 170 ft at a full pool elevation of 1536 ft NGVD29. Figure 17 shows the Long Lake Dam, spillway and powerhouse facilities. There are 8 Tainter gates on the dam. Aside from leakage these gates are kept closed to allow as much storage (normal pool is with gates closed) and power generation as possible. Table 5 lists several dam facility specifications.



Figure 17: Long Lake Dam and Powerhouse

Long Lake is located furthest downstream in the system model. Table 5 provides some important physical characteristics of the reservoir.

Table 5. Long Lake Dam and Reservoir Specifications

Specification	ft	m
Top of Dam Elevation	1537	468.48
Spillway Crest Elevation	1508	459.64
Spillway Gate Type	Vertical lift (8)	
Spillway Gate Height	29	8.84
Spillway Gate Width	25	7.62
Normal Full Pool Elevation	1536	468.18
Max Forebay Elevation	1536	468.18
Min Forebay Elevation	1512	460.86
Max Draw down	24	7.32
Turbine Inlet Elevation	1499	456.9

Long Lake was modeled as a one-branch system. Figure 18 shows a cross section of the model grid for Long Lake and Figure 19 shows a plan view of the model grid indicating the segment orientation. Details of the grid setup are given in Table 6.

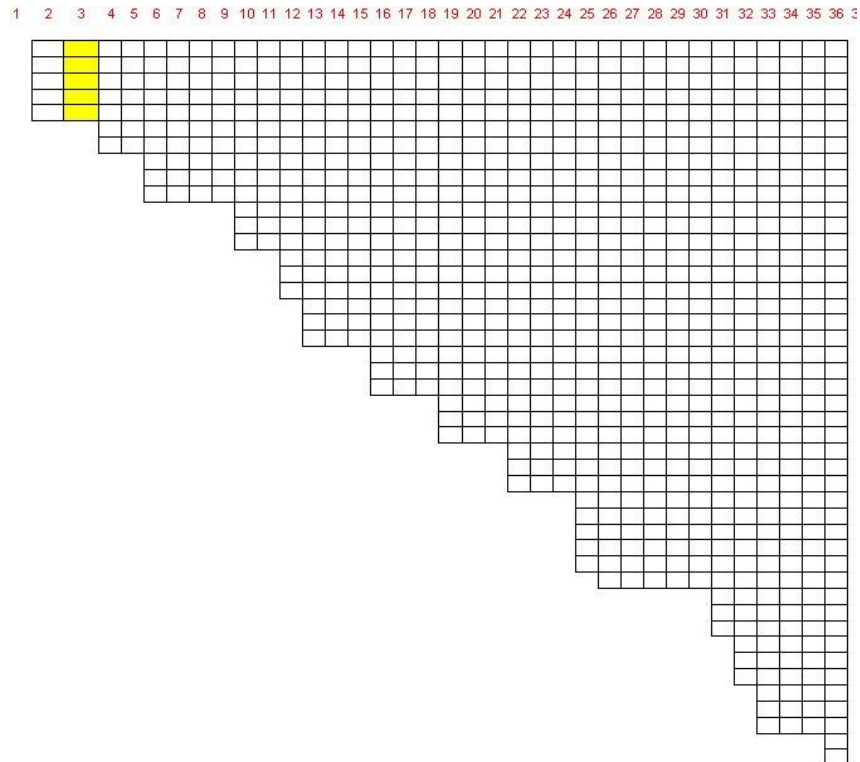


Figure 18: Long Lake Segment and Layers.

CALIBRATION

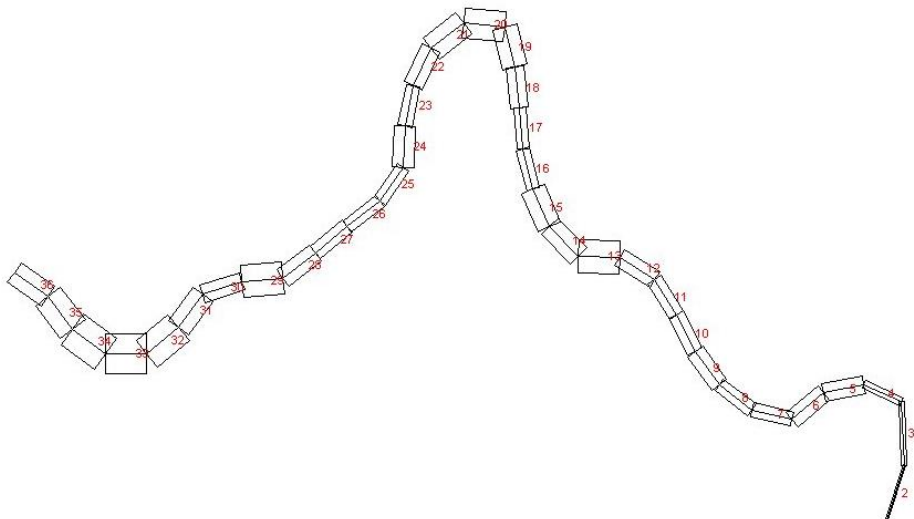


Figure 19: Long Lake segment layout.

Table 6. Computational Grid Setup

Branch	Start RM	End RM	Layer Height, m	# of seg-ments	DLX Range, m	Bottom Elev. m
1	57.77	32.50	1.0	37	1070.8 to 1666.0	422.10

Initial/Boundary Conditions

Inflows to Long Lake consist of the upstream boundary condition from the Spokane River and a tributary inflow from the Little Spokane River. Figure 20 and Figure 21 show the upstream inflow and temperature to Long Lake. Figure 22 and Figure 23 show the inflow and temperature from the Little Spokane River. Figure 24 shows the outflow from Long Lake.

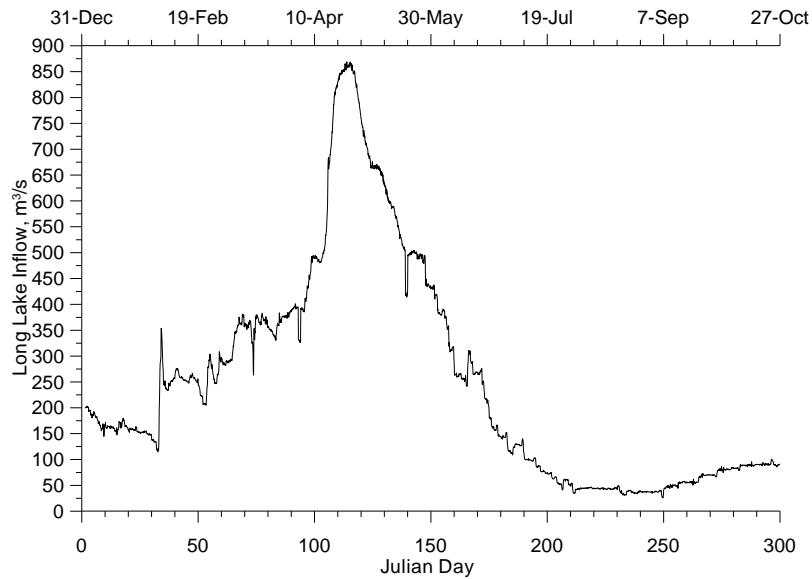


Figure 20. Long Lake 2000 upstream inflow

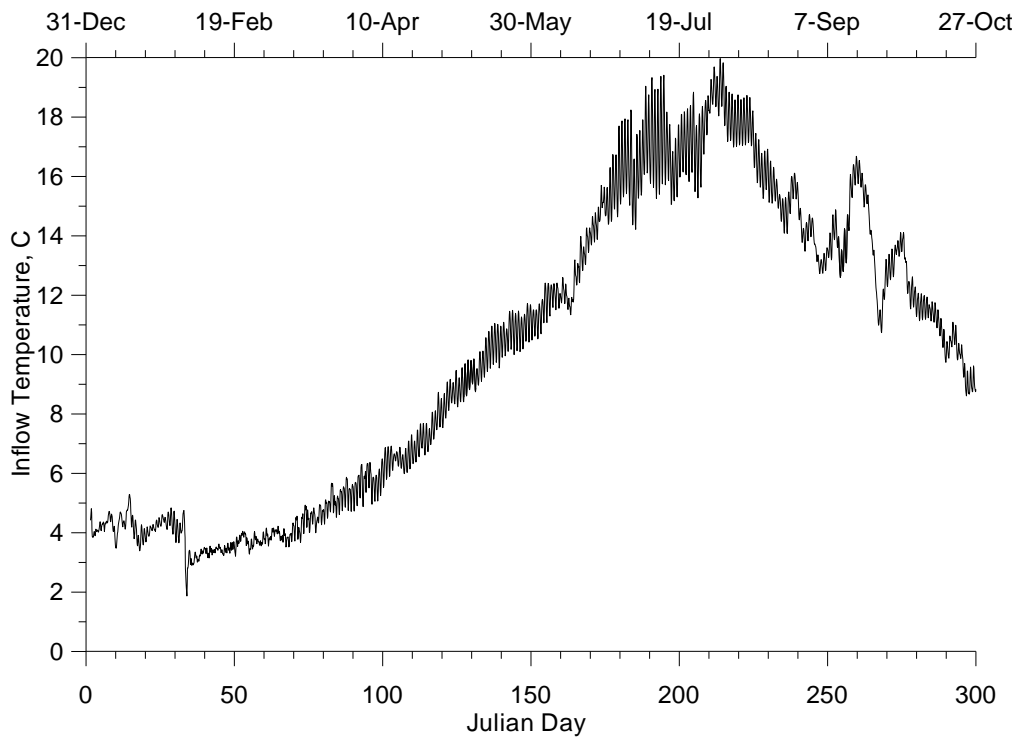


Figure 21. 2000 Long Lake upstream inflow temperatures

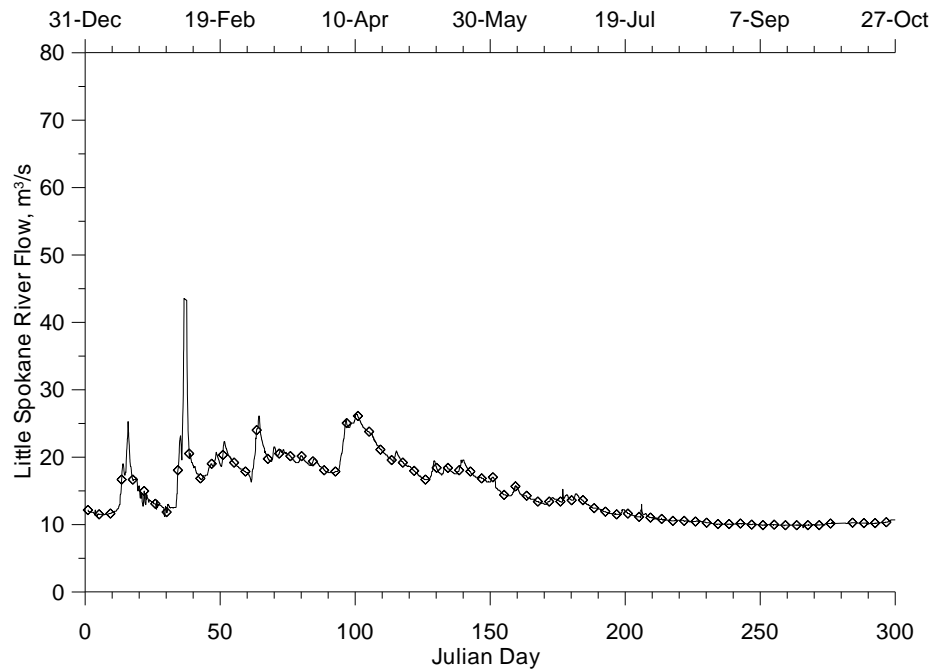


Figure 22. Little Spokane River flow 2000

CALIBRATION

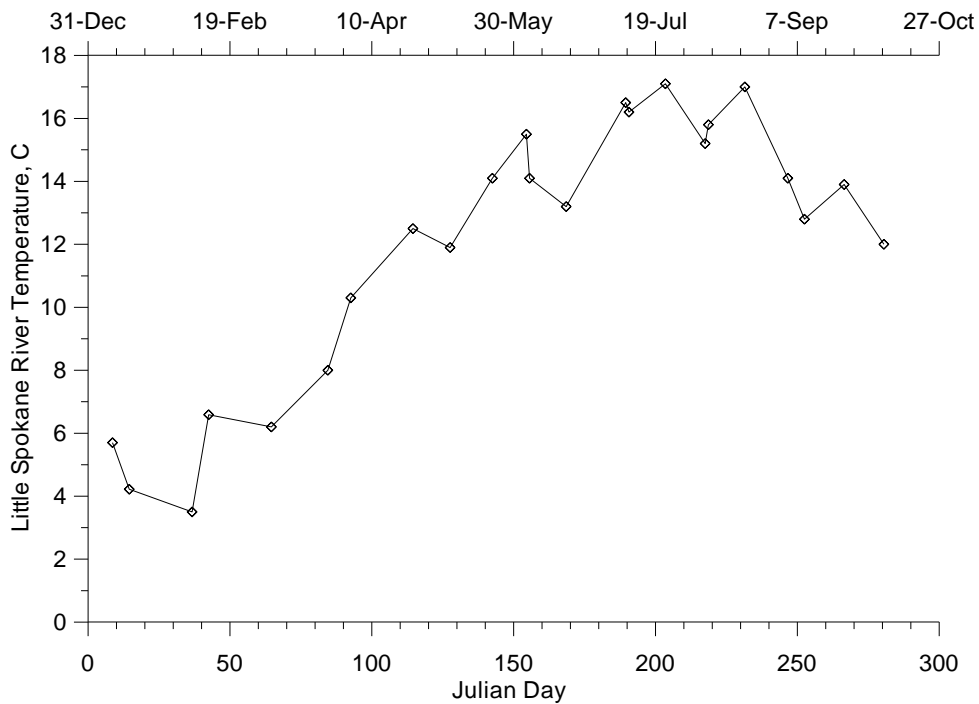


Figure 23. Little Spokane River temperature, 2000

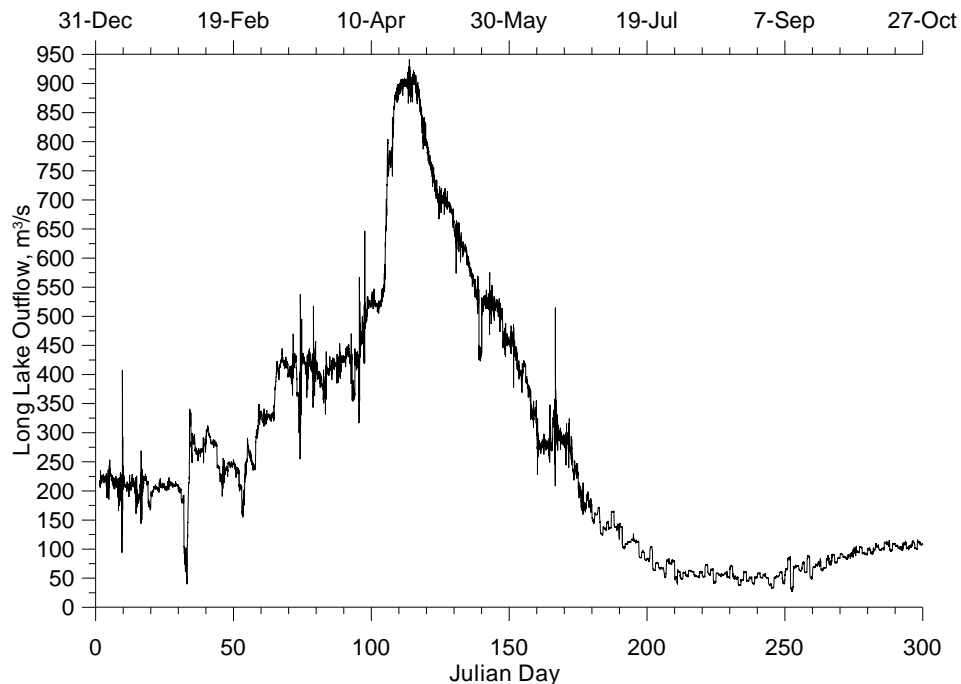


Figure 24. Long Lake outflows, 2000

Table 7 shows the file names of the inputs to the Long Lake model and the output files generated by the model.

Table 7. Long Lake model input and output files

File Type	File Name	Description
control file	w2_con.csv	Model control file (developed from w2_con.xlsx)
bathymetry file	bth.csv	Segment lengths, initial water surface elevation, segment orientation, layer thickness and cell widths
meteorological file	met00jr6.csv	Time series file containing temperature, dew point temperature, wind speed, wind direction and cloud cover data (based on solar radiation)
Wind sheltering file	wsc.csv	Wind sheltering coefficient for each segment and variable over time
Shade file	shade.csv	Shade file for characterizing vegetative and topographic shade or static shade values
Aerator input file	w2_aerate.npt	Input parameters for using aeration
Environmental Performance Criteria Input File	w2_envirprf.npt	Input parameters for specifying environmental performance criteria
Habitat volume input file	w2_habitat.npt	Input parameters for calculating habitat volumes
Selective withdrawal input file	w2_selective.npt	Input parameters for selective withdrawal feature
Water surface elevation file	wl_LL00.dat	Observed water surface elevations
branch inflow files	Qin_br1.csv	Flow rate file for branch 1 inflow
	Tin_br1.csv	Temperature file for branch 1 inflow
	Cin_br1.csv	Concentration file for branch 1 inflow
Branch outflow files	qll_00.csv	Flow rate file for branch 1 outflow
tributary files	LSPKQ00.csv	Flow rate file for tributary 1 (Little Spokane River)
	LSPKT00.csv	Temperature file for tributary 1
	LSPKC00.csv	Concentration file for tributary 1
distributed tributary files	Qwb1.csv	Flow rate file for distributed tributary
	DisTribT.csv	Temperature file for distributed tributary
	DisTribC.csv	Concentration file for distributed tributary
model output files	snp1.opt	Snapshot file
	tsr_#_seg#.csv	Time series files
	qwo_36.csv	Long Lake outflow file for segment 36 (dam segment)
	two_36.csv	Long Lake outflow temperature for segment 36 (dam segment)
	cwo_36.csv	Long Lake outflow concentration for segment 36 (dam segment)
	qwo_str1_seg36.csv	Outflow file time series for structure #1 at segment 36 (dam segment)
	two_str1_seg36.csv	Outflow temperature time series for structure #1 located at segment 36 (dam segment)
	cwo_str1_seg36.csv	Outflow constituent time series for structure #1 located at segment 36 (dam segment)
	W2_Output.w2l	Binary output file for W2_Tool Post-Processor

CALIBRATION

Multiple Water Body Cascade

This example focuses on using 3 waterbodies of a river system that cascade from one-to-the-other in linear fashion with the multiple processor approach discussed in Part 3 of the User Manual. The purpose of this example is to show how one can reduce computational time for running multiple waterbodies.

The model user has several choices on how to run this system of 3 waterbodies:

- Run all 3 waterbodies as one model. This simulation may be simpler to manage since all files are in one directory, but the model will take the longest time to run since all waterbodies will be limited to the shortest numerical time step in the 3 waterbody domain.
- Run the upper waterbody (WB1) first, then copy the outflow from WB1 to the next waterbody (WB2) and then run WB2. Then repeat this for running the last waterbody 3 (WB3). This is often well-suited to using a batch file to transfer the files automatically and using CLOSEC=ON to close the dialog box automatically. Each waterbody will run at its maximum time step independent of the other waterbodies and hence will be faster than the first choice.
- Use the multiple waterbody model where the code manages the transfer of information from one waterbody to the other and runs the models simultaneously based on upstream data availability. This is similar to the earlier choice except that instead of waiting for the run from upstream to run to completion, the downstream model starts running when information is available from upstream. With multiple cores, the waterbodies run on separate computer cores and the run finishes close to the time of the run of the limiting waterbody.

The example is from a multiple waterbody model of the Chehalis River in Washington, USA. The Chehalis River Basin is located in southwest Washington State (see Figure 25). The drainage area to the Chehalis River is over 2000 square miles, with area existing within five counties: Lewis, Thurston, Grays Harbor, Pacific, and Cowlitz (WADOE, 2001). The Chehalis River originates in Coast Range east of Willapa Bay, and also drains the western foothills of the Cascades and the southern Olympic Mountains. It ultimately flows into Grays Harbor and the Pacific Ocean, totaling over 125 miles in length.

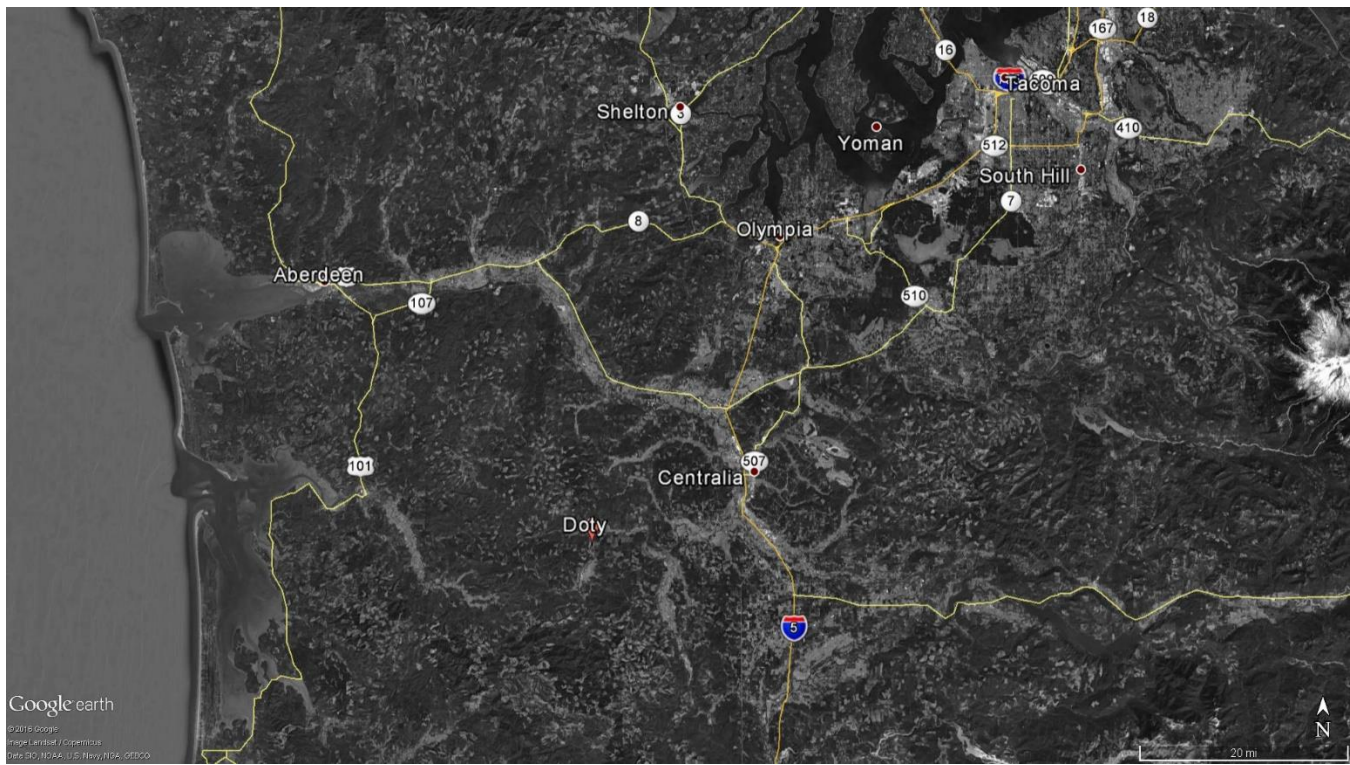


Figure 25. Chehalis River study area from near Doty, through Centralia to Aberdeen in southwestern Washington State (Google earth, 2017).

The Chehalis River was modeled from upstream of Pe Ell (river mile 108) to Porter, WA (river mile 33.3). Only the mainstem Chehalis River was modeled and was discretized into 10 model branches and 9 waterbodies. The physical characteristics of the river varied widely, and multiple branches allowed for separate characteristics (such as branch slope) unique to each branch to be implemented in the model. The upstream reaches had steep gradients with riffles and pools. It is the first 3 waterbodies or first 3 branches that were used in this example (see Figure 26). Table 8 shows the characteristics of each waterbody.

CALIBRATION

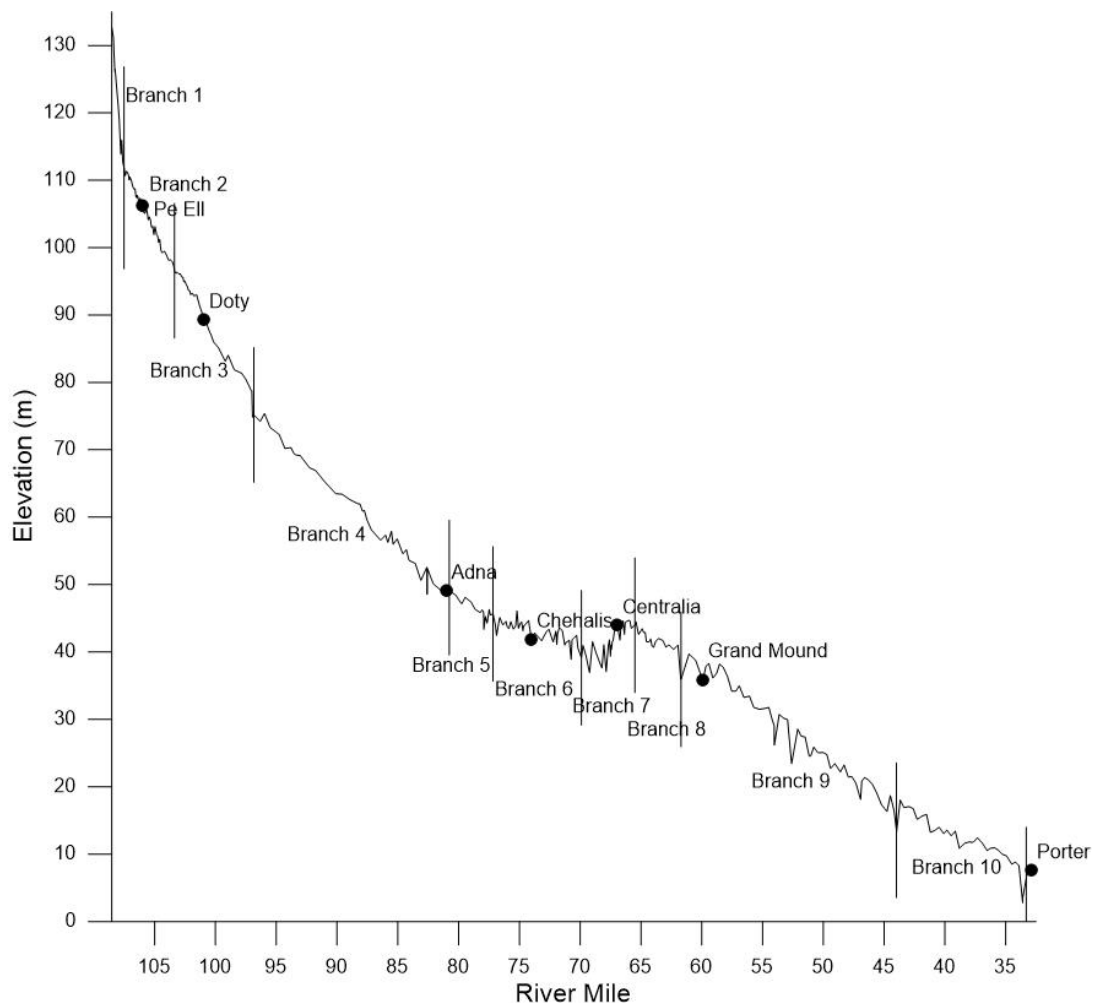


Figure 26. Longitudinal profile of the Chehalis River thalweg (vertical lines show model branch breaks). Only the first 3 branches were modeled in this example.

Table 8. Summary of waterbody and branch segments and layers for the 3 waterbodies in this example.

Water-body	Branch	Start-ing Ac-tive Seg-	End-ing Active Seg-ment	Num-ber of Seg-ments	Branch Length (m)	Num-ber of layers	Vertical layer Thick-ness (m)	SLOPE
1	1	2	6	5	2000	20	1	0.01600
2	2	2	21	20	8000	20	1	0.00200
3	3	2	30	29	11600	20	1	0.00200

For this example, follow the steps outlined in the User Manual Part 3 for using this model feature. The model user starts running the first waterbody, then starts running the second water body, then once output has stated in the second water body, the model user starts the third water body. The model waits until enough output has been generated by the upstream model before starting on the downstream models.

Each model waterbody runs on a different model processor. Overall this approach has saved considerable computational time compared to running the model all under one model environment.

Particle Tracking

This example is for a reservoir that has a particle release defined by the input file, "particle.csv". The User Manual Part 3 describes in detail the input file format and the model output files that describe the particle paths and histogram of the time history of the particles in terms of temperature, velocity and depth the particles experienced over time. This code also shows how to use the feature where the longitudinal eddy viscosity and diffusivity scale with the predicted longitudinal velocity, which affect the random movement of the particles in the x-direction.

The reservoir grid with one waterbody and 6 branches is shown in Figure 27. The side view of branch 1 is shown in Figure 28. The dam is located at the end of branch 1 at segment 64. A primary withdrawal is at segment 84 in branch 2. Hence, many of the particles released near the dam travel upstream into branch 2 to the withdrawal at segment 84.

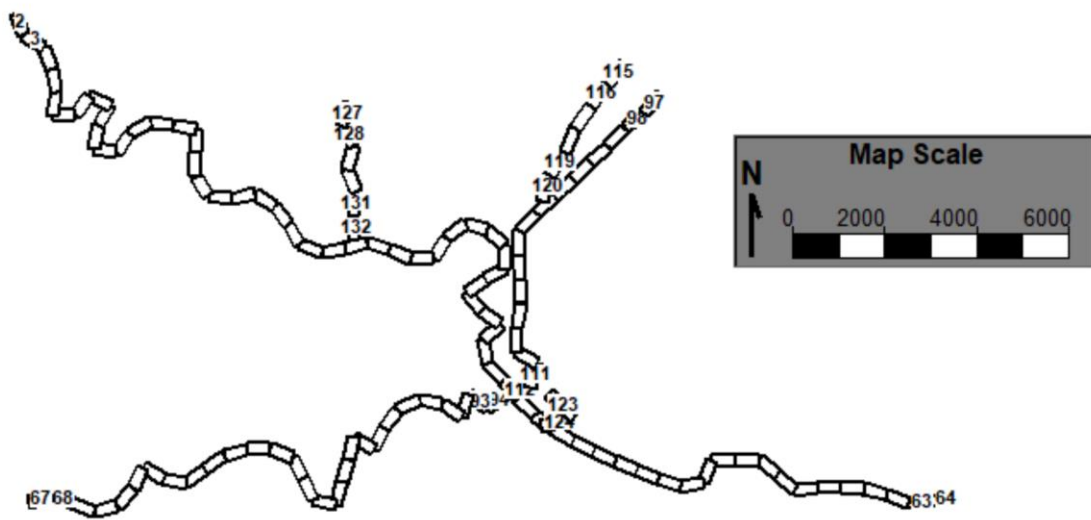


Figure 27. Particle tracking reservoir grid example.

CALIBRATION

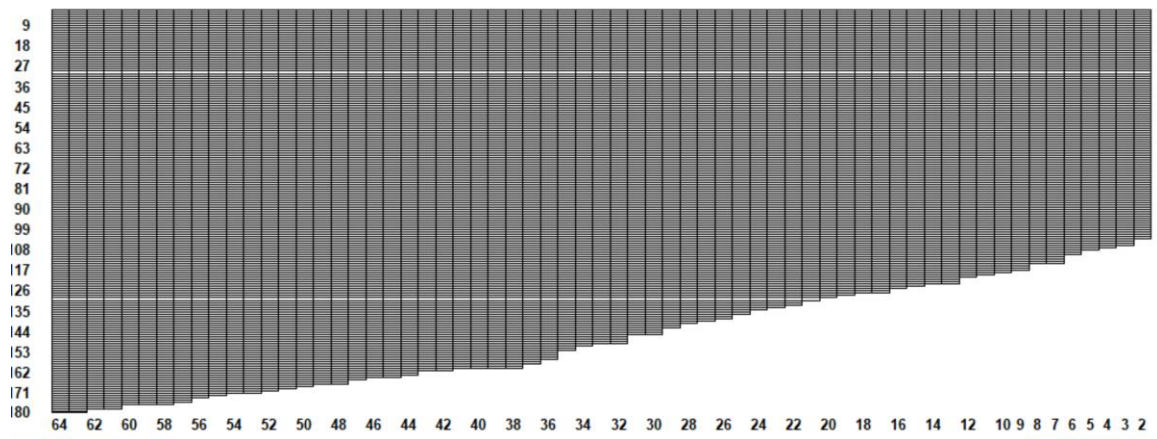


Figure 28. Side view of model grid for branch 1 in particle release example.

A typical example of using Tecplot to plot the particle paths is shown in Figure 29.

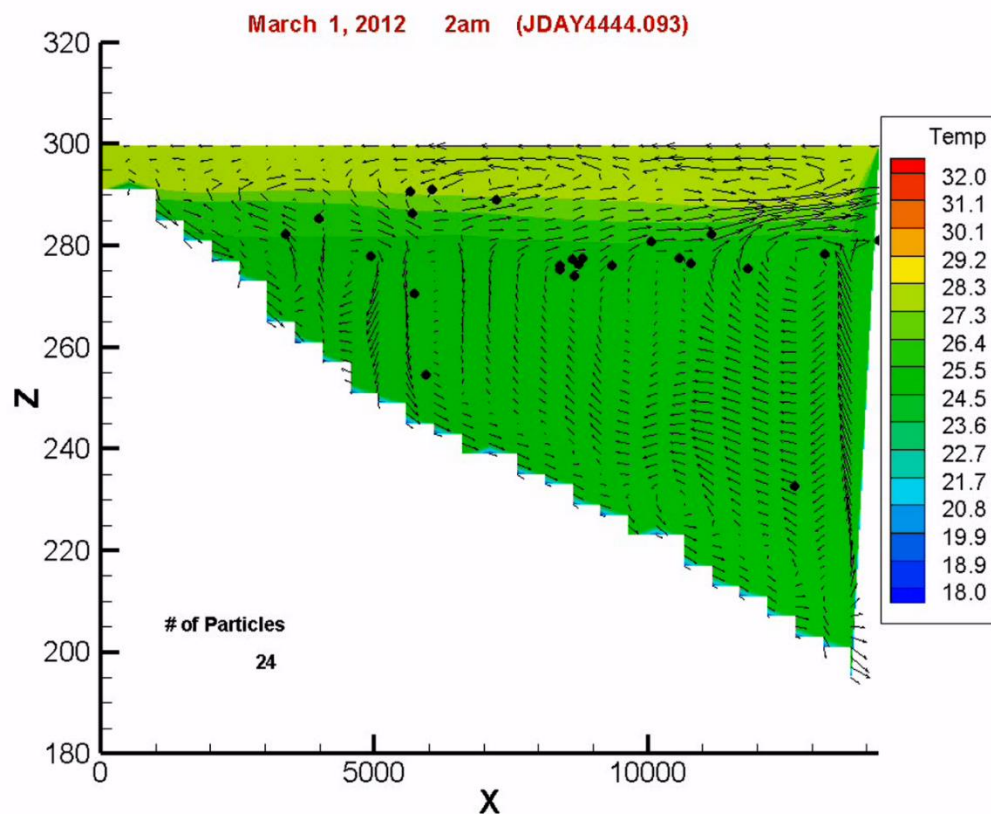


Figure 29. Branch temperature, velocity and particles in Tecplot frame.

Sediment Diagenesis Example

The sediment diagenesis model example plan view of the grid is shown in Figure 30. Figure 31 shows the side view of the main branch 1. The grid consists of 270 segments, 1 waterbody, 7 branches, and 43 layers of 1 m vertical grid spacing.

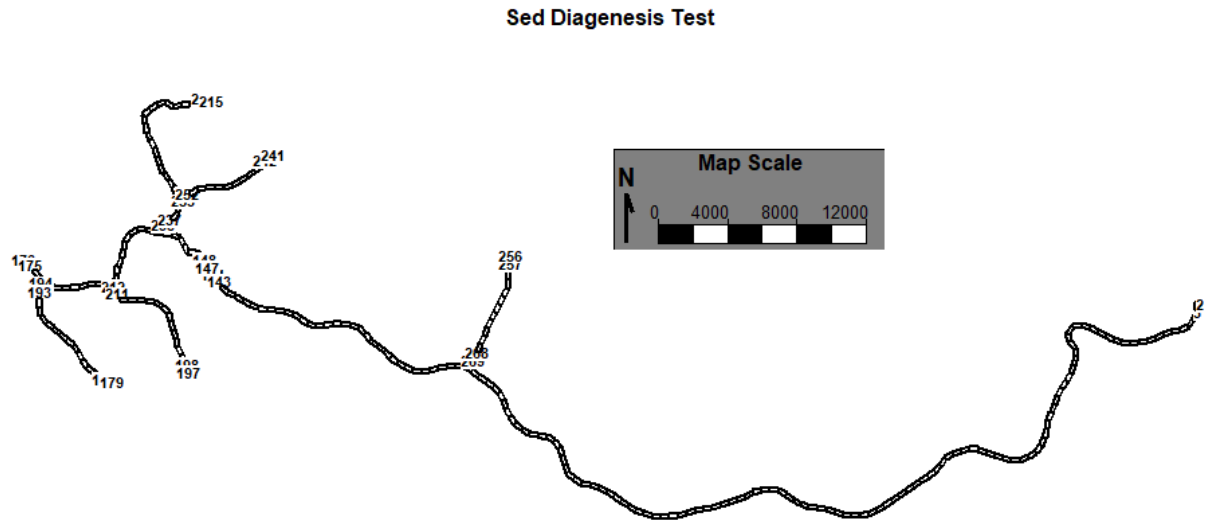


Figure 30. Sediment diagenesis model grid example.

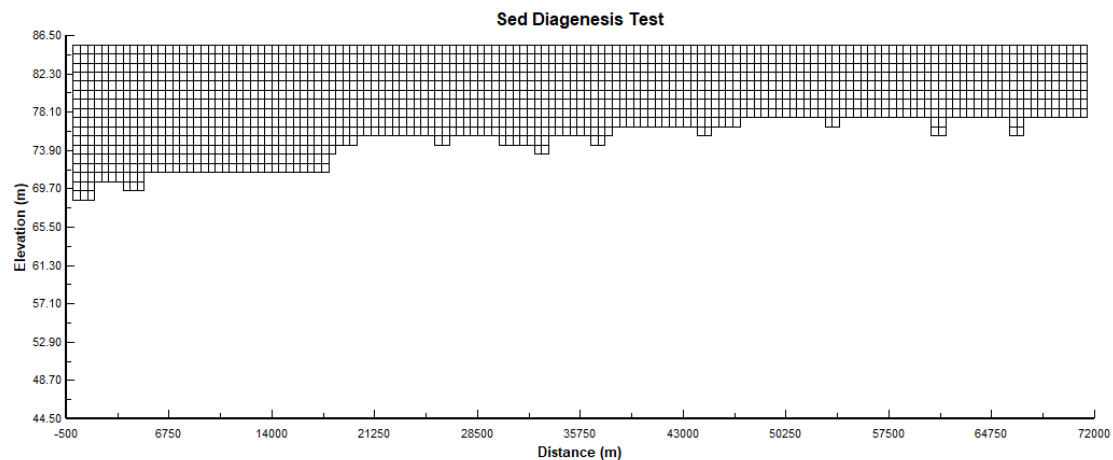


Figure 31. Side view of Branch 1 of sediment diagenesis example.

The file for setting up the sediment diagenesis example is `w2_diagenesis.npt` which is described in detail in the User Manual Part 3. Once a simulation is performed, a set of files (also described in User Manual Part

CALIBRATION

3) are output by the model to evaluate the sediment diagenesis model. Some of these output files are shown in Figure 32.

-  Diagenesis_CH4_Sediments.csv
-  Diagenesis_H2S_Sediments.csv
-  Diagenesis_POC_Sediments.csv
-  Diagenesis_PON_Sediments.csv
-  Diagenesis_POP_Sediments.csv
-  DiagenesisAerobicLayer.csv
-  DiagenesisBottomLayer.csv
-  DiagenesisBubbleReleaseSummary.csv
-  DiagenesisBubbles.csv
-  DiagenesisBubblesAtmosphereRelease.csv
-  DiagenesisConstituent.csv
-  DiagenesisSedDissGasOutput.csv
-  DiagenesisSedimentGasOutput.csv
-  DiagenesisSOD.csv
-  DiagenesisSODCSODNSOD.csv

Figure 32. Typical output files from the sediment diagenesis example.

Spokane River

This example shows how to use a river model and to explore the periphyton and river shading in the CE-QUAL-W2 model. The first example uses old input file formats, while the other example has csv format inputs.

The Spokane River reach between Upper Falls Dam (RM 74.1) and Nine Mile Pool (RM 62.0) is simulated in this example (Figure 33). The Spokane wastewater treatment plant is located at RM 67.4 (segment 27) and Hangman Creek is located at RM 72.4 (segment 11).

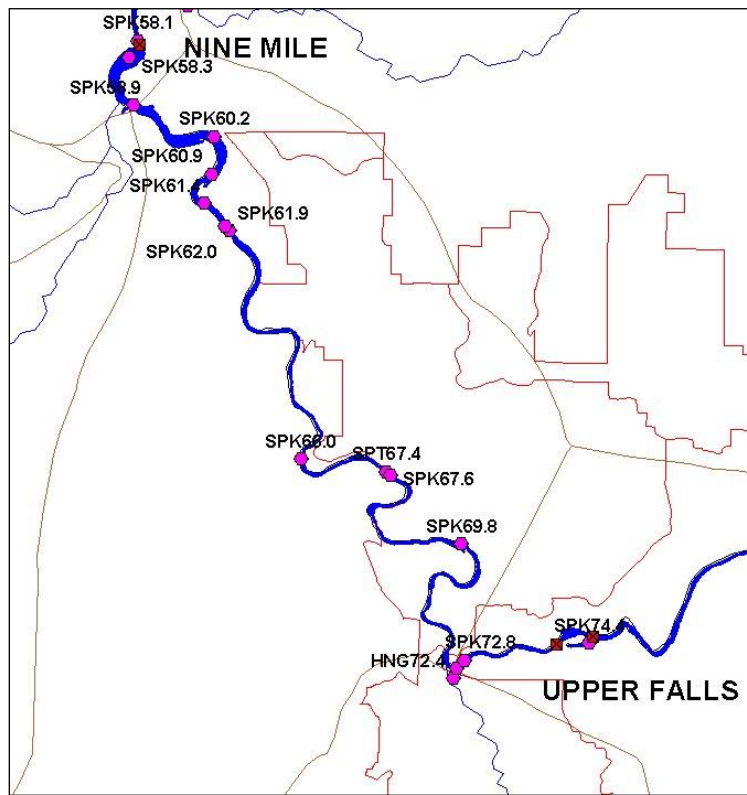


Figure 33. Spokane River between Upper Falls Dam and Nine Mile Dam.

The segments are oriented as shown in Figure 2 below. The side view of the grid is shown in Figure 3.

CALIBRATION

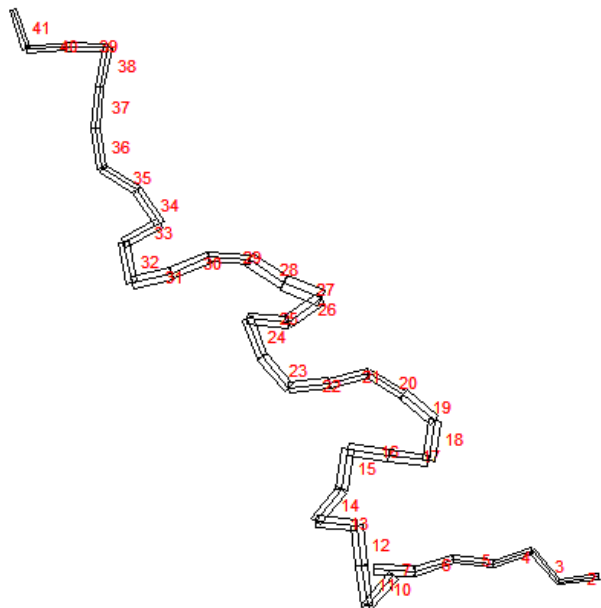


Figure 34. Model segment layout.

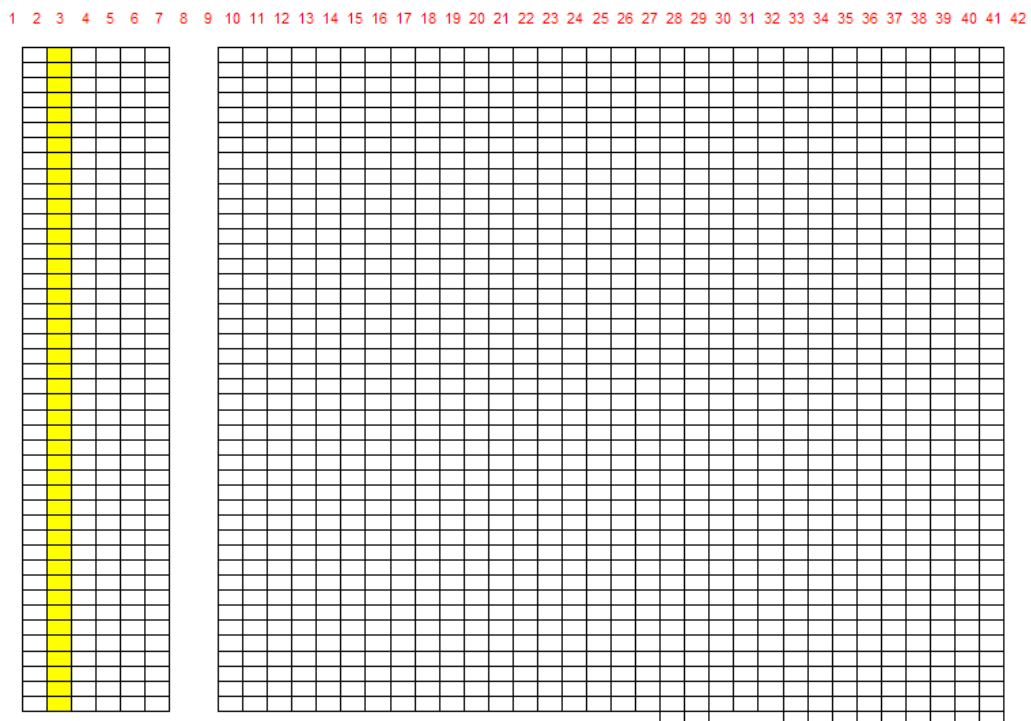


Figure 35. Model vertical layers for Spokane River model.

Tributary inputs are located at segments 11 and 27 representing a tributary Hangman Creek and the Spokane WWTP, respectively. A listing of model files and their description is shown in Table 9.

Table 9. Model files for the Spokane River example.

File Type	File Name	Description
control file	w2_con.csv from the Excel file w2_con_SpokaneRiver.xlsx	Model control file
bathymetry file	bth1.csv	Segment lengths, initial water surface elevation, segment orientation, layer thickness and cell widths
meteorological file	met.csv	Time series file containing temperature, dew point temperature, wind speed, wind direction and cloud cover data (based on solar radiation)
Wind sheltering file	wsc.csv	Wind sheltering coefficient for each segment and variable over time
Shade file	shade.csv	Shade file for characterizing vegetative and topographic shade or static shade values
Aerator input file	w2_aerate.npt	Input parameters for using aerator feature
Environmental Performance Criteria Input File	w2_envirprf.npt	Input parameters for specifying environmental performance criteria
Habitat volume input file	w2_habitat.npt	Input parameters for calculating habitat volumes
Selective withdrawal input file	w2_selective.npt	Input parameters for selective withdrawal feature
branch inflow files	qin_br8.npt	Flow rate file for branch 1 inflow
	tin_br8.csv	Temperature file for branch 1 inflow
	cin.csv	Concentration file for branch 1 inflow
tributary files	Hangq01.npt SPKwwtpq01.npt	Flow rate file for tributary 1 (Hangman Creek) Flow rate file for tributary 2 (Spokane wwtp)
	hangT01.npt SPKwwtp01.npt	Temperature file for tributary 1 Temperature file for tributary 2
	hangmanc.csv spokanewwtpc.csv	Concentration file for tributary 1 Concentration file for tributary 1
	qdt_br8.npt tdt_br9.npt	Flow rate file for distributed tributary 1 Flow rate file for distributed tributary 2
distributed tributary files	tdt_br8.npt tdt_br9.npt	Temperature file for distributed tributary 1 Temperature file for distributed tributary 2
	cdt8.csv cdt9.csv	Concentration file for distributed tributary 1 Concentration file for distributed tributary 2
	snp1.opt	Snapshot file
model output files	tsr_1_seg2.csv to tsr_7_seg41.csv	Time series files
	qwo, two, cwo files	Withdrawal output files at segment 10 and 41.
	Spokane.w2l	Binary output file for W2_Tool Post-Processor

CALIBRATION

SysTDG Columbia River – Bonneville Reservoir

This is an application on the Columbia River using the SYSTDG model for estimating the discharge TDG at Bonneville dam. The model consists of 1 waterbody, 1 branch, and 77 model segments as shown in Figure 36. The main branch 1 of the Columbia River side view is shown in Figure 37.

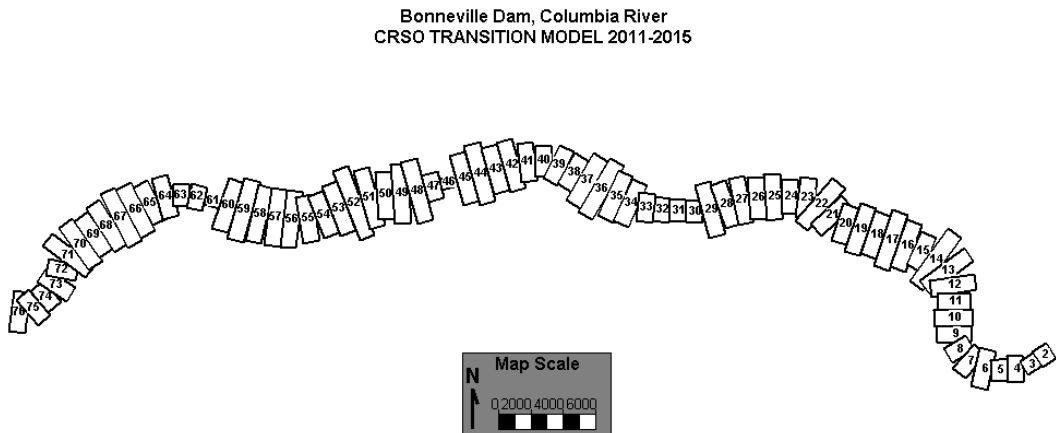


Figure 36. Bonneville pool CE-QUAL-W2 model.

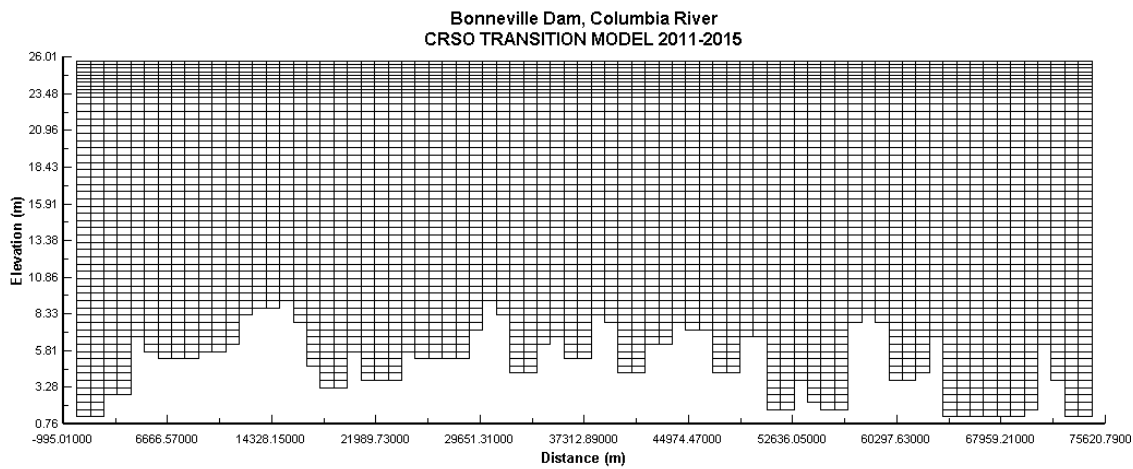


Figure 37. Side view of Bonneville pool in the Columbia River.

This example illustrates how to turn on TDG and use the state variable N2 gas and O2 gas to predict TDG gas concentrations in the pool area and at the dam as a result of spillway operation. The special input file, w2_systdg.npt, is described in the User Manual Part 3. The SysTDG algorithm only operates on gates. Hence, gates were used for the spillways and power house withdrawals since specified flows can be prescribed for a gate just as a withdrawal or structure.

3. Examples of Model Applications – Tom Cole

This first section was written by Tom Cole, retired Environmental Laboratory, Waterways Experiments Station, and includes a useful information on modeling in general and in using the CE-QUAL-W2 model. He provides an overview of using the model and going through a calibration process for a reservoir, estuary and a river system.

Model Preparation

Input checks. A preprocessor program, pre.exe, performs checks of the control file for many errors that can be detected by the preprocessor. Errors are written to the file [PRE.ERR](#) and warnings are written to the file [PRE.WRN](#). If no errors are detected, then input from the control file is written to the file [PRE.OPT](#). All errors should be corrected before proceeding any further. Warnings should be investigated to ensure that what is being input into the model is what is intended. The preprocessor should be run periodically during the calibration phase to ensure that errors have not been introduced into the input files. However, do not assume that all is necessarily well if no warnings or errors are reported.

Additionally, the user should check preprocessor output against inputs to ensure they are correct. Further evaluation of control file input data must be performed by the user to ensure data the user thinks he has input into the model is what the model is actually receiving. Additionally, *all* time-varying input data should be plotted and screened for errors. These plots will need to be included in any final report and can eliminate a number of problems early on in the project.

Calibration

The next step is to begin calibration runs. Much of the literature refers to this step as calibration and verification in which model coefficients are adjusted to match an observed data set (calibration) and then the model is run on another “independent” data set without adjusting model coefficients to see if the model reproduces observed data in the prototype (verification in most circles, but variously called confirmation, validation, substantiation, etc. as numerous water quality modelers object to the word verification).

This separation is artificial and wrong. If a model does not reproduce observed data (and, more importantly, trends in data) for the “verification” data, then any good modeler will adjust coefficients, review model assumptions, include new processes, or collect additional data to adequately match both sets of data. Often, application to additional sets of data improves the fit to the first. The artificiality of this concept has led to applications in which modelers have used May, June, and July data for “calibration” and August, September, and October data of the same year for “verification” so they can state the model has been “calibrated/verified”.

The following examples will further illustrate the artificiality of the current concept of “calibration/verification”. Consider the following summary of observed data.

CALIBRATION

Year	Flow	Stratification	Fall algal bloom	Minimum DO at dam
1989	high	weak	yes	0 ppm
1990	low	strong	no	3 ppm
1991	average	medium	yes	1 ppm
1992	average	medium	yes	1 ppm
1993	low	strong	yes	1 ppm
1994	high	weak	no	3 ppm

Based on the currently accepted definition of calibration/verification, which of the years should be chosen for calibration and which should be chosen for verification? A case could be made for 1989 for calibration and 1994 for verification because of a fall phytoplankton bloom in 1989 and its absence in 1994. Additionally, the minimum dissolved oxygen at the dam was different between the years. If the model were to reproduce this behavior, then confidence could be placed in the model's ability to reproduce dissolved oxygen and phytoplankton blooms for the correct reasons. However, both years were years of high flow and using them would not test the model's ability to reproduce prototype behavior under different flow regimes.

Cases could be made for other combinations of calibration/verification years and different modelers would probably choose different calibration/verification years, so there doesn't appear to be one "correct" answer. In actuality, there is a correct answer. Model all the years and model them continuously. Modeling them continuously would eliminate separate calibration and verification years or data sets so the model could not be considered "calibrated and verified". However, if the model reproduces the wide variation in prototype behavior between all the years, a lot more confidence can be placed in the model's ability to reproduce prototype behavior for the "right" reasons than if the model were calibrated for one year and verified for another year.

Another example of the problems with the currently accepted "calibration/verification" approach to establishing model credibility is illustrated in the following table.

Year	Dominant algae	Flow	Minimum DO at dam
1979	diatoms	average	5 ppm
1986	greens	average	3 ppm
1994	bluegreens	average	0 ppm

Which year should be used for calibration and which year should be used for verification? Again, the best approach would be to model all three years, but since data do not exist for all the intervening years from 1979 to 1994, the simulation could not be continuous. An analysis of the data indicates a clear progression of eutrophication from 1979 to 1994 based on phytoplankton progression and increasing hypoxia. According to the current concept of "calibration/verification", all kinetic coefficients should be the same for all simulation years. However, the different dominant phytoplankton groups will have different growth, mortality, respiration, excretion, and settling rates and different light and nutrient growth rate half-saturation constants between the years. Keeping these values constant between calibration years would be inappropriate if only modeling one algae group. With multiple algae groups this would be a good test of the model's ability to model algal succession.

Additionally, the sediment oxygen demand has clearly changed because of eutrophication, so the values used in the zero-order sediment compartment should be different for the three years if the modeler only used the zero-order model. This highlights a weakness of this approach since it does not change over time. The model though can use the first order and sediment diagenesis models which over this limitation. As

can be seen from just these two examples, all years should be considered calibration years and rate coefficients in some cases should change between different calibration data sets if the prototype is to be represented accurately.

Another concept associated with “calibration/verification” of a model is a post audit. Post audits are recommended whenever management changes are made as a result of modeling studies. A post audit involves making the management changes and then collecting data to see if the hoped for changes in prototype behavior based on model guidance have taken place. This appears to be a very reasonable concept and straightforward test of a given model’s simulation capabilities and, if the hoped for changes occur, then a great deal of confidence can be placed in the model’s simulative capabilities.

But what if the changes in water quality such as an improvement in minimum dissolved oxygen or extent of hypoxia does not occur? Can one then conclude that the model is not very good and little confidence can be placed in model results? The answer is no and the reason why is that no model can be used to predict the future. A model can only be used to determine what might have occurred if a particular set of boundary forcing functions were to occur in the prototype.

For example, hypoxia in Chesapeake Bay is a result of not only nutrient and organic matter loading, but also the degree of stratification that inhibits vertical mixing and reaeration. The degree of stratification is in large part a function of freshwater inflow. The higher the inflow, the greater the areal extent of density stratification in the Bay resulting in a greater areal extent of hypoxic waters. Suppose a model of the Bay “predicted” that a 40% nitrogen loading reduction decreased the areal extent of hypoxia by 20%. Based on this result, loadings were then reduced by 40% for five years and hypoxia did not decrease but actually increased during this time period.

Since the exact opposite occurred from what the model predicted, can the modeling study be concluded to be a failure? The answer is no. Suppose that the model results assume average freshwater river inflows and the five years after implementing loading reductions were high flow years, which increased the extent of hypoxia compared to an average flow year due strictly to physical effects. The only way to tell if the conclusions based on the model study were erroneous would be to model the five years using observed boundary conditions for this period and see if the model reproduced the observed increase rather than decrease in hypoxia. Thus, if a post audit yielded water quality different from expected water quality based on model results, this has no reflection on a given model’s ability to reproduce water quality in the prototype. Again, models cannot be used to predict the future, only what might have been.

Ideally, calibration should involve multiple data sets encompassing as many variations and extremes as possible in the prototype. A model’s ability to reproduce prototype behavior under a variety of conditions gives the modeler more confidence in the model’s ability to accurately simulate the prototype under proposed conditions. To put it very simply, a model is a theory about behavior in the real world. A theory is continuously tested against ***all*** observed data, and, if it does not match the data, then the theory should either be modified or a new one developed that more closely agrees with observed data.

Model data/comparison. The model produces the following output files for displaying results:

1. **[Profile file \[PRFFN\]](#)**. This file was used to plot observed versus predicted vertical profiles for temperature and constituents at a given segment. It is rarely used for this now. See the spreadsheet output file instead for plotting up profile data.
2. **[Time series file \[TSRFN\]](#)**. This file is used to plot time histories of water surface elevations, flows, temperatures and constituent concentrations for user specified computational cells.

CALIBRATION

This file also contains information to plot out the time history of the variable timestep and average timestep.

3. [**Contour plot file \[CPLFN\]**](#). This file is used to plot contours of temperature and constituents along the waterbody length.
4. [**Vector plot file \[VPLFN\]**](#). This file was used to plot velocity vectors determined from horizontal and vertical velocities in model versions up to and including Version 3.6. Since Version 3.7, this file is used by the W2Tools post-processor to output all information of a model run in order to produce contours, profiles, velocity vectors, time series, contour animations, and model-data comparisons.
5. [**Spreadsheet file \[SPRFN\]**](#). This file is similar to the profile except the output is suitable for importing into a spreadsheet type database for subsequent plotting.
6. [**Withdrawal output files \[WDOFN\]**](#). For each water withdrawal the model outputs the flow, temperature, and concentration of any water withdrawal over time.

A description of the output from each file and how to use the information is given Part 3 of the User Manual. The current release version requires the user to develop plotting capabilities from these files. This is most often done using the [**spreadsheet output file**](#) and [**time series output file**](#) and developing macros to process the data.

Calibration is an iterative process whereby model coefficients are adjusted until an adequate fit of observed versus predicted data is obtained. Unfortunately, there are no hard and fast guidelines for determining when an adequate fit is obtained. The user must continually ask himself "is the model giving useful results based on model formulations, assumptions and input data?". If it is not, then the user must determine if the inability of the model to produce useful results is due to the use of the model in an inappropriate manner (i.e., hydrostatic approximation is invalid, one phytoplankton group is not sufficient to capture phytoplankton/nutrient/DO interactions, wind speed function for evaporation is inappropriate for the waterbody, etc.), model formulations are insufficient to describe known prototype behavior, or if input data are insufficient to describe the system dynamics.

Another important point to keep in mind during calibration is that a model may give inadequate results for a given spatial and/or temporal scale, but at another scale may reasonably represent the dynamics of the prototype. For example, the model may fail to predict a short-term phytoplankton bloom using monthly inflowing phytoplankton and nutrient concentrations but may adequately represent phytoplankton production over the summer stratification period. The model may thus be useful in determining a waterbody's long-term response to nutrient loading reductions but be inadequate in addressing short-term responses to a nutrient reduction strategy. In summary, it is not always necessary for model output to match all of the observed data for the model to provide meaningful results.

The usual sequence for calibration is to first calibrate the water budget (or water surface elevation), then calibrate temperature (preferably salinity for estuarine applications), and finally water quality. Keep in mind water quality calibration can affect temperature/salinity calibration. A description of each follows. Calibration is separated into different sections for river, lake/reservoir, and estuarine applications.

Lake/Reservoir

Water budget

The water budget is checked by comparing predicted elevations with observed elevations. Errors in the water budget are generated by the following:

1. **Incorrect bathymetry.** The user should carefully check the volume-area-elevation table produced by the model to ensure it closely matches the project volume-area-elevation table. If it does not, then the bathymetry should be checked carefully to ensure there are no errors. In some cases, additional sediment range surveys may be necessary to adequately define the bathymetry. It may also be necessary to include branches that were not included in the initial bathymetry. Also, keep in mind that development of the original volume-area-elevation table was subject to the same errors used in developing the volume-area-elevation table for the application. In some applications, the new volume-area-elevation table was deemed more accurate than the original.
2. **Storm events.** Errors in the water budget due to storm events can be determined by comparing predicted with observed elevations using output from the time series plots. If the error is generated during storm events, then the user should check to see if precipitation must be included and/or if more tributaries need to be included than were originally specified. The user may need to use a hydrologic model to determine inflows during storm events for ungaged tributaries. An alternative method is to apportion inflows for ungaged tributaries based on their watershed areas.
3. **Incomplete inflow data.** A substantial amount of inflow is often unaccounted for when using gauged inflows. The unaccounted inflows can include minor tributary, precipitation, stormwater, and wastewater treatment plant contributions. The distributed tributary option provides the user with a means to account for these contributions. This option distributes inflows into every branch segment weighted by the segment surface area.
4. **Evaporation.** If evaporation in the region is significant and is not accounted for in inflows, then it should be included using the evaporation option [\[EVC\]](#).
5. **Seepage.** Seepage gains or losses can be significant for some waterbodies. The model user can specify a withdrawal or a low level structure to simulate losses at a dam face. Several applications required specifying seepage losses through the dam in order to properly calibrate temperature.
6. **Inaccurate Inflow/Outflow Measurements.** Gauged inflows and reservoir outflows are notoriously inaccurate with typical measurement errors of 5-10%. The model is very sensitive to inflow/outflow error measurements that can result in significant errors in water level predictions.

Typically, the user will first plot observed versus predicted water surface elevations for the simulation period after all the inflow/outflow data have been collected and the model is running to completion. The latest version contains a program for computing reservoir water balances that will initially compute the additional flows necessary for reproducing observed water surface elevations, but it will not normally generate a perfect water balance. The computed flows can then be manually adjusted to more closely match observed water surface elevations. Normally, the computed flows are initially incorporated using the distributed tributary option in the model with interpolation turned off so that the model sees the flows as a step function since this is how the flow is computed by the utility. Using this option, the flows necessary to compute the water balance are distributed into the surface layer weighted according to segment surface area.

Keep in mind that this method only provides the necessary flows to complete the water balance. The user must decide how to incorporate them into the model in a realistic fashion as the method of incorporation can have a large impact on temperature and water quality calibration – another fork in the road in the “art” of water quality modeling. The recommended procedure is to first plot up and analyze the computed flows to see if they provide any information as to the source of the error.

CALIBRATION

For example, if the majority of the computed flows are negative and the inflows are deemed accurate, then this would indicate that the outflow has been underestimated. It could be due to seepage into groundwater or seepage through the dam. If the hypolimnetic temperatures were also being underpredicted, which would indicate that the hypolimnetic residence time was being overpredicted, then incorporating the computed flows into an additional outflow could solve both problems at once. The point to be made is that various methods of incorporating the computed flows during temperature and water quality calibration should be tried to determine if they have an effect on temperature or water quality. Whichever method improves the calibration is the method to use. The following plot illustrates the accuracy normally expected for a reservoir water surface elevation calibration. The computed elevations overlay the observed elevations.

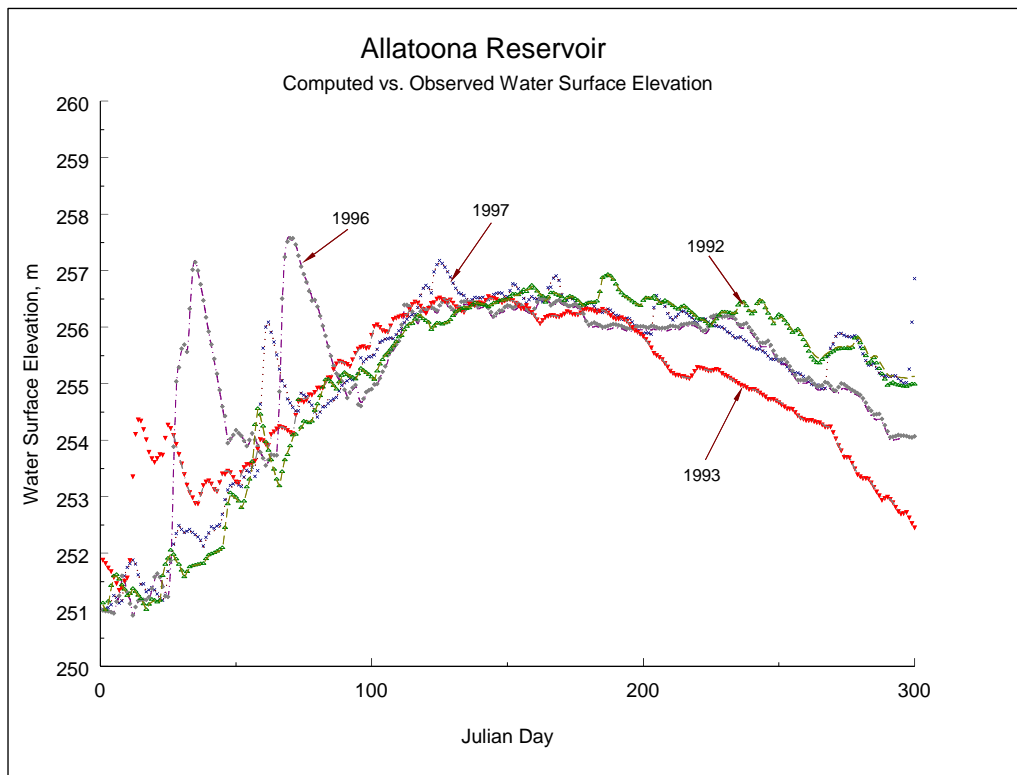


Figure 38. Allatoona Reservoir computed (lines) vs. observed (symbols) water surface elevations for 1992, 1993, 1996, and 1997.

Hydrodynamics and Temperature

The earliest one-dimensional mechanistic reservoir models included only temperature. As a result, temperature was the only model prediction that could be used for hydrodynamic calibration. Since temperature is affected by surface and bottom heat exchange and is therefore nonconservative, it is not the best parameter for calibrating hydrodynamics. Salinity, which is conservative, has historically been considered the ideal constituent for hydrodynamic calibration. However, this is generally feasible only for estuarine applications where salinity is routinely monitored. Dissolved solids are not conservative and are generally *not* a good substitute for salinity during calibration except in waterbodies where the conservative assumption is appropriate. The previous three sentences echo the prevailing sentiment of hydrodynamic modelers.

In reality, there is no “ideal” constituent that should be used for hydrodynamic calibration. Each constituent can contribute knowledge about the system and can have an impact on the hydrodynamic calibration.

Experience has shown that dissolved oxygen and phytoplankton are often much better indicators of proper hydrodynamic calibration than either temperature or salinity. There are several reasons for this. First, gradients in dissolved oxygen and phytoplankton are often present at different locations in the water column than either temperature or salinity gradients. Consequently, they can provide additional information as to the correctness of the hydrodynamic calibration beyond either temperature and/or salinity alone. Second, dissolved oxygen is much more dynamic than either temperature or salinity and readily responds to wind events including seiching, with the anoxic zone often moving several kilometers over a day in response to the hydrodynamics. Phytoplankton distributions are also affected by the hydrodynamics. Further discussion and examples will be presented in the section on water quality calibration. Nevertheless, temperature and/or salinity should always be the first step during hydrodynamic calibration, with the hydrodynamic calibration further refined during water quality calibration.

Computed velocities can be compared with velocity and flow measurements obtained from an acoustic Doppler current profiler (ADCP) to additionally evaluate the model’s hydrodynamic performance. However, care must be taken when comparing model velocities with observed velocities to ensure ADCP measurements are comparable to the laterally averaged velocities generated by the model.

Coefficients affecting temperature and their default values are given in [Table 10](#). The eddy viscosities, Chezy coefficient, and wind sheltering coefficient directly affect hydrodynamics that affect heat and constituent transport. The remaining coefficients directly affect temperature that affects hydrodynamics. Of these, the last two coefficients affect temperature only if constituents are modeled. See Part 3 of the User’s Manual for a more detailed description of these coefficients and their effects.

Table 10. Coefficients affecting thermal calibration

Coefficient	FORTRAN Name	Default
Longitudinal eddy viscosity	[AX]	$1 \text{ m}^2 \text{ sec}^{-1}$
Longitudinal eddy diffusivity	[DX]	$1 \text{ m}^2 \text{ sec}^{-1}$
Chezy coefficient or Manning’s n	[FRICT]	$70 \text{ m}^2 \text{ sec}^{-1}$ or 0.035
Wind sheltering coefficient	[WSC]	Calibration parameter
Solar radiation absorbed in surface layer	[BETA]	0.45
Extinction coefficient for pure water	[EXH20]	0.45 m^{-1}
Extinction coefficient for inorganic solids	[EXINOR]	0.01 m^{-1}
Extinction coefficient for organic solids	[EXORG]	0.2 m^{-1}

In addition to the above coefficients, temperature predictions are also affected by the surface heat exchange algorithm specified, mainstem and tributary inflows, inflow temperatures and their placement, outlet and withdrawal specifications, the numerical solution scheme, and bathymetric and meteorological data. Again, always represent the prototype as accurately as possible.

CALIBRATION

Applications on over 400 waterbodies under a wide variety of conditions have shown the model generates remarkably accurate temperature predictions using default values when provided accurate geometry and boundary conditions. The wind-sheltering coefficient [WSC] has the most effect on temperature during calibration and should be adjusted first. Previous applications varied the wind sheltering coefficient from 0.5-0.9 for mountainous and/or dense vegetative canopy and 1.0 for open terrain. In a very few cases, the wind-sheltering coefficient [WSC] has been increased above 1.0 to account for funneling effects on systems with steep banks (or when measured wind data do not reflect the wind field on the lake). The user should also run sensitivity analyses on the other coefficients to gain a "feel" for how they affect temperature predictions.

Calibration problems. Difficulties during temperature calibration can often be traced to the following:

1. **Inflows and Inflow temperatures.** Accurate inflows and inflow temperatures are desirable for all applications, but they are critical for waterbodies with short residence times or during high inflow periods. Temperature calibration will be difficult using monthly inflow temperatures for a waterbody with a one week residence time. Methods exist for generating more frequent inflow temperatures based on flow and meteorological data (Ford and Stein, 1986), but there is no substitute for actual measurements.
2. **Meteorological data.** Many difficulties are associated with extrapolating weather station meteorological data to a waterbody site. Weather stations are typically located in different terrain and at large distances from the prototype. Frontal movements can occur at different times over the waterbody and meteorological station resulting in model predictions that are in closer agreement either earlier or later than the actual comparison date. Methods for addressing these problems include adjustment of the wind sheltering coefficient [WSC], use of an alternative meteorological station, averaging data from several meteorological stations, separating a waterbody into regions applying data from different meteorological stations, and comparison of observed data using model output either before or after the observed date. If the user has the luxury of obtaining calibration data before applying the model, portable weather stations exist which can be deployed on the waterbody. Obviously, this is the preferred method.
3. **Outflow data.** The addition of the selective withdrawal algorithm in Version 2.0 has reduced many of the previous problems of accurately representing outflows. However, problems still arise. In the application of CE-QUAL-W2 to Bluestone Reservoir, Tillman and Cole (1994) were unable to reproduce observed temperature stratification without limiting the lower withdrawal layer. Subsequent investigation showed that withdrawal was limited by trash accumulation that effectively acted as a submerged weir. This was a problem generated by inadequate knowledge of the prototype and not a problem with the model. Indeed, this is an example of a model giving insight into the behavior of the prototype.
4. **Bathymetry.** Several previous applications of the model encountered difficulties during temperature calibration until the bathymetry was revisited. Check the assumptions made during the development of the bathymetry to ensure they are not the source of the problem. Starting points include grid resolution that affects the models ability to define sharp thermal gradients and bottom slope, volume-area-elevation accuracy that can have a marked effect on hypolimnetic temperatures since the volumes are generally small near the bottom, and water surface areas that affect the area available for surface heat exchange. Branch definition has also been found to have an effect on temperature predictions.

In order to illustrate how accurate reservoir temperature modeling has become with CE-QUAL-W2, [Table 11](#) lists calibration results for 70 reservoir thermal simulations. The statistic presented is the absolute mean error (AME) computed as follows:

$$AME = \frac{\sum |Predicted - Observed|}{\text{number of observations}}$$

Although a number of other statistics have been used when evaluating model results, the AME provides the best indication of model performance since it is directly interpretable. For example, an AME of 0.5°C means that the model results are, on the average, within 0.5°C of the observed data. As can be seen, model predictions for all the reservoirs are within 1°C and most of them are much less.

Table 11. Reservoir thermal simulations with error statistics for station closest to dam.

	Reservoir	# years	AME, °C		Reservoir	# years	AME, °C
1	Allatoona	4	0.6	36	Monroe	4	0.7
2	Alum Creek	1	0.5	37	Neely Henry	2	0.6
3	Barkley	1	0.5	38	Neversink	3	0.4
4	Bluestone	2	0.5	39	Norman	3	0.7
5	Brownlee	2	0.6	40	Oxbow	1	0.3
6	Bull Run 1	2	0.5	41	Oahe	2	0.9
7	Bull Run 2	2	0.7	42	Occoquan	1	0.9
8	Burnsville	1	0.9	43	Paint Creek	1	0.4
9	Caesar Creek	1	0.6	44	Paintsville	1	0.4
10	Cannonsville	5	0.7	45	Patoka	3	0.7
11	Cave Run	4	0.8	46	Pepacton	3	0.6
12	C.J. Strike	2	0.7	47	Pineflat	5	0.6
13	Croton	1	0.7	48	Powell	1	0.7
14	Cumberland	1	0.5	49	J. Percy Priest	3	0.8
15	Deer Creek, OH	1	0.4	50	Quabbin	1	0.7
16	Deer Creek, ID	5	0.8	51	Richard B. Russell	3	0.5
17	DeGray	8	0.9	52	Rhodiss	2	0.6
18	Fishtrap	1	0.8	53	Riffe	1	0.7
19	Fort Peck	2	0.7	54	Rimov	1	0.5
20	Francis Case	2	0.7	55	Rondout	3	0.5
21	Herrington	1	0.7	56	Sakakawea	2	0.7
22	Hickory	1	0.5	57	Schoharie	2	0.8
23	J.W. Flanagan	1	0.5	58	Shasta	1	0.6
24	Jordanelle	3	0.7	59	Shepaug	1	0.6
25	J. Strom Thurmond	5	0.9	60	Stonewall Jackson	2	0.5
26	James	1	0.6	61	Toledo Bend	1	0.7
27	Houston	6	0.5	62	Taylorsville	2	0.9
28	Lanier	2	0.9	63	Tolt	1	0.5
29	Loch Raven	1	0.9	64	Travis	1	0.3
30	Long Lake	1	0.5	65	Wabush	1	0.6
31	Lost Creek	1	0.6	66	Wachusett	4	0.7
32	Maumelle	2	0.7	67	Weiss	2	0.6
33	Mayfield	1	0.6	68	West Point	3	0.8
34	Moehnetaisperre	1	0.4	69	Walter F. George	2	0.6
35	Mountain Island	1	0.7	70	Youghiogheny	2	0.8

The following examples illustrate CE-QUAL-W2's ability to reproduce observed temperatures on a variety of systems with widely varying temperature regimes. On all plots, x's represent observed data and their widths are scaled to represent $\pm 0.5^\circ\text{C}$. The dotted lines represent computed model values. The absolute mean error (AME) and root mean square error (RMS) are also included for each date in order to help in interpreting the predictive capability of the model. These statistics should always be included in plots of computed versus observed data since plots can often be misleading depending upon the scale of the x and

CALIBRATION

y axes and the size of the marker used to represent the observed data (a common technique used to make model results appear better than they actually are).

Pineflat Reservoir. Pineflat Reservoir is located in California near the base of the Sierra Madre mountain range. One of its primary uses is for providing irrigation water during the summer growing season. Consequently, the reservoir is drawn down as much as 70 m over the summer during drought years. The model was used to provide operational guidance for a temperature control device that will be installed in the reservoir to optimize the storage of cold water for downstream releases at the end of summer.

[Figure 39](#) shows the results of temperature predictions for 1989. The thermal regime exhibits two thermoclines starting in early spring. As can be seen, the reservoir was drawn down over 40 m during the summer. During 1993, the development of the two thermoclines was delayed until the end of summer ([Figure 40](#)). CE-QUAL-W2 correctly captured the thermal regimes for both years and the differences in the thermal regimes between the two years.

Sensitivity analyses showed that temperature predictions were very sensitive to inflow temperatures. Calibration consisted of adjusting inflow temperatures to more closely match in-pool temperature profiles. Because calibration showed the importance of accurate inflow temperatures in order to properly calibrate the model, additional fieldwork was done to obtain accurate inflow temperatures. During this effort, it was discovered that the location where inflow temperatures were taken showed a lateral variation in the river of over 5°C due to hypolimnetic discharges from an upstream reservoir that did not completely mix laterally. Additionally, during extreme drawdown, it was shown that inflow temperatures increased by nearly 2°C from measured temperatures as the upstream boundary of the model moved downstream approximately 10 km due to the large drawdowns that the reservoir was periodically subjected to.

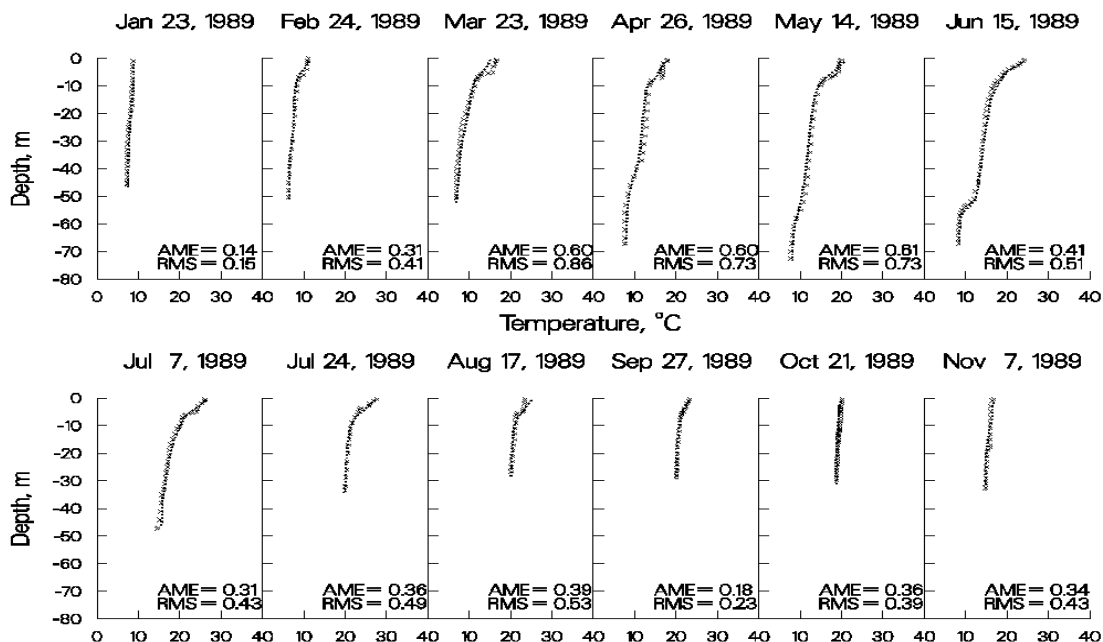


Figure 39. 1989 Pineflat Reservoir computed versus observed temperatures.

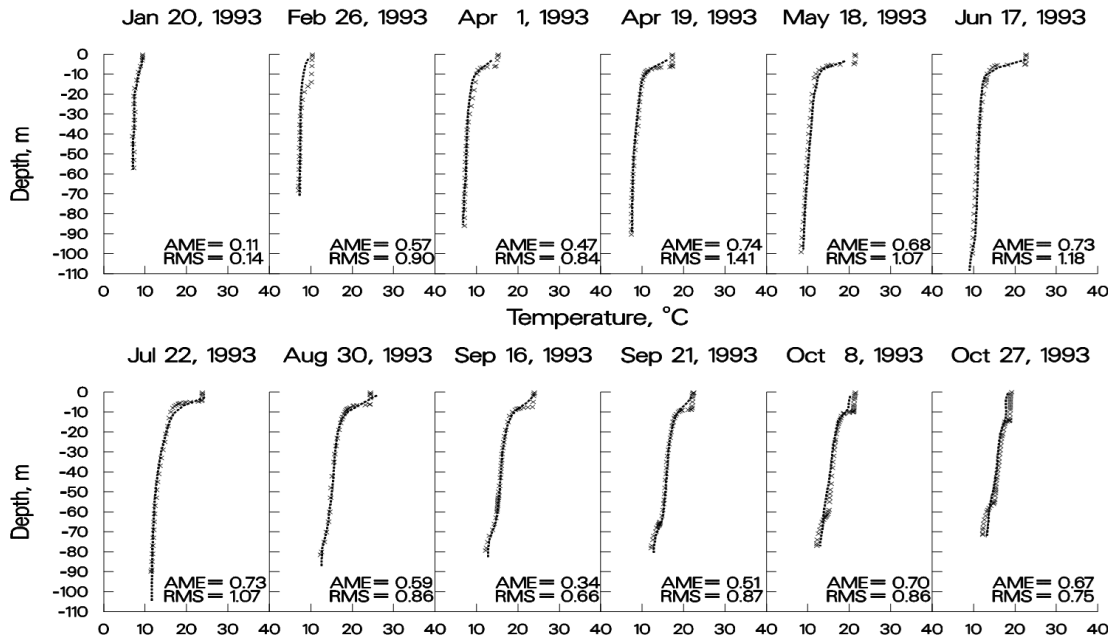


Figure 40. 1993 Pineflat Reservoir computed versus observed temperatures.

Bluestone. Bluestone Reservoir is located in the mountains of West Virginia. The reservoir has an average hydraulic retention time of less than a week during the summer. When first calibrating for temperature, the model predicted essentially no thermal stratification during the summer whereas the observed data showed strong stratification beginning at a depth of about eight meters. Based on the short residence time during the summer, model predictions seemed quite reasonable. However, stratification was present in both 1981 and 1983 indicating that stratification was not a rare occurrence.

A number of mechanisms were proposed to explain the observed stratification including groundwater seepage and extreme wind sheltering. Including these in the model did not result in any improvements in model predictions. Finally, the lower limit of selective withdrawal was set at the depth corresponding to the outlet elevation. Results of the simulation are shown in [Figure 41](#) and [Figure 42](#). Subsequent investigations at the reservoir revealed that accumulated debris at the level of the trash racks was acting like a submerged weir that limited the bottom of the withdrawal zone to the elevation of the trash racks. This is an example of a model providing insight into previously unknown behavior of the prototype.

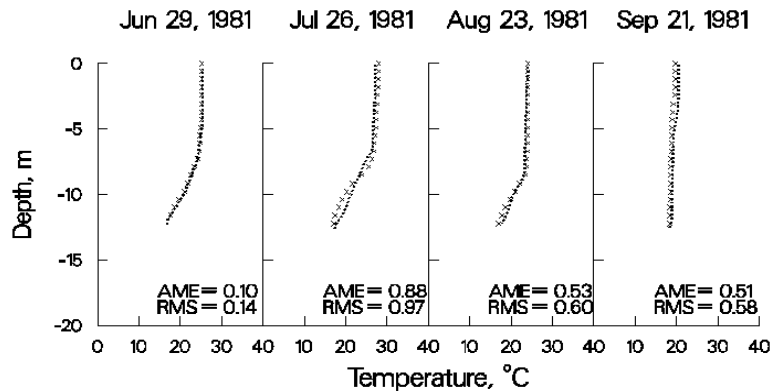


Figure 41. 1981 Bluestone Reservoir computed versus observed temperatures.

CALIBRATION

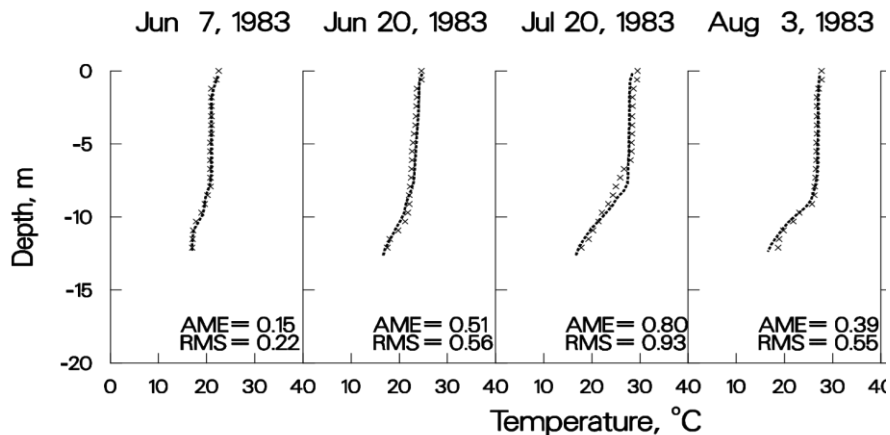


Figure 42. 1983 Bluestone Reservoir computed versus observed temperatures.

Richard B. Russell. Richard B. Russell (RBR) is located immediately upstream of J. Strom Thurmond Reservoir (JST) on the Savannah River bordering Georgia and South Carolina. The model was used to investigate the effects of proposed pump-storage operations in which water would be pumped into RBR from JST and reused for hydropower operations during peak energy demands. An important concern was what effect pump-storage operations would have on the thermal regime in RBR. The model was subsequently applied to 1996, a year in which extensive pump-storage operations occurred. In order to simulate the effects of pump-storage, the model code was altered to allow dynamic linkage of RBR and JST reservoirs.

This is a stringent test of the model's simulation capabilities because the dynamic linkage required accurate temperature simulations in RBR in order to provide accurate inflow temperatures to JST. Likewise, accurate temperature predictions were required in JST in order to provide accurate temperatures entering RBR during pumpback.

[Figure 43](#)-[Figure 45](#) show the results of the simulations. The model correctly predicted the approximately 4°C increase in hypolimnetic temperatures compared to previous years that did not have pump-storage operations. No calibration was involved for this simulation. Results are from the first run of the model for 1996 using default hydrodynamic/temperature calibration parameters and a wind-sheltering coefficient determined from calibration to two previous years that did not include pump-storage operations.

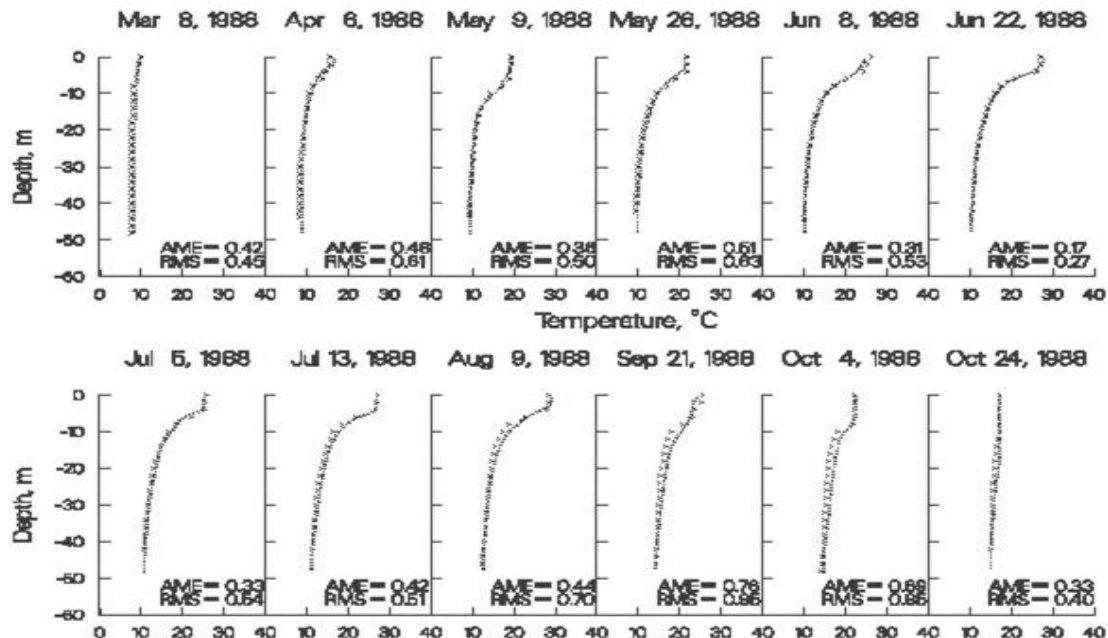


Figure 43. 1988 Richard B. Russell computed versus observed temperatures.

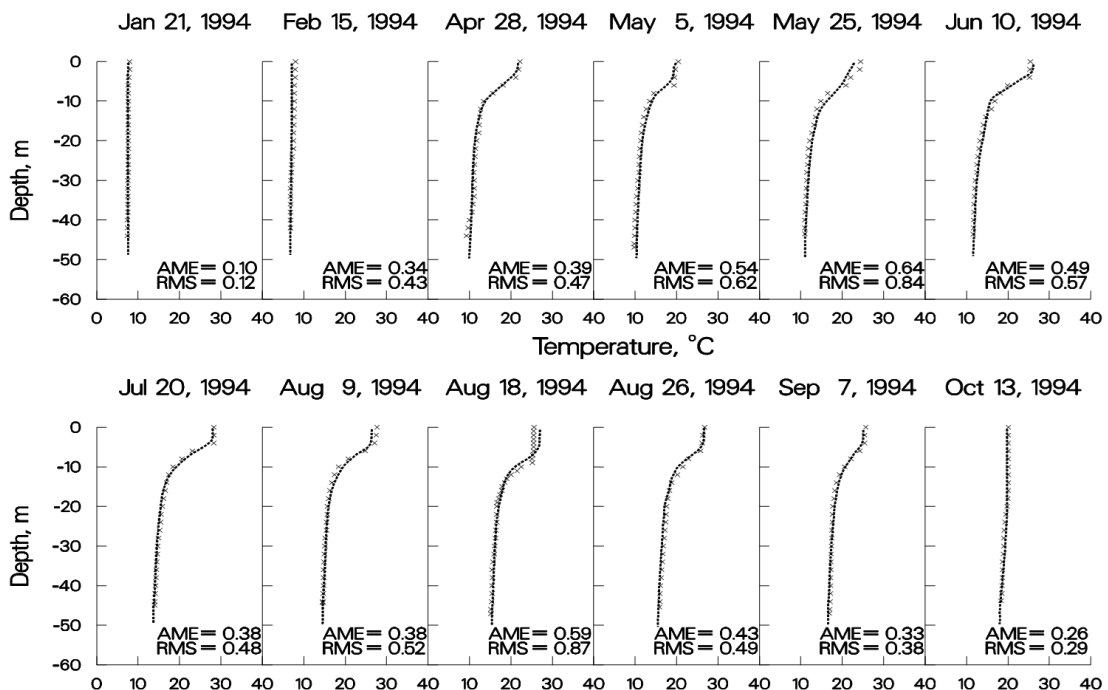


Figure 44. 1994 Richard B. Russell computed versus observed temperatures.

CALIBRATION

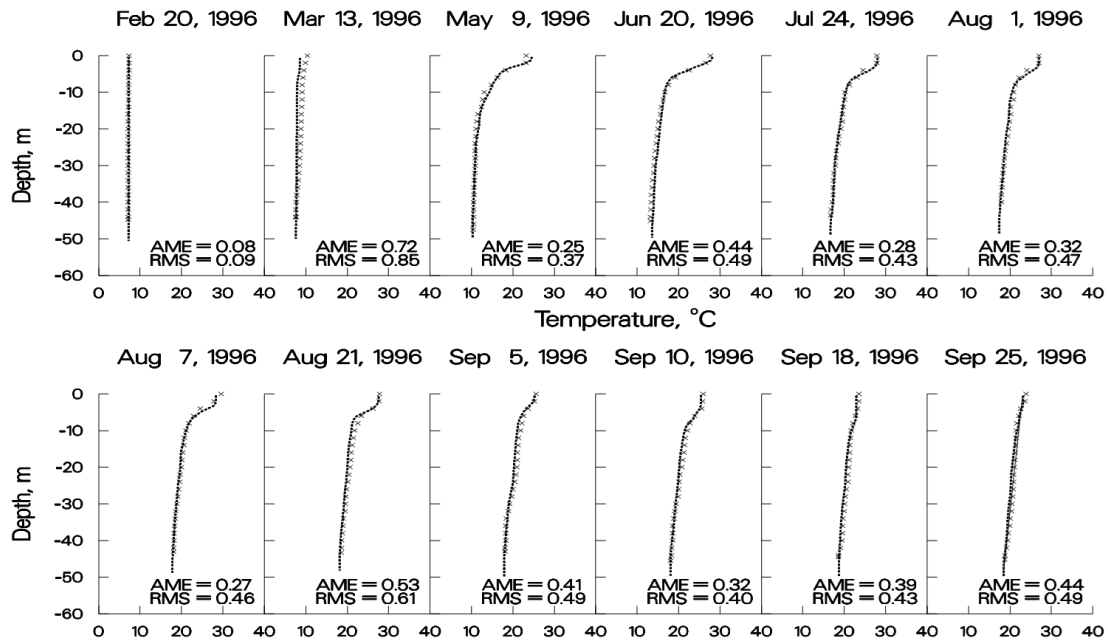


Figure 45. 1996 Richard B. Russell computed versus observed temperatures.

Paintsville Reservoir. Paintsville Reservoir is a US Army Corps of Engineers reservoir located in Kentucky. The reservoir's thermal regime is typical of deep-storage reservoirs with hydraulic retention times greater than four months. [Figure 46](#) illustrates the model's ability to reproduce the springtime development of the thermocline, the strong thermocline present in late summer, and fall overturn.

During initial calibration, the model consistently overpredicted hypolimnetic temperatures. No parameter adjustment (wind-sheltering or light absorption/extinction) resulted in an acceptable calibration. Realizing that hypolimnetic temperatures are influenced by residence time, a sensitivity analysis was performed in which the widths were increased uniformly (thus increasing hypolimnetic residence time) until the predicted hypolimnetic temperatures matched the observed temperatures. Subsequently, it was determined that the original development of the bathymetry did not include two branches that accounted for approximately 15% of the storage in the reservoir. In this case, calibration consisted of ensuring that the volume-elevation relationship was accurately described.

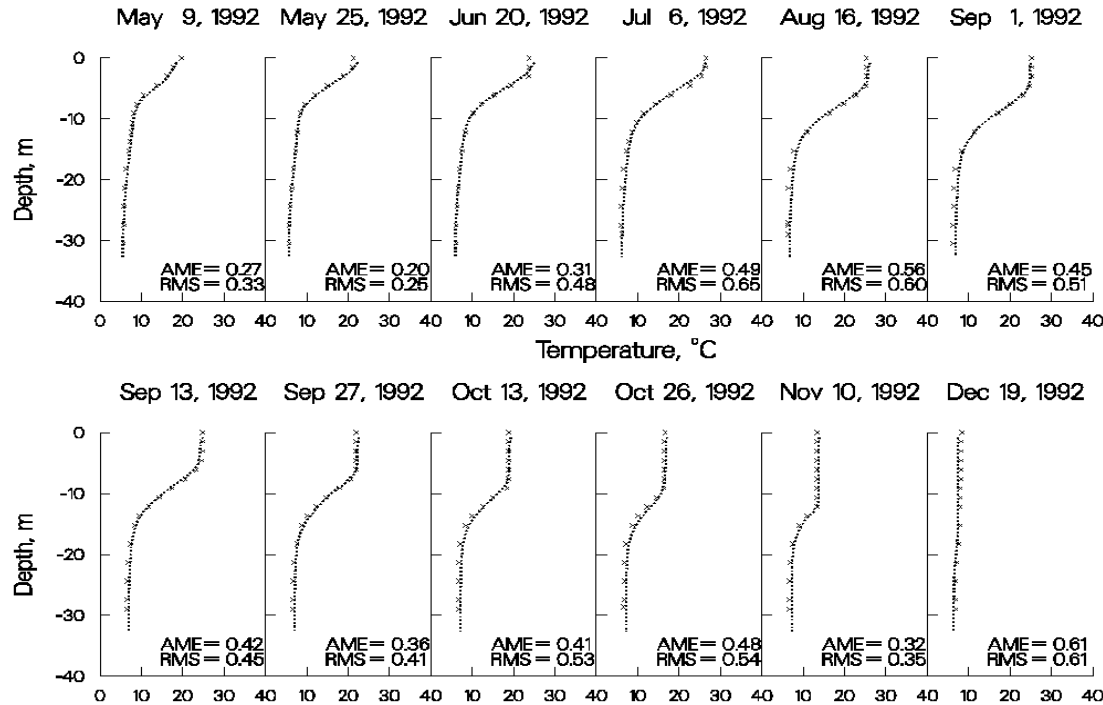


Figure 46. Paintsville Reservoir computed versus observed temperatures.

Brownlee Reservoir. Brownlee Reservoir is located on the Snake River in Idaho and is operated by Idaho Power. Brownlee's thermal regime is very distinctive with the thermocline starting at approximately 30 m below the water surface. [Figure 47](#) and [Figure 48](#) illustrate the model's ability to simulate the thermal regime in Brownlee.

During initial temperature calibration, the model predicted hypolimnetic temperatures greater than 15°C, whereas the observed temperatures were always near 5°C. No parameter adjustment allowed for adequate temperature calibration. An analysis of the system showed that the theoretical residence time during the summer was less than two months indicating that model predictions of warmer hypolimnetic temperatures were more reasonable than the observed data.

Additionally, the thermal structure in Brownlee exhibits a well-mixed epilimnion approximately 30 m in depth. Wind mixing could not supply sufficient energy to account for the depth of the epilimnion. Therefore, it was concluded that outflow dynamics had to be responsible for the observed thermal regime. As in the Bluestone application, the bottom layer for selective withdrawal was set at approximately the same depth as the thermocline. Subsequent investigations revealed the presence of a ledge below the outlet that was limiting the outflow to the level of the observed thermocline.

CALIBRATION

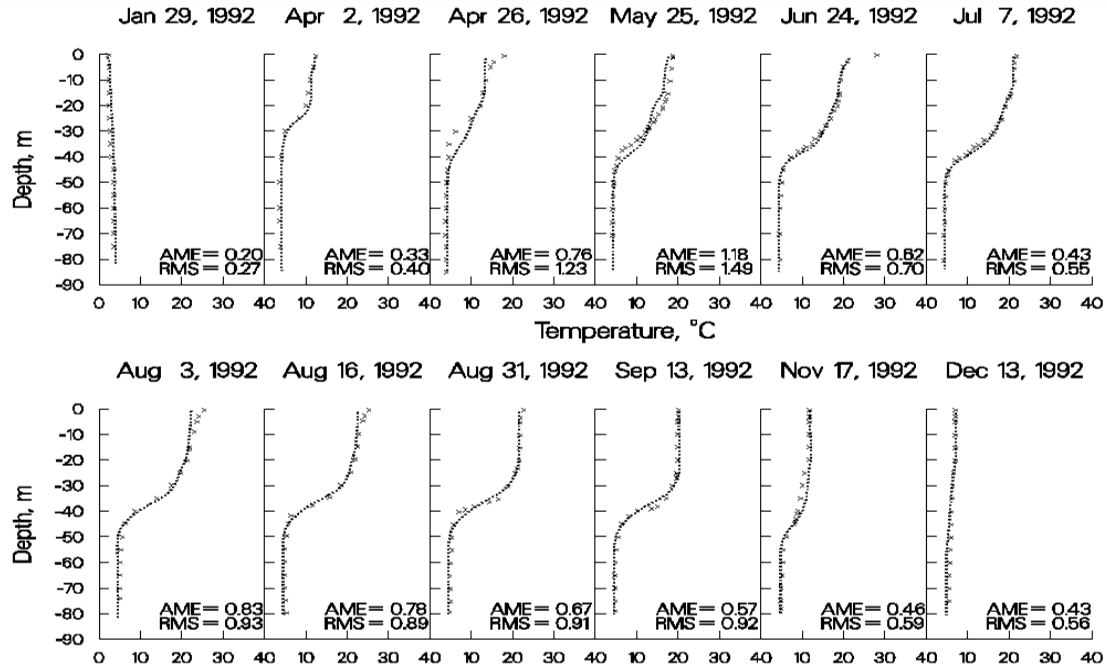


Figure 47. 1992 Brownlee Reservoir computed versus observed temperatures.

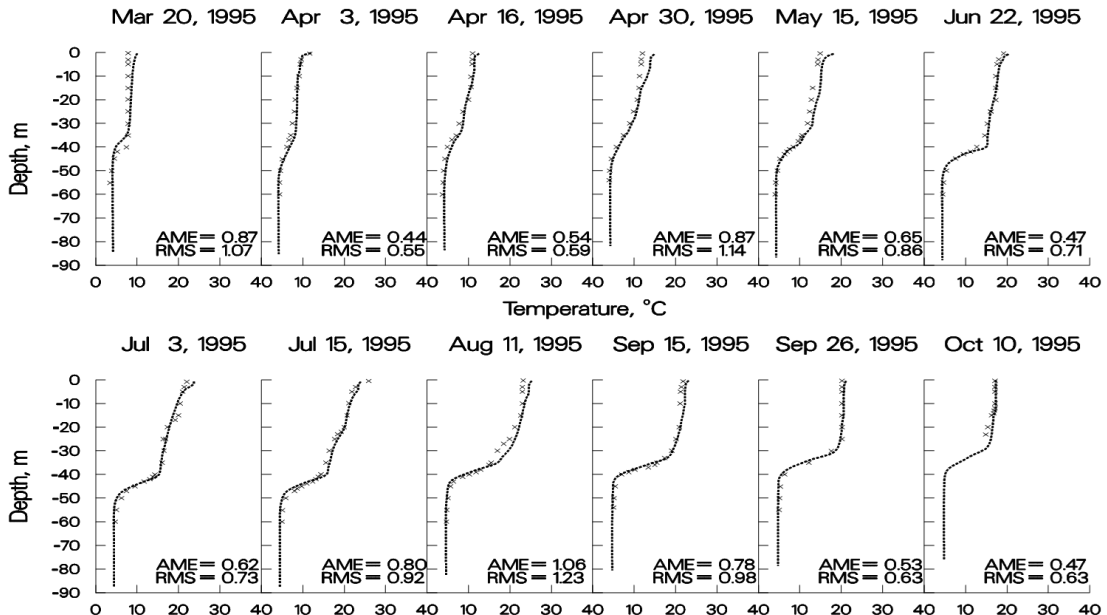


Figure 48. 1995 Brownlee Reservoir computed versus observed temperatures.

C.J. Strike Reservoir. C.J. Strike Reservoir is located on the Snake River in Idaho upstream of Brownlee Reservoir and is also operated by Idaho Power. Stratification is not nearly as pronounced as in Brownlee Reservoir due to the smaller volume of C.J. Strike and subsequent shorter residence time.

As noted in the discussion for Brownlee Reservoir, the relatively short residence time during the summer should result in considerable hypolimnetic heating as cold water is withdrawn and replaced by warmer Model Examples and Applications

waters from above. Temperature calibration consisted of adjusting the wind-sheltering coefficient until adequate agreement was obtained between computed and observed temperatures.

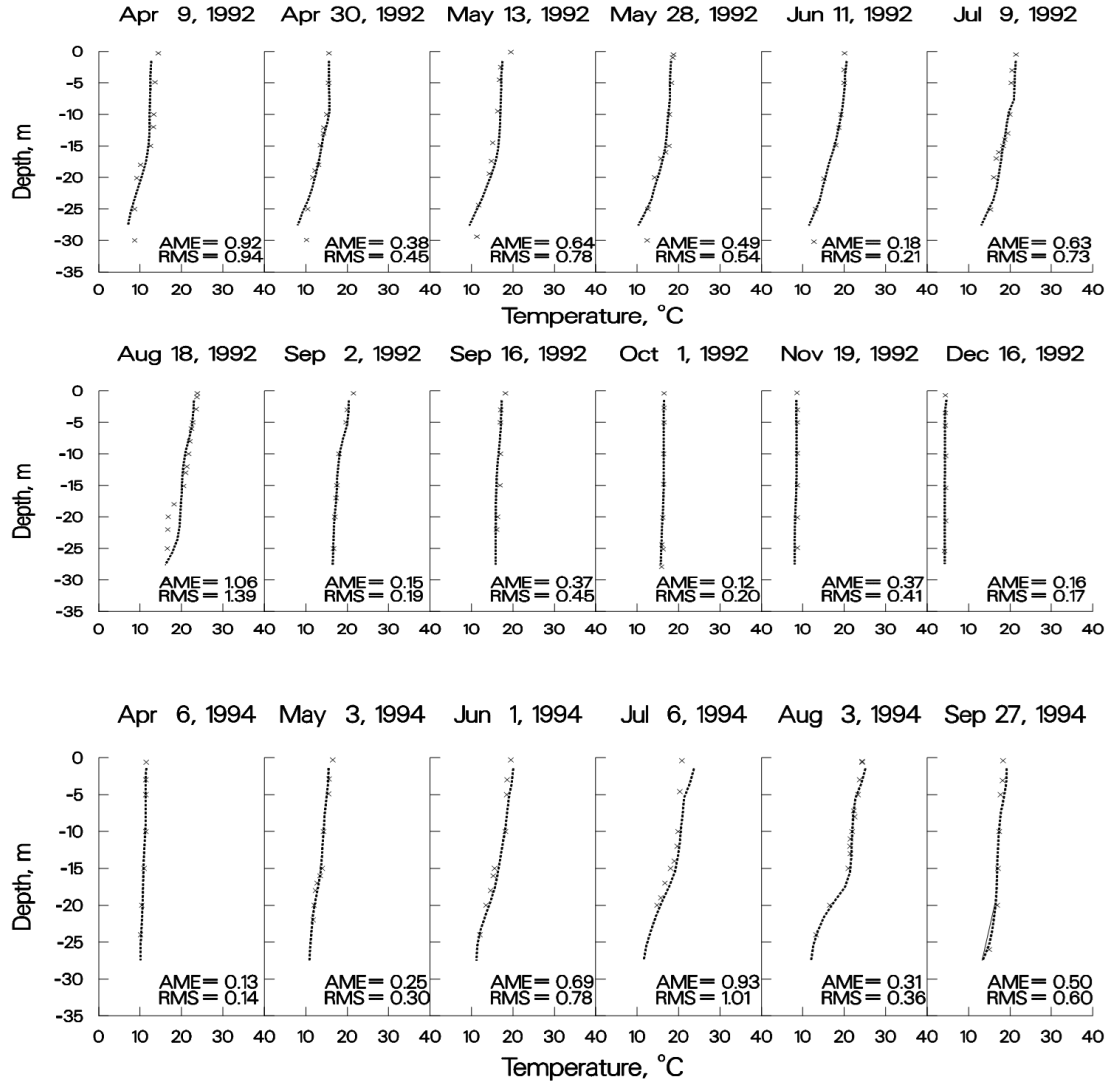


Figure 49. C.J. Strike Reservoir computed versus observed temperatures.

These examples illustrate the models ability to reproduce complex thermal regimes that differ widely depending upon a particular reservoir's morphometry, location, surrounding terrain, and operations with a minimum of parameter adjustment. The only parameter adjusted was the wind-sheltering coefficient that was used to adjust wind speeds taken at a given meteorological station to the reservoir surface. Values ranged from 0.6 for small reservoirs located in mountainous terrains to 1.0 for large reservoirs located in open terrain.

The preceding discussion is not meant to imply that the model is "plug and play" and requires no calibration with regards to temperature. Greater discrepancies between computed and observed temperature profiles were always present at the beginning of thermal calibration for all the presented examples.

CALIBRATION

Aside from adjustment of wind sheltering, calibration consisted of determining whether known inaccuracies in a given forcing function could be responsible for the discrepancies in the computed temperature profiles and then describing the forcing function more accurately. This procedure included the following:

1. Adjustment of volume-elevation relationship to ensure that residence time was accurately represented
2. Adjustment of bottom elevation to ensure that computed and observed bottom elevations for the deepest station were at least as deep as the observed data
3. Adjustment of inflow temperatures to more closely match temperatures at the most upstream station
4. Generation of more frequent inflow temperatures based on equilibrium temperature
5. Using more frequent outflow data than daily average values, particularly for peaking hydro-power systems
6. Ensuring that the outflow distribution for multi-level outlets was accurately described
7. Ensuring sufficient longitudinal/vertical grid resolution
8. Obtaining more frequent meteorological data than daily average values
9. Limiting the bottom zone for selective withdrawal (all instances were eventually physically justified in the prototype)
10. Including additional sources of outflow due to dam leakage or seepage to groundwater
11. Ensuring multiple branch descriptions were accurately represented
12. Using the most accurate numerical scheme (ULTIMATE with **[THETA]** set to 0.55) and including the effects of vertical turbulence **[VISC]** and internal gravity waves **[CELC]** in the autosteping stability requirements

As a result of the numerous thermal applications of the model, an important concept that has emerged is that the more accurately the behavior of the prototype is described, the more accurately the model responds. Always keep this in mind during model calibration.

Water Quality

The following discussion can serve as a starting point for reservoir water quality calibration. However, each application is different and requires knowledge about prototype behavior and the dominant water quality processes that are occurring in the prototype before ever attempting to model water quality. Black box application of any model is a recipe for failure.

Dissolved Oxygen. Once the user has a good understanding of the dominant water quality processes occurring in the prototype and ensures they are accurately represented in the model, then the user should begin dissolved oxygen calibration. The zero-order SOD should be used initially as it is essentially a pure calibration parameter that allows for back calculating the oxygen uptake rate in the water column. If dissolved oxygen profiles in the water column are exactly matched, then the values for SOD used in calibration are very close to the actual uptake rates of dissolved oxygen in the water column. The problem with using only the zero-order SOD for water column DO calibration is that the model will not be sensitive to load increases/decreases that directly affect water column DO uptake and sediment nutrient recycling that affect phytoplankton primary production.

However, this is seldom the case, particularly where loadings to the system in the form of allochthonous organic matter (or CBOD), autochthonous organic matter due to phytoplankton production, and/or ammonium are important forcing functions for water column dissolved oxygen that are subject to change over time. Unfortunately, for systems where allochthonous loadings of organic matter are important, rarely are there sufficient boundary condition data to adequately represent the loadings to the system.

Particular care should be paid to the timing and duration of events involving phytoplankton, epiphyton, and dissolved oxygen. If the model does not represent the onset, extent, and duration of anoxic conditions, then nutrient dynamics will not be represented either. They in turn affect phytoplankton production that affects dissolved oxygen. Timing of the onset of dissolved oxygen depletion is greatly influenced by the temperature rate multipliers used for organic matter and the sediments. A change in the lower temperature [OMT1] of 1°C in the temperature rate formulation can shift the initial uptake of water column dissolved oxygen by as much as two weeks. The same effect can be obtained by adjusting the value of the multiplier [OMK1]. Much of the art in water quality modeling is involved in calibrating phytoplankton/nutrient/DO dynamics.

The following plots illustrate the model's ability to reproduce widely varying reservoir dissolved oxygen regimes. With the exception of the zero-order SOD rates, all kinetic coefficients were set to their default values thus ensuring that the model was applied with a minimum of "curve fitting". In all likelihood, using the same values for kinetic parameters such as phytoplankton growth and settling rates is not correct. However, the point to be made is that the model is capable of reproducing very different water quality regimes without having to resort to extensive, site-specific parameter manipulations.

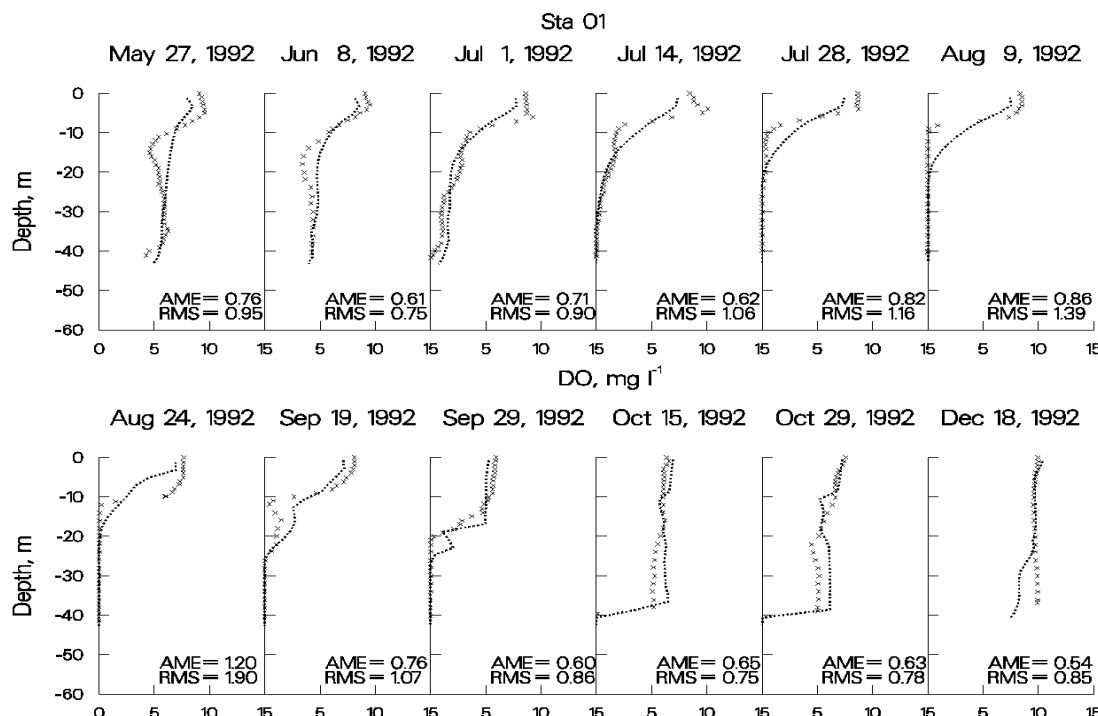


Figure 50. Allatoona Reservoir computed vs. observed DO.

CALIBRATION

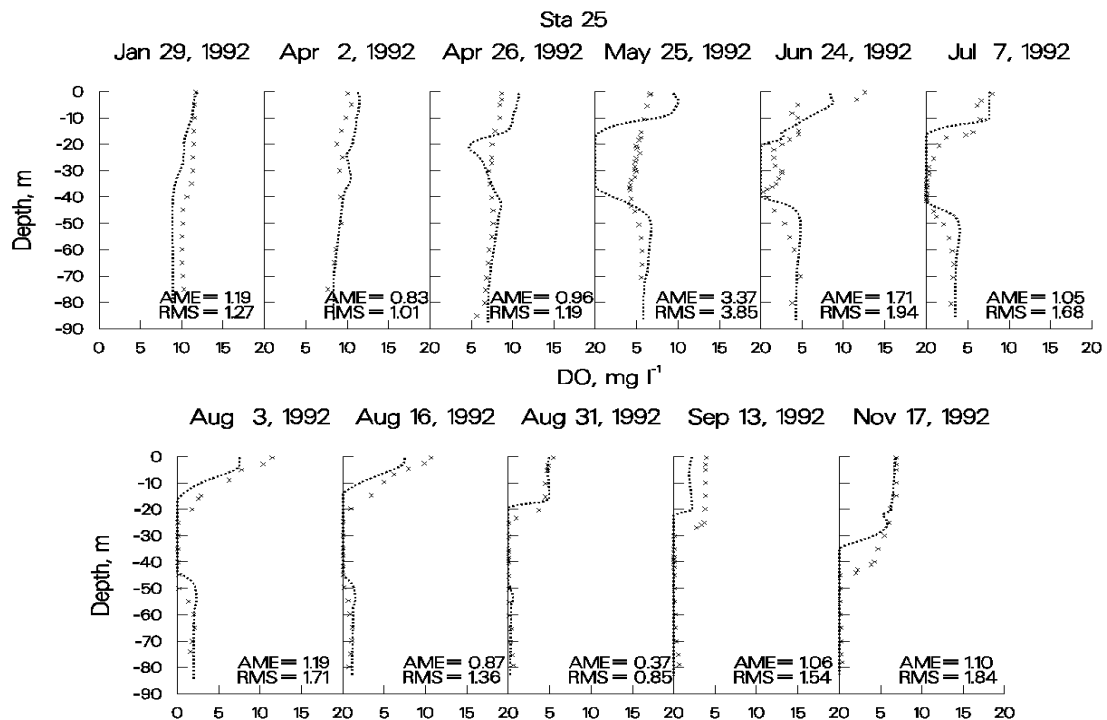


Figure 51. Brownlee Reservoir computed vs. observed DO.

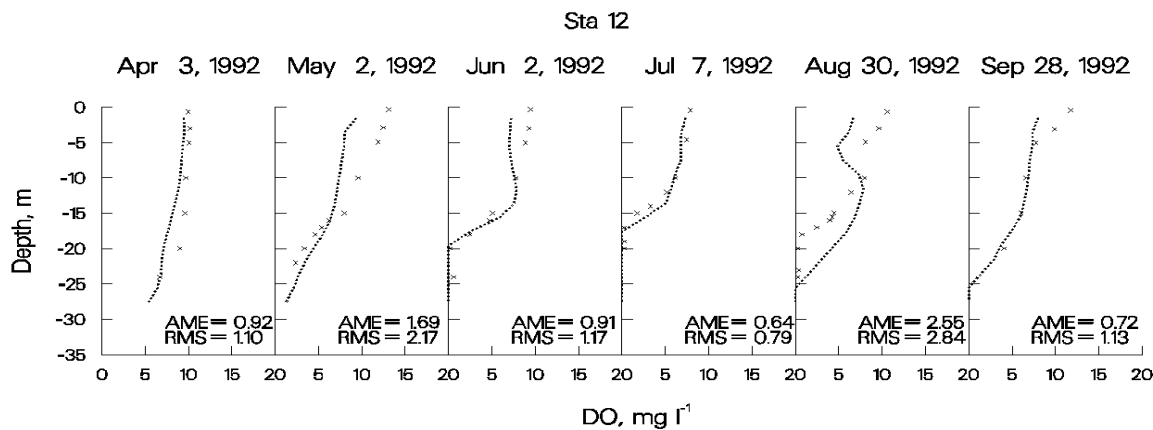


Figure 52. C.J. Strike Reservoir computed vs. observed DO.

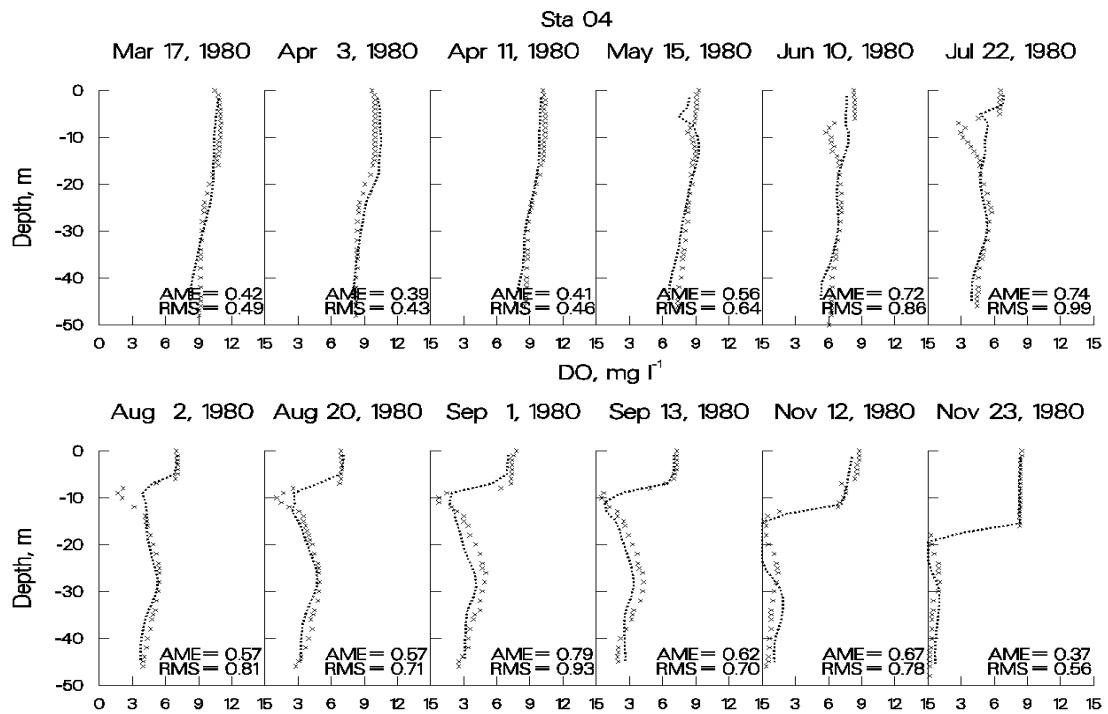


Figure 53. DeGray Reservoir computed vs. observed DO.

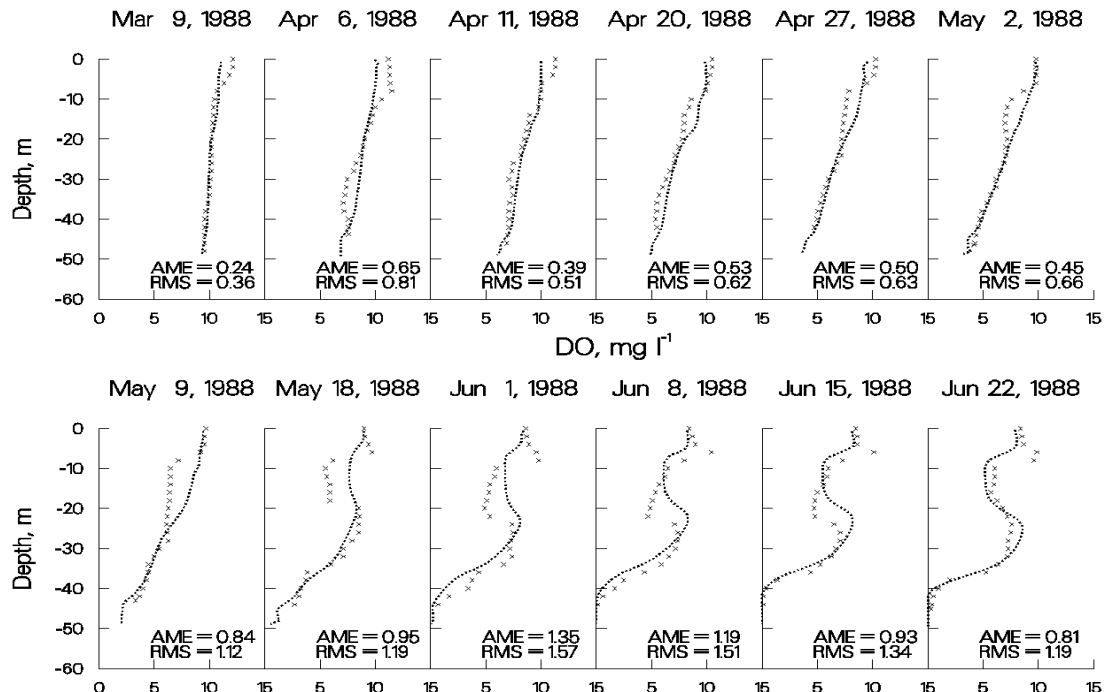


Figure 54. Richard B. Russell Reservoir computed vs. observed DO, March through June, 1988.

CALIBRATION

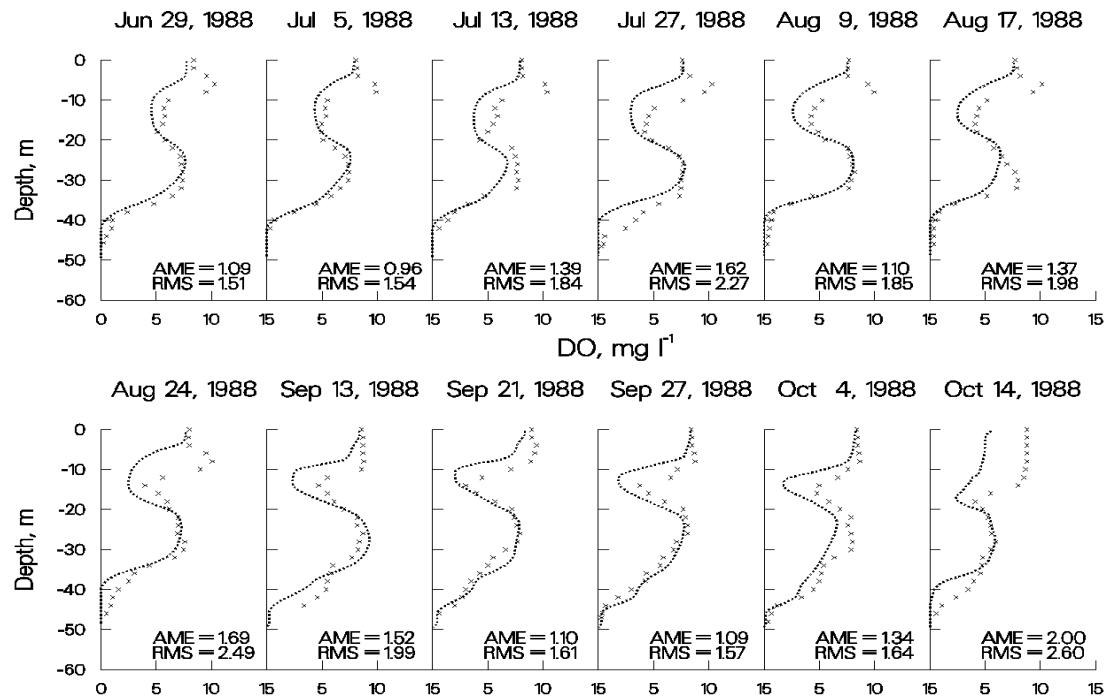


Figure 55. Richard B. Russell Reservoir computed vs. observed DO, June through October, 1988.

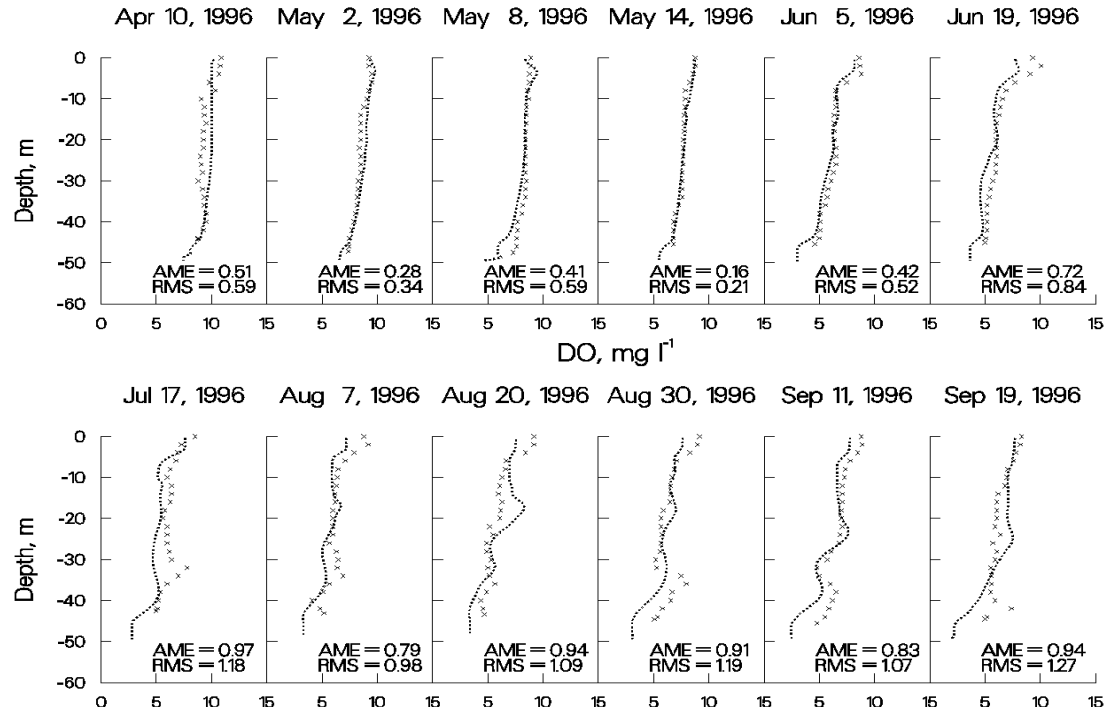


Figure 56. 1996 Richard B. Russell computed vs. observed DO.

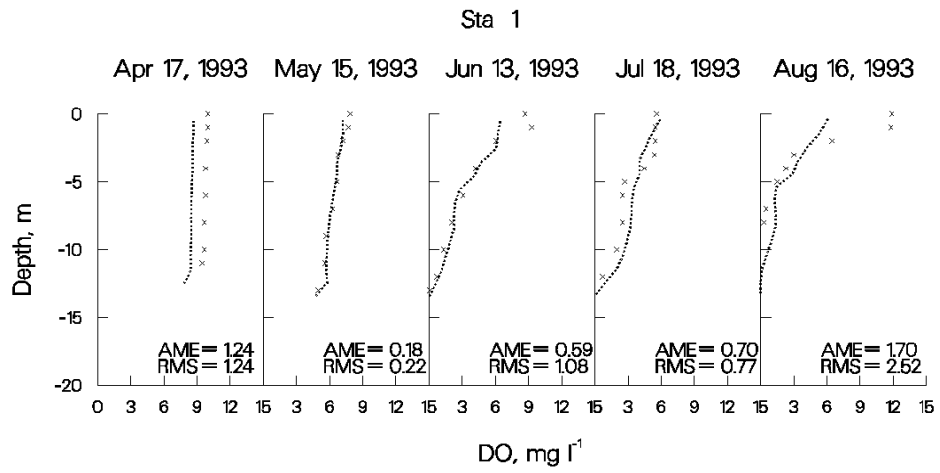


Figure 57. Neely Henry Reservoir computed vs. observed DO.

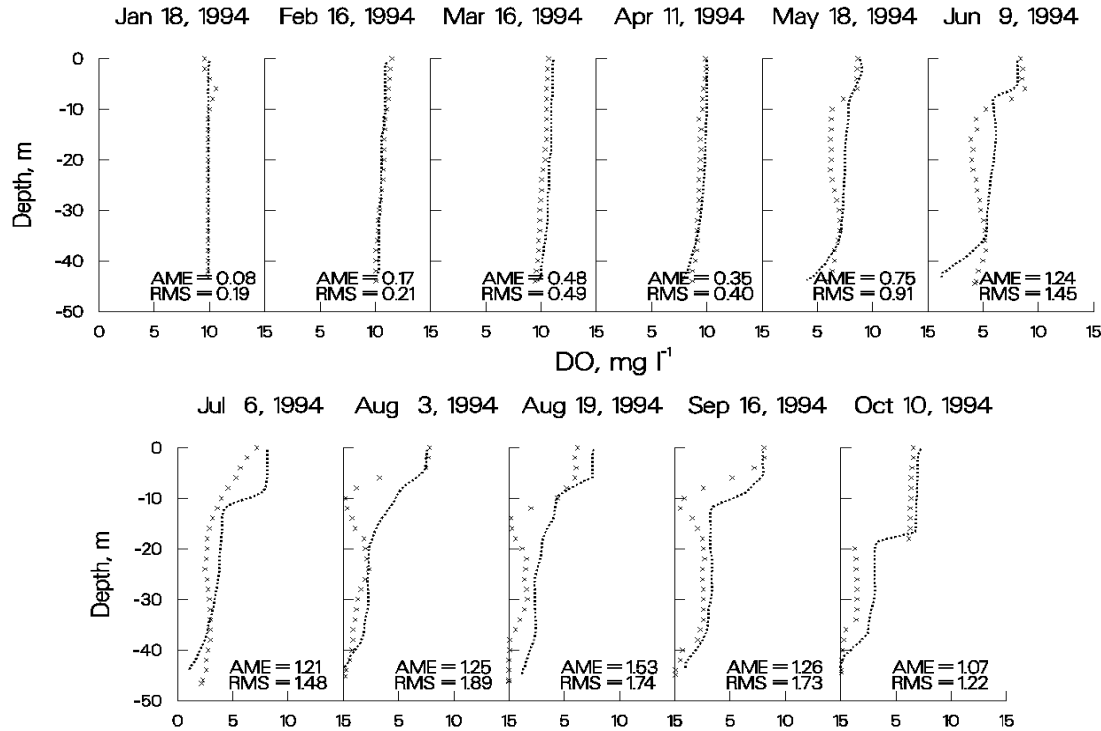


Figure 58. J. Strom Thurmond Reservoir computed vs. observed DO.

CALIBRATION

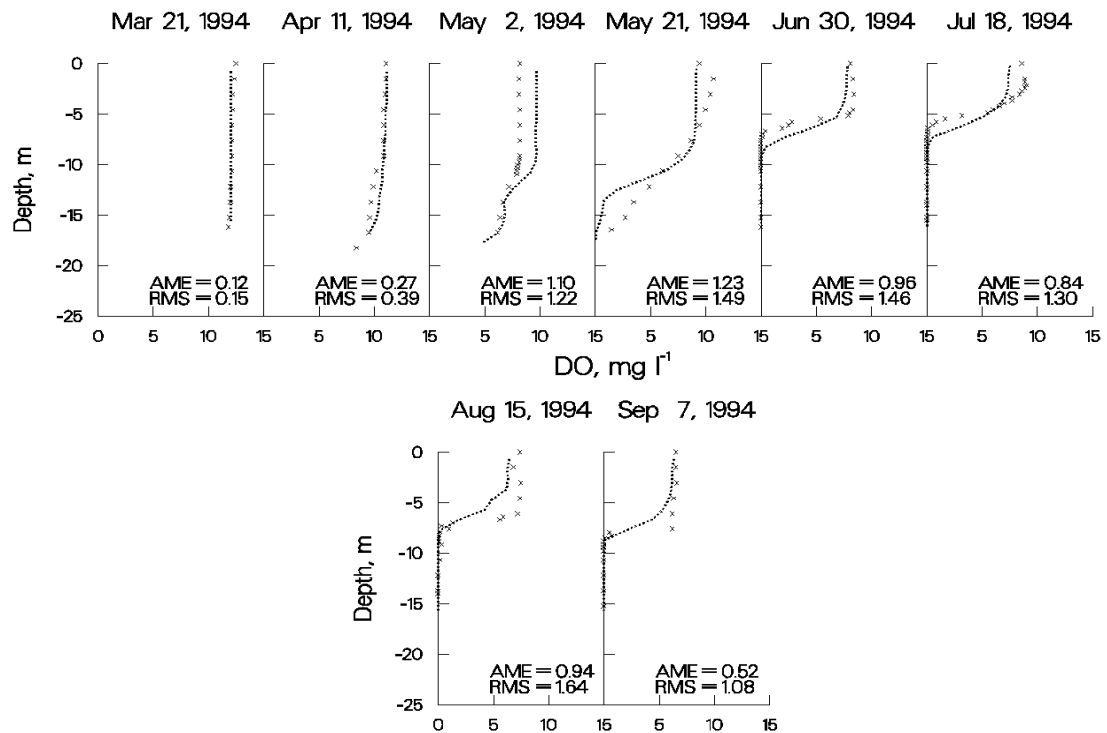


Figure 59. Monroe Reservoir computed vs. observed DO.

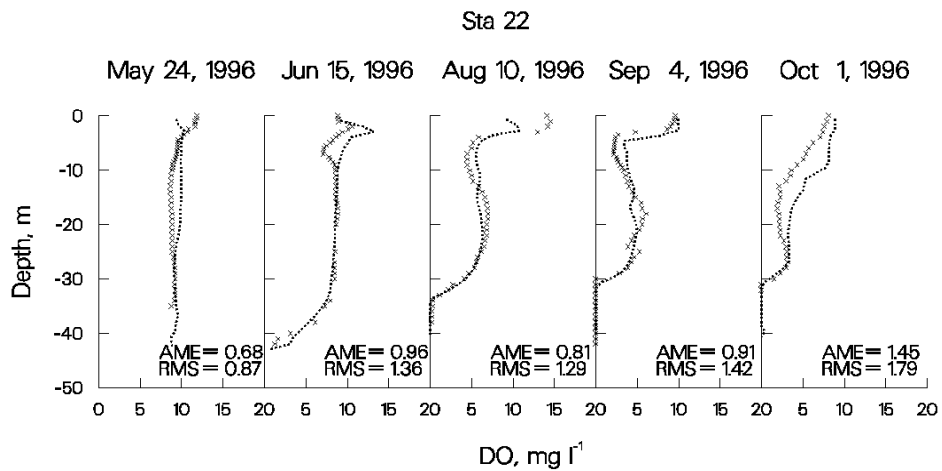


Figure 60. Rimov Reservoir computed vs. observed DO.

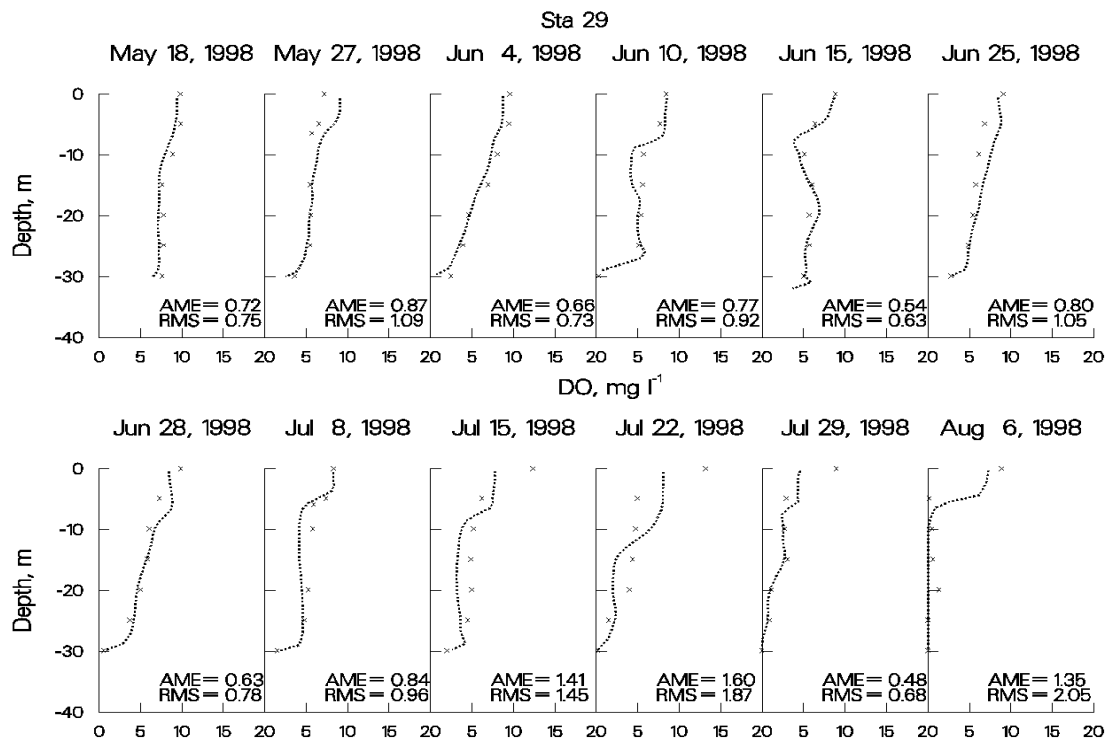


Figure 61. Shepaug Reservoir computed vs. observed DO.

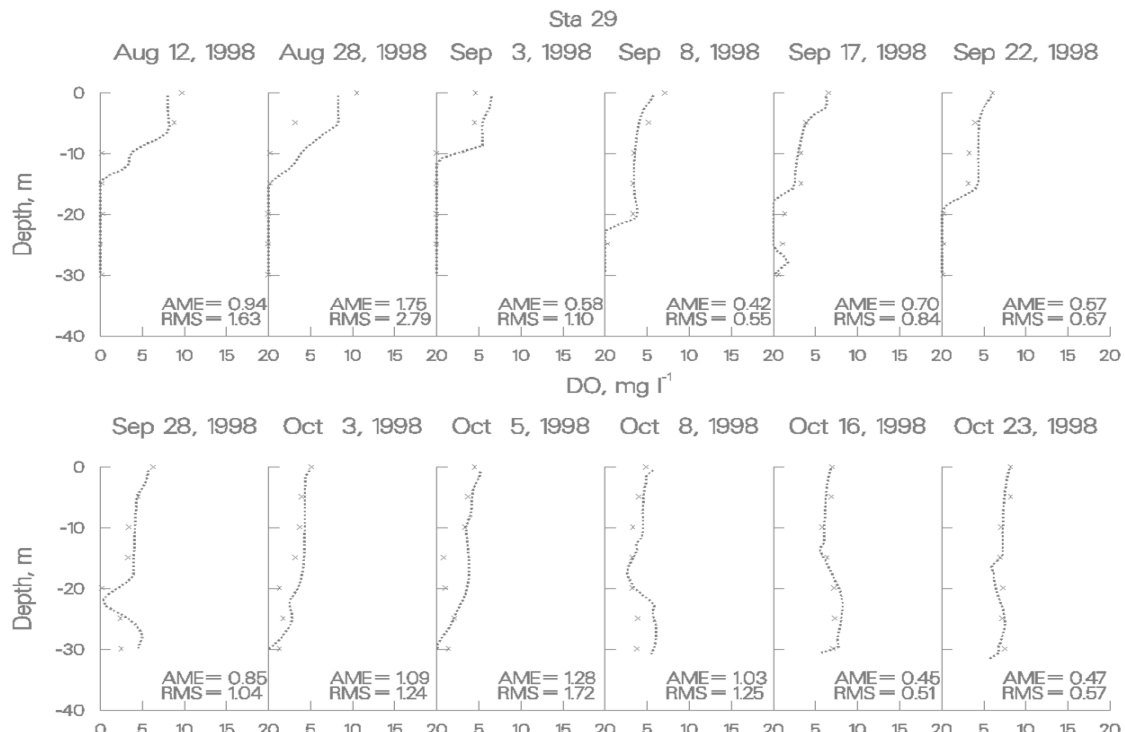


Figure 62. Shepaug Reservoir computed vs. observed DO.

CALIBRATION

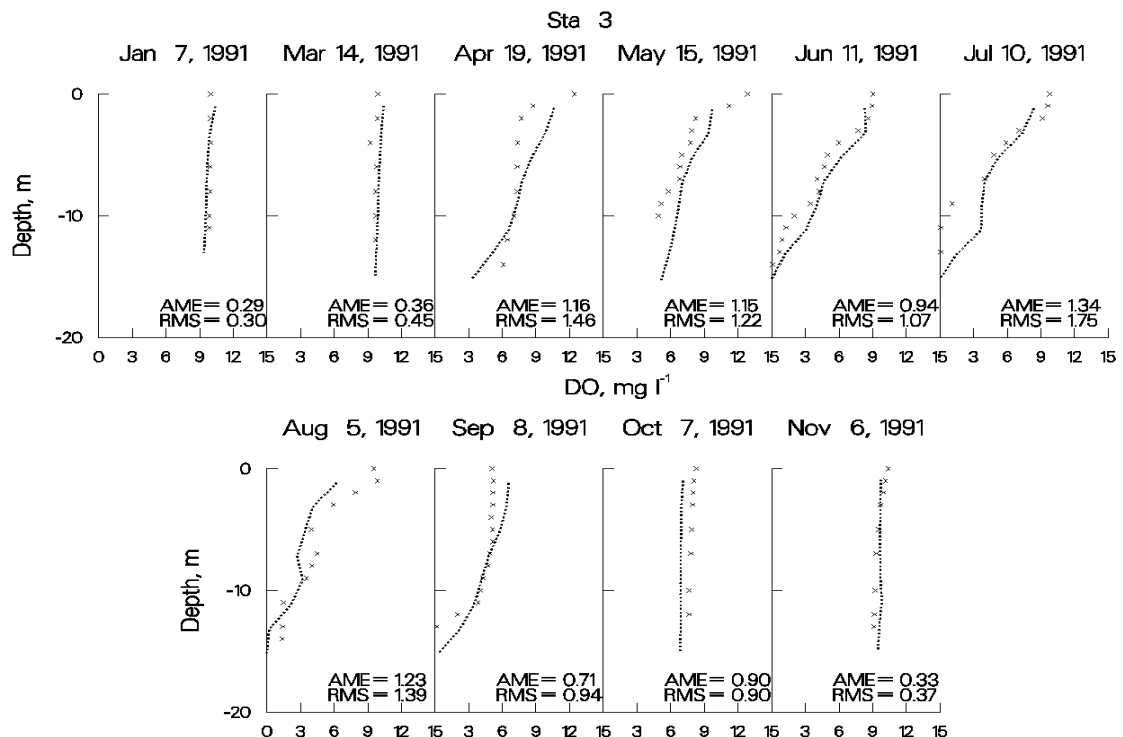


Figure 63. Weiss Reservoir computed vs. observed DO.

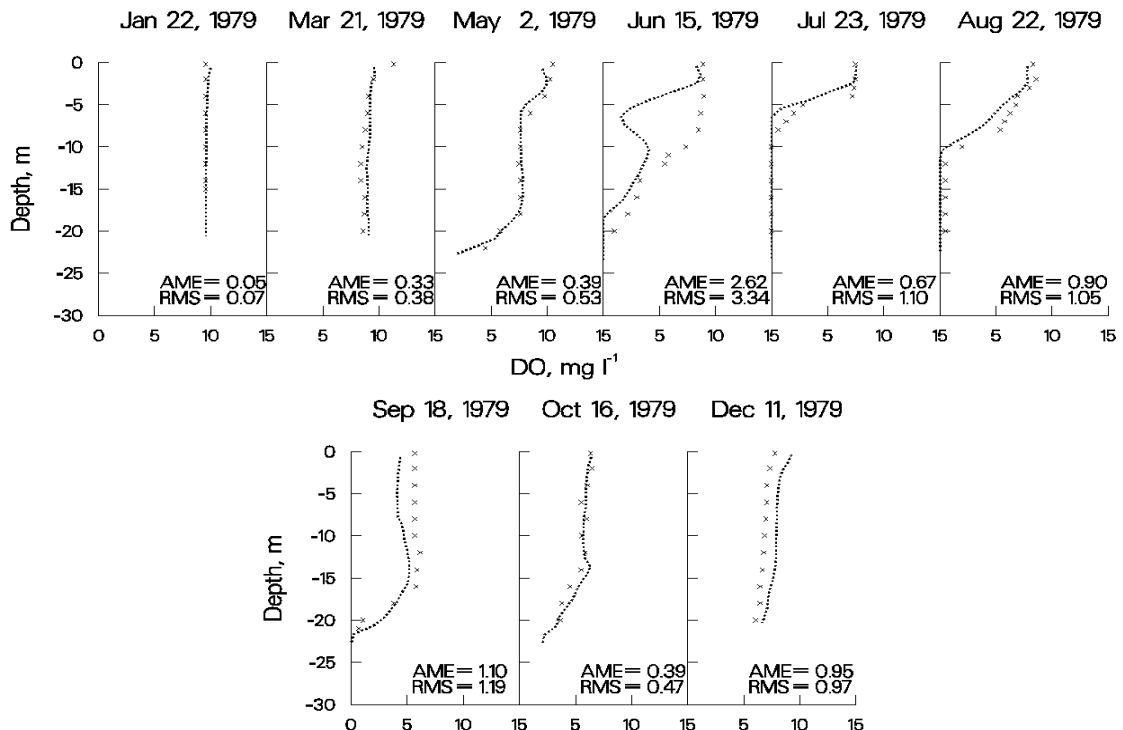


Figure 64. West Point Reservoir computed vs. observed DO.

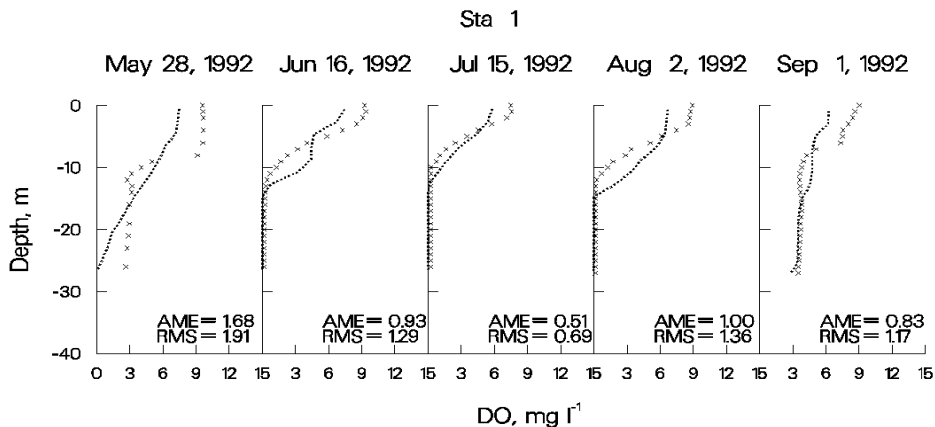


Figure 65. Walter F. George Reservoir computed vs. observed DO.

As can be seen from the previous figures for computed versus observed DO comparisons, the model has reproduced a wide range of DO regimes with a high degree of accuracy using mostly default kinetic parameters. The largest discrepancies between computed and observed DO occur in the epilimnion during middle to late summer where the model consistently underpredicts supersaturated DO. The problem is that if the model is correctly predicting very low nutrient levels during these times (typically at detection levels), then there are insufficient nutrients in the water column to support the observed levels of primary production indicated by supersaturated conditions. This is a shortcoming of all currently used water quality models and indicates insufficient understanding of phytoplankton/nutrient dynamics in the photic zone. A great deal of research needs to be done in this area in order to improve our ability to model phytoplankton primary productivity.

Another possible problem during dissolved oxygen calibration is during fall overturn when anoxic hypolimnetic water mixes with epilimnetic water. For the most part, the model reproduces dissolved oxygen fairly well during overturn ([Figure 64](#)), but in some applications the model has consistently underpredicted dissolved oxygen and in other applications the model has consistently overpredicted hypolimnetic concentrations.

There are three possible causes for this behavior. The first is the reaeration formula is not appropriate for the waterbody. For reservoirs, the model has accurately reproduced epilimnetic dissolved oxygen concentrations on so many systems that this is probably not the case. The second possibility is that the volumes of epilimnetic and hypolimnetic volumes are sufficiently off to affect the final mixed dissolved oxygen concentration. Depending upon the direction of the volume error, this can result in either over or underprediction. The third possibility in the case of overprediction is that reduced substances including ammonium, iron, manganese, and sulfides have been released from the sediments in sufficient quantities to exert an appreciable oxygen demand. The model includes only the effect of ammonium on dissolved oxygen. In this case, the code would need to be altered to include their effects on dissolved oxygen. All of these scenarios should be investigated if accurate reproduction of dissolved oxygen during fall overturn is important to simulate.

Nutrients. Given accurate boundary conditions for phosphorus, ammonium, and iron and accurate simulations of metalimnetic/hypolimnetic dissolved oxygen, hypolimnetic concentrations of these nutrients are relatively easy to reproduce. Again, this is basically a back calculation of the sediment fluxes to match observed hypolimnetic concentrations.

CALIBRATION

Epilimnetic concentrations of phosphorus during the growing season are typically at or below detection levels in both the model and the prototype, so they are also relatively easy to reproduce. Fall concentrations can be more complicated, particularly if iron and manganese have built up during the summer in an anoxic hypolimnion. In this case, the iron compartment should be turned on so that iron is released in the hypolimnion. The model includes phosphorus sorption onto iron hydroxides that form during fall overturn and settle into the sediments, thus removing phosphorus from the water column.

Epilimnetic ammonium and nitrate levels are more difficult to reproduce as some phytoplankton show a preference for ammonium over nitrate and the degree to which they exhibit this preference is different between groups. In addition, water column nitrate undergoes denitrification when the water column goes anoxic and also diffuses into the sediments where it undergoes denitrification in the anaerobic layer under both oxic and anoxic conditions. The ammonium preference factor [ANPR], the water column denitrification rate [NO3DK], and the sediment nitrate uptake rate [NO3S] are calibration parameters that can be adjusted to better match observed concentrations of these nutrients.

Phytoplankton. The following plots illustrate the model's ability to reproduce a spring phytoplankton bloom in Rimov Reservoir, Czech Republic. Tremendous amounts of data were collected to analyze the spring bloom. Chlorophyll α samples were taken at 1 m depth intervals over upper 10 m of the water column at six stations approximately every three days for over a month. The plots include six stations along the length of the reservoir starting upstream and progressing towards the dam.

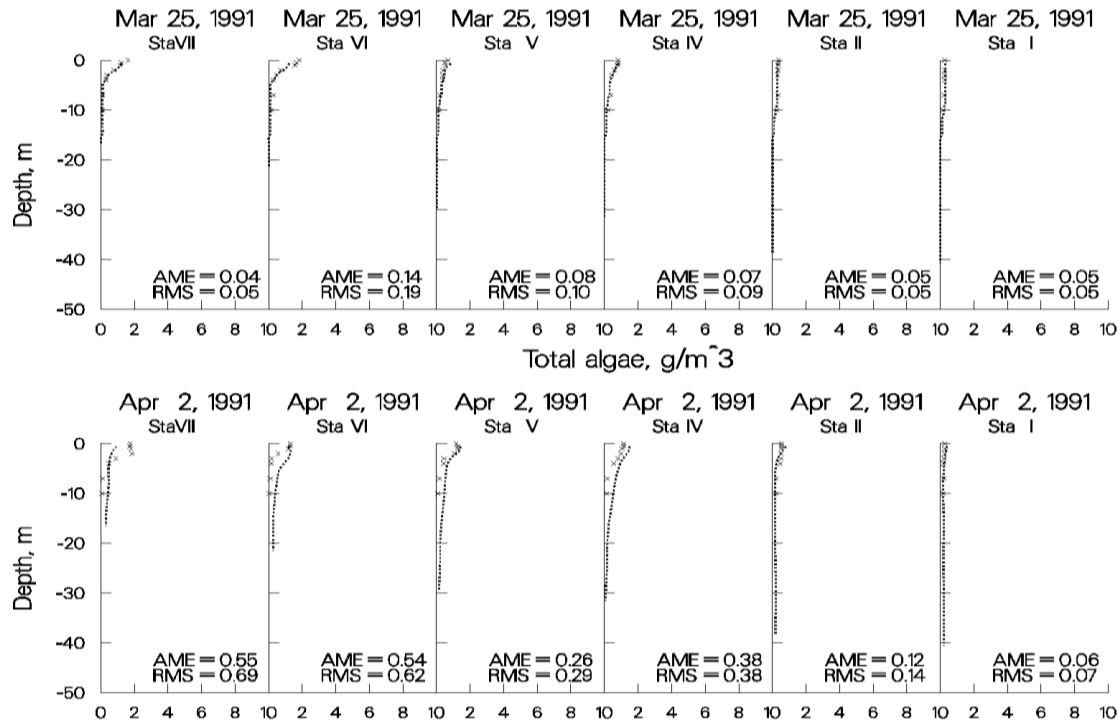


Figure 66. Rimov Reservoir computed vs. observed phytoplankton biomass.

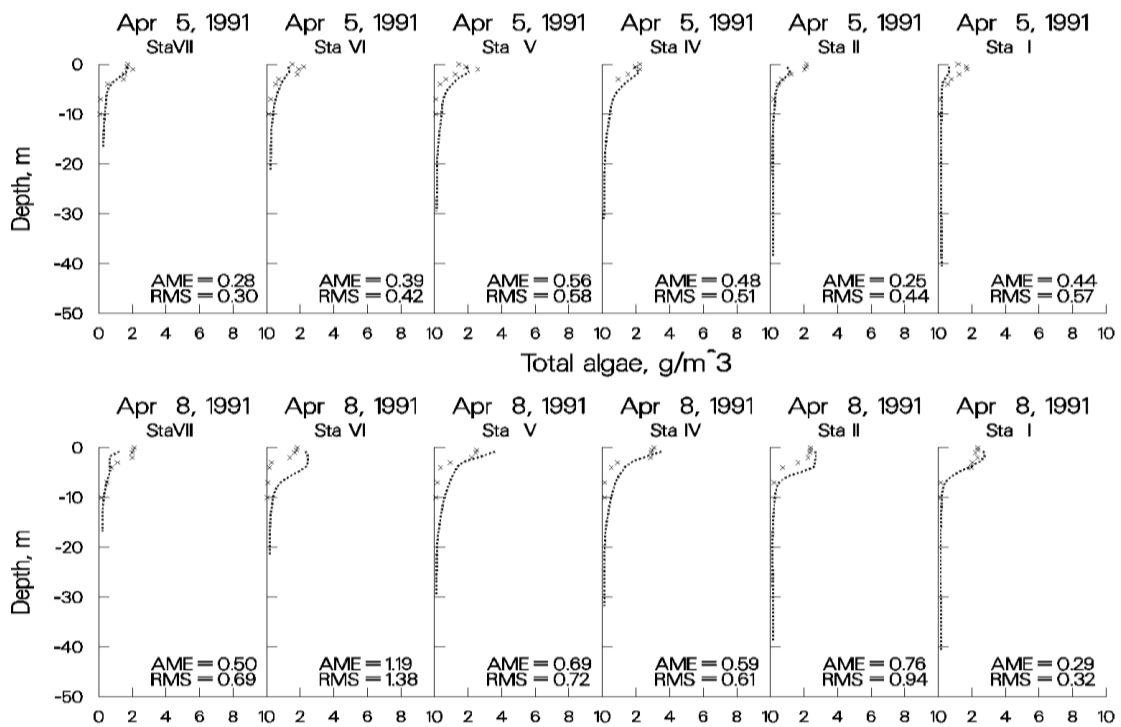


Figure 67. Rimov Reservoir computed vs. observed phytoplankton biomass.

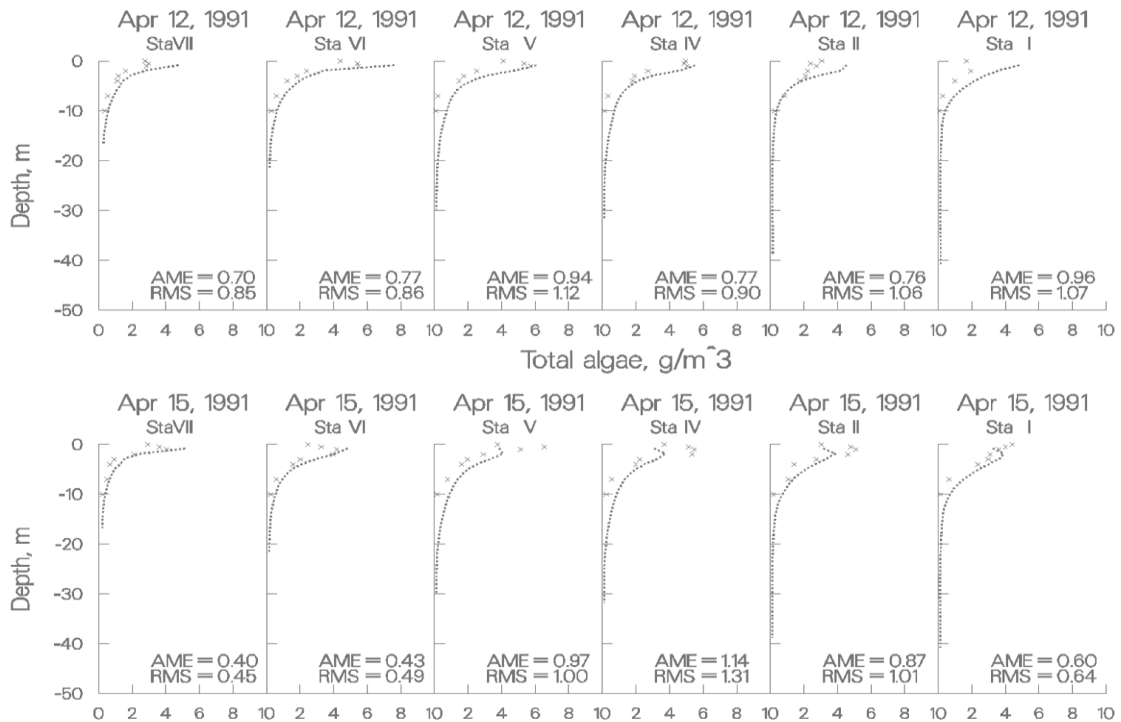


Figure 68. Rimov Reservoir computed vs. observed phytoplankton biomass.

CALIBRATION

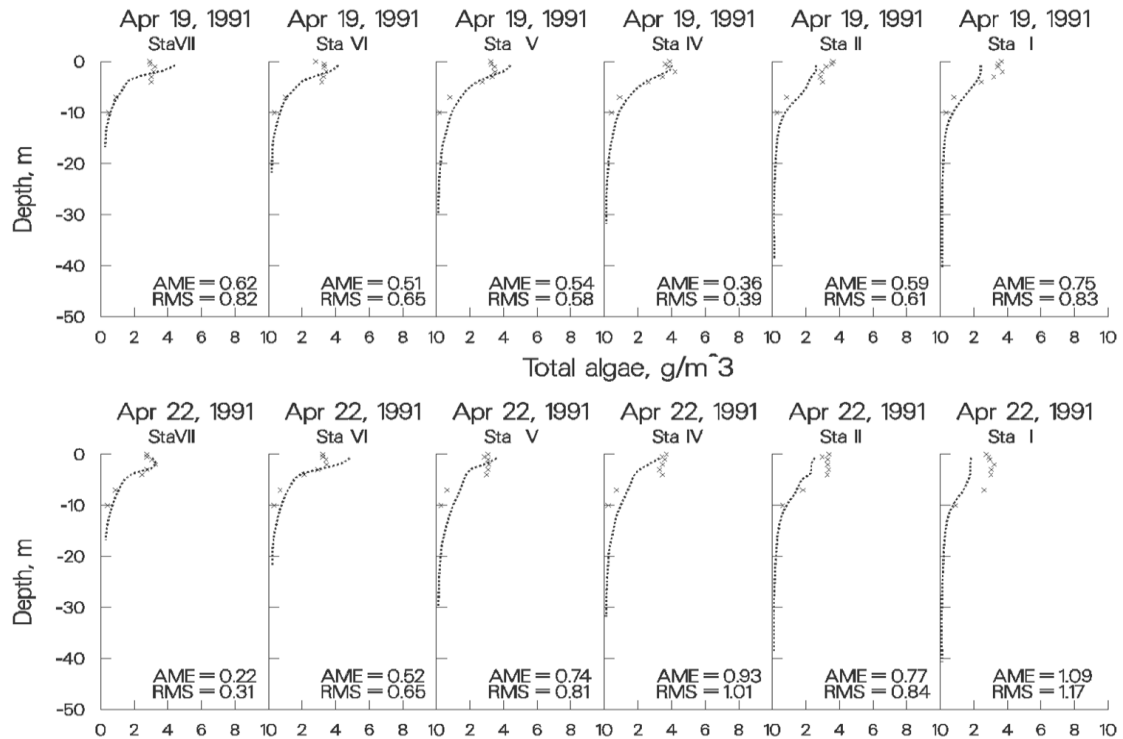


Figure 69. Rimov Reservoir computed vs. observed phytoplankton biomass.

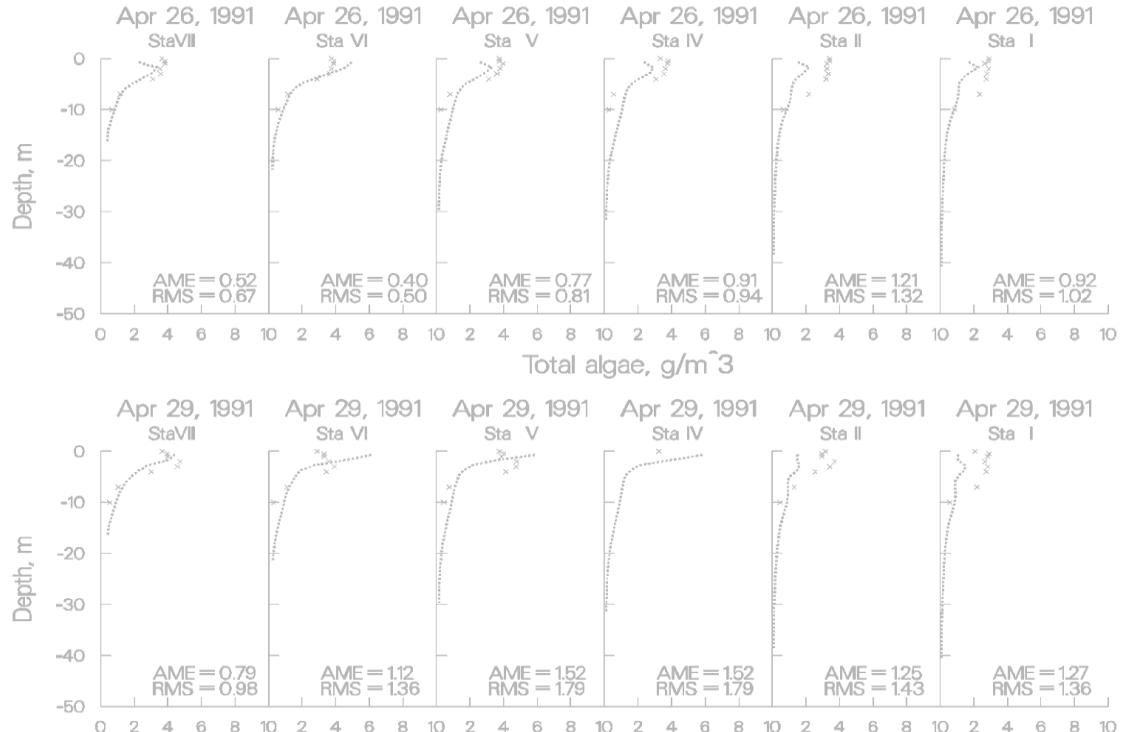


Figure 70. Rimov Reservoir computed vs. observed phytoplankton biomass.

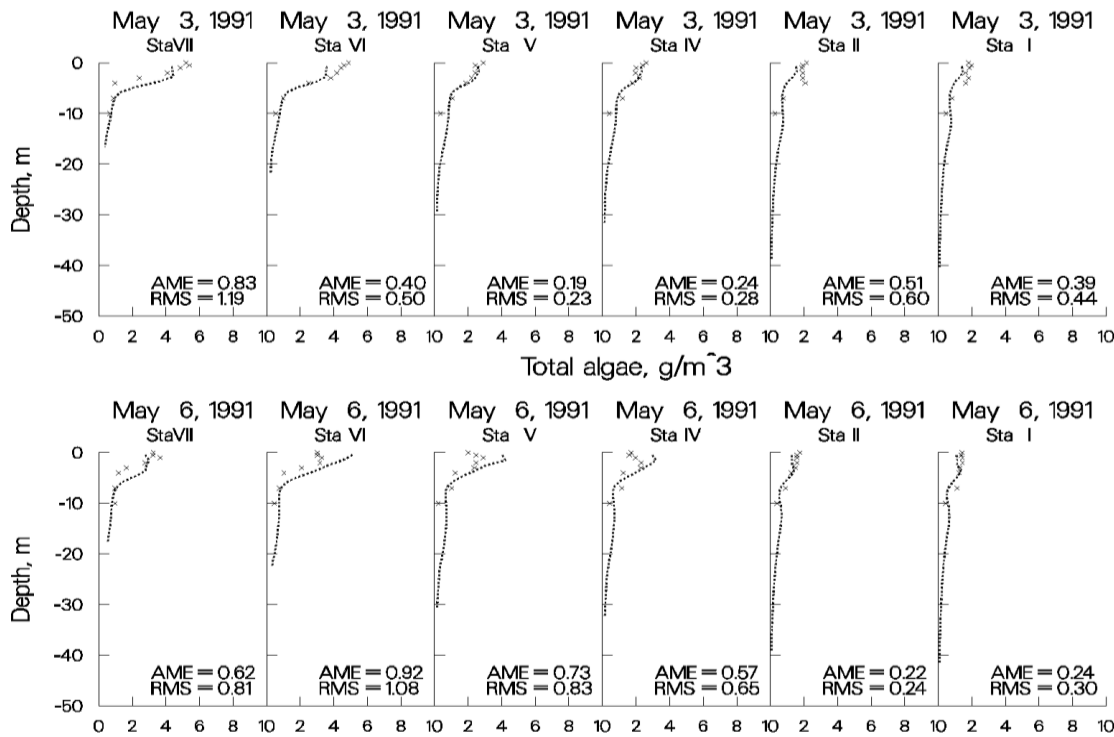


Figure 71. Rimov Reservoir computed vs. observed phytoplankton biomass.

The following plots illustrate how important it is to describe the system accurately. The plots show results of the Rimov phytoplankton simulation in which the wind direction was inadvertently changed by 90°. The importance of wind direction and its influence on the spring phytoplankton bloom was noted by limnologists who originally collected the 1991 data. Note the difference at the most downstream station on April 8 compared to the previous plot of April 8 using the correct wind direction. This also illustrates that the model can be a powerful limnological investigative tool when trying to determine how important different forcing functions are to the limnology of a reservoir.

CALIBRATION

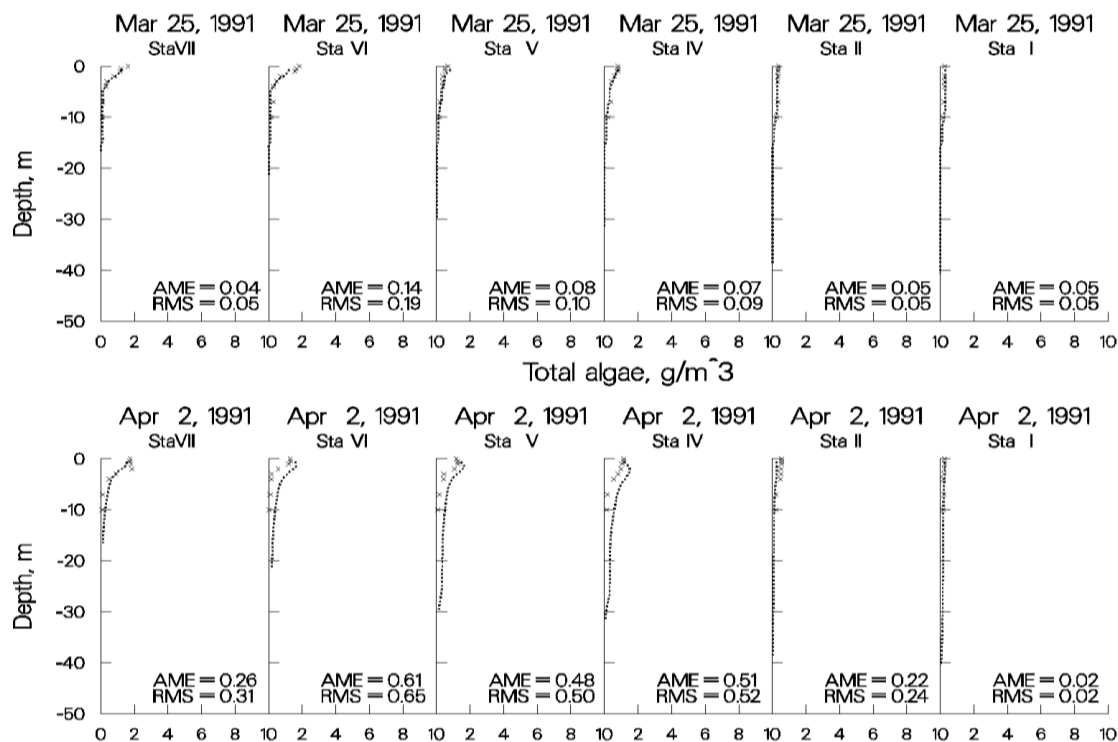


Figure 72. Rimov Reservoir computed vs. observed phytoplankton with wind rotated 90°.

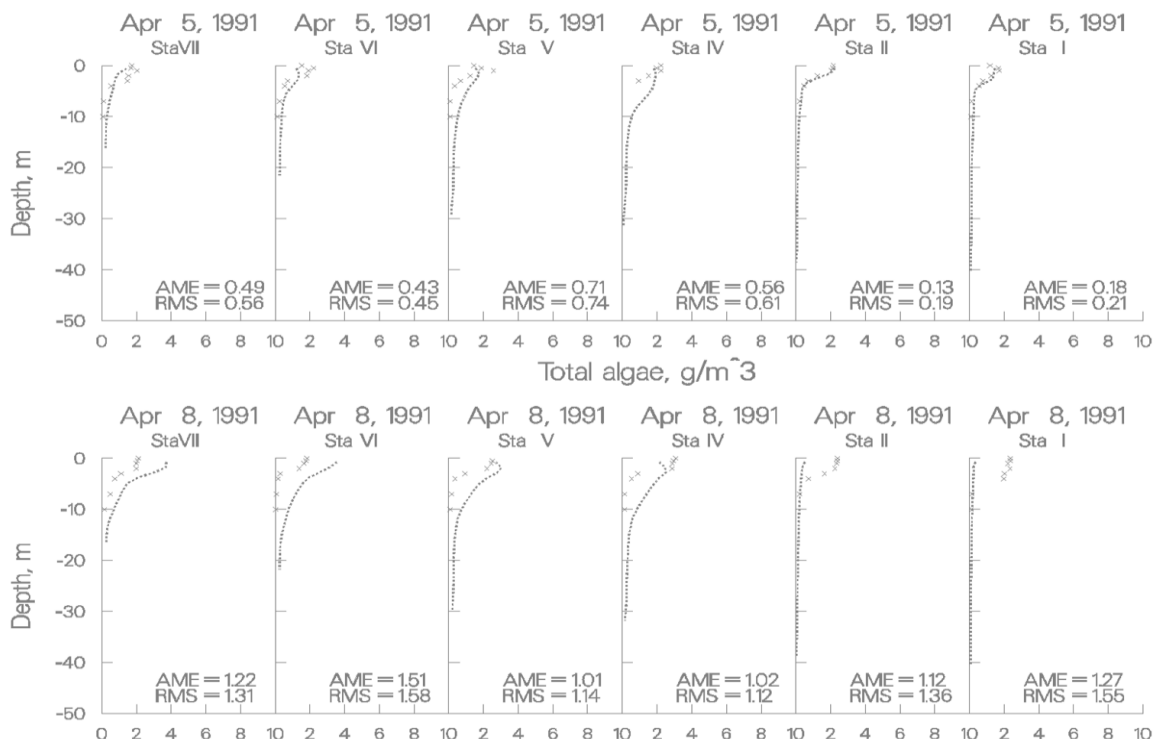


Figure 73. Rimov Reservoir computed vs. observed phytoplankton with wind rotated 90°

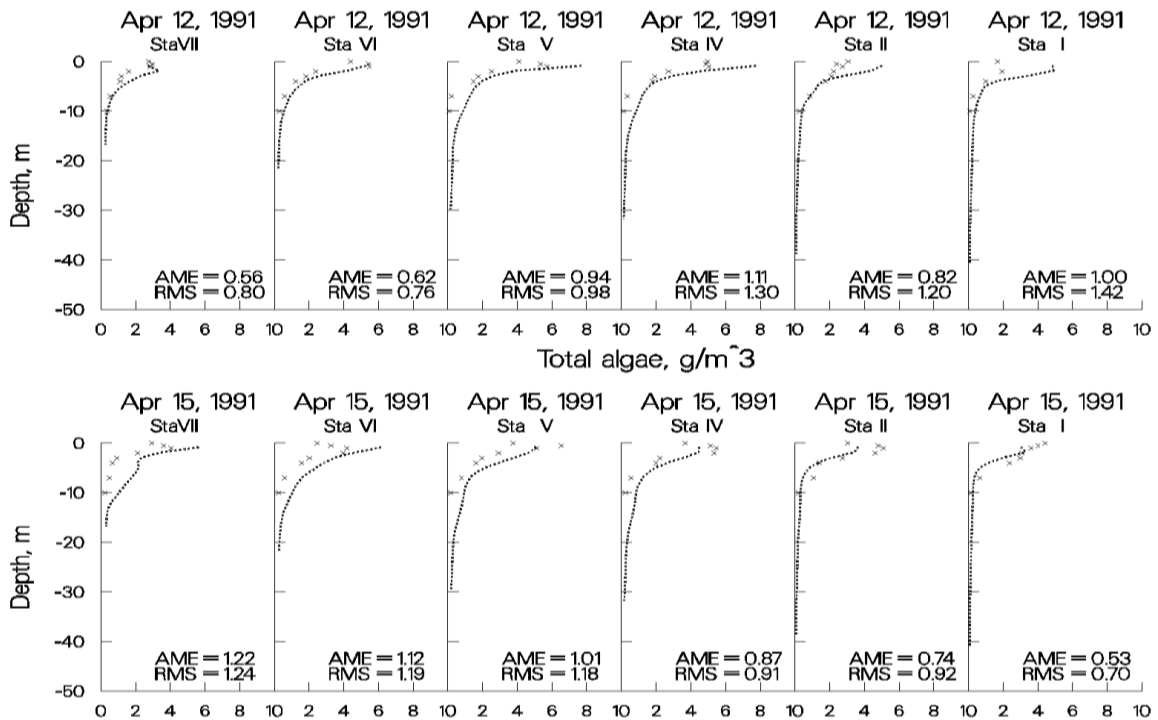


Figure 74. Rimov Reservoir computed vs. observed phytoplankton with wind rotated 90°.

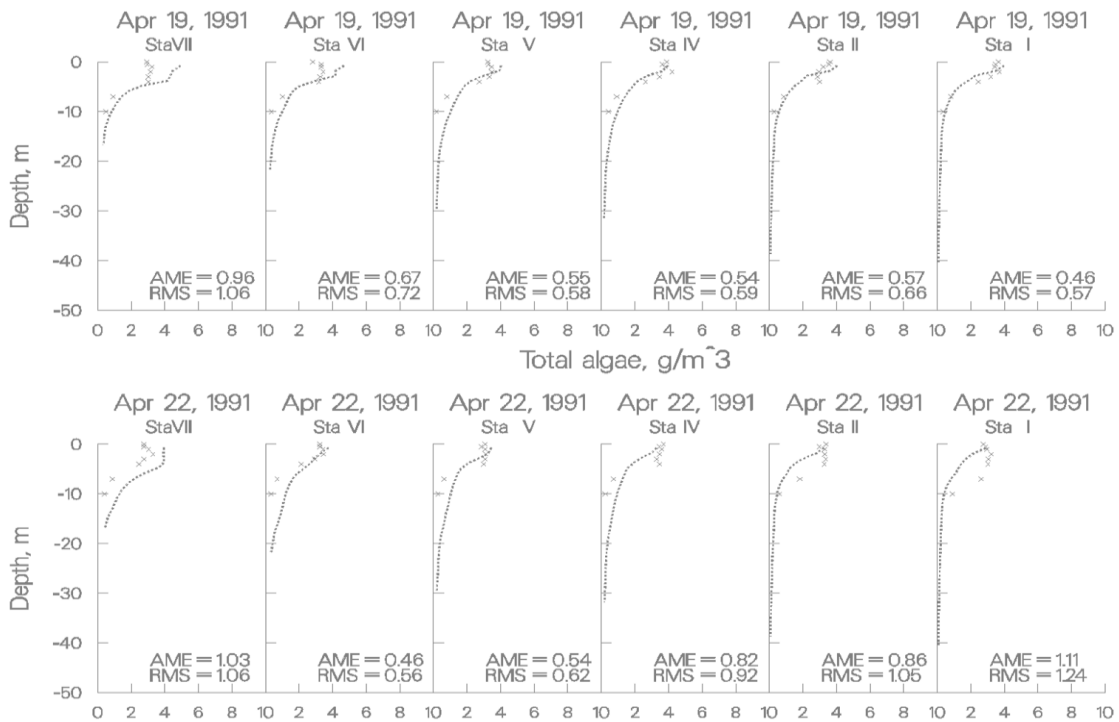


Figure 75. Rimov Reservoir computed vs. observed phytoplankton with wind rotated 90°.

CALIBRATION

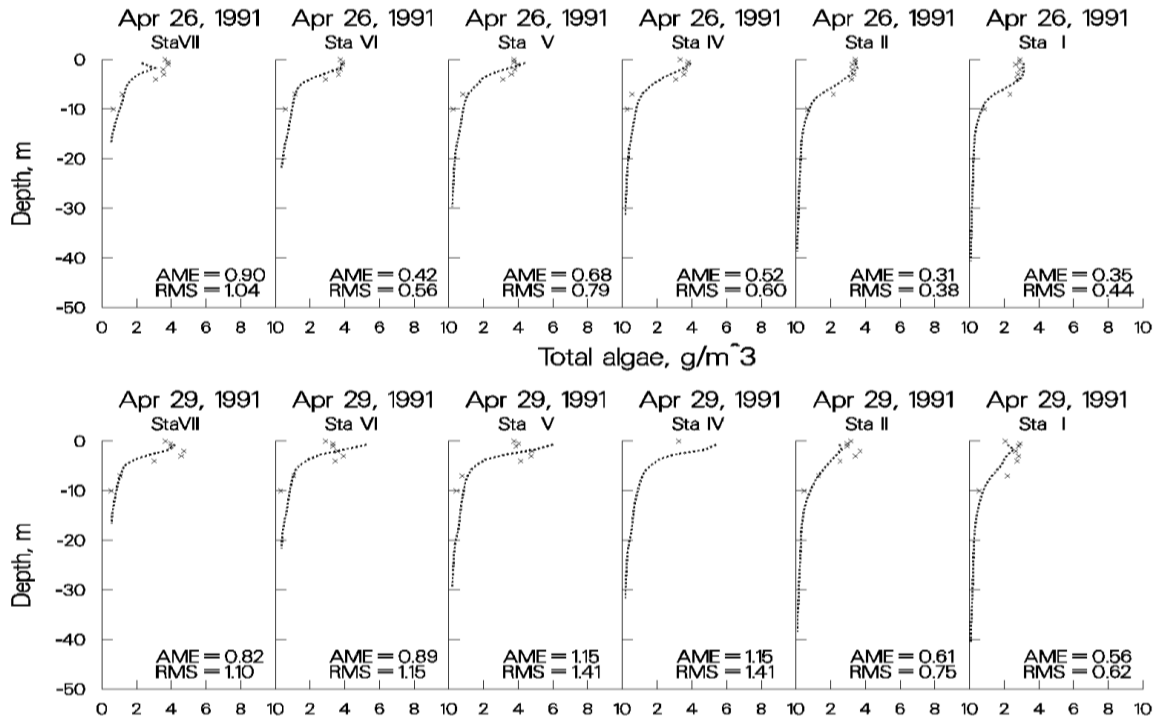


Figure 76. Rimov Reservoir computed vs. observed phytoplankton with wind rotated 90°.

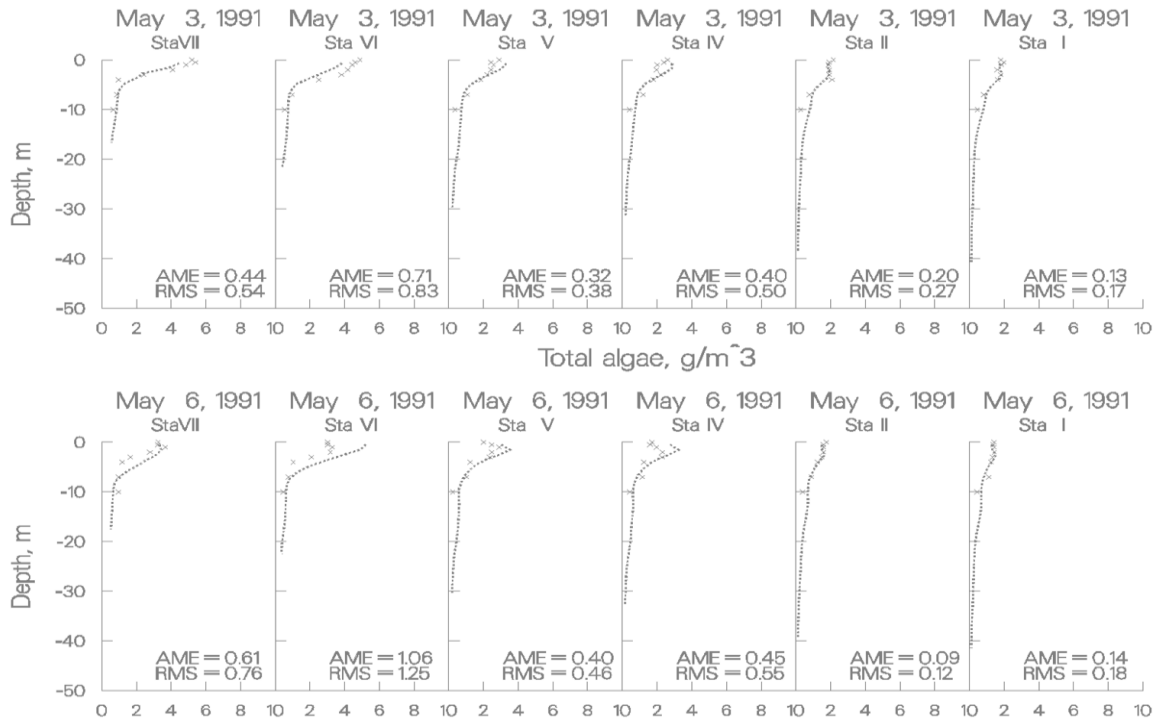


Figure 77. Rimov Reservoir computed vs. observed phytoplankton with wind rotated 90°.

The following plots illustrate the importance of accurate inflow boundary conditions for phytoplankton in Rimov Reservoir. Inflow phytoplankton concentrations were inadvertently set to 0.05 g m^{-3} rather than the observed concentrations when converting from V2 to V3. Again, the researchers who collected the original data concluded that the spring phytoplankton bloom was first initiated in Rimov because of inflowing phytoplankton. The model concurs with this conclusion and again illustrates how powerful a limnological investigative tool the model can be.

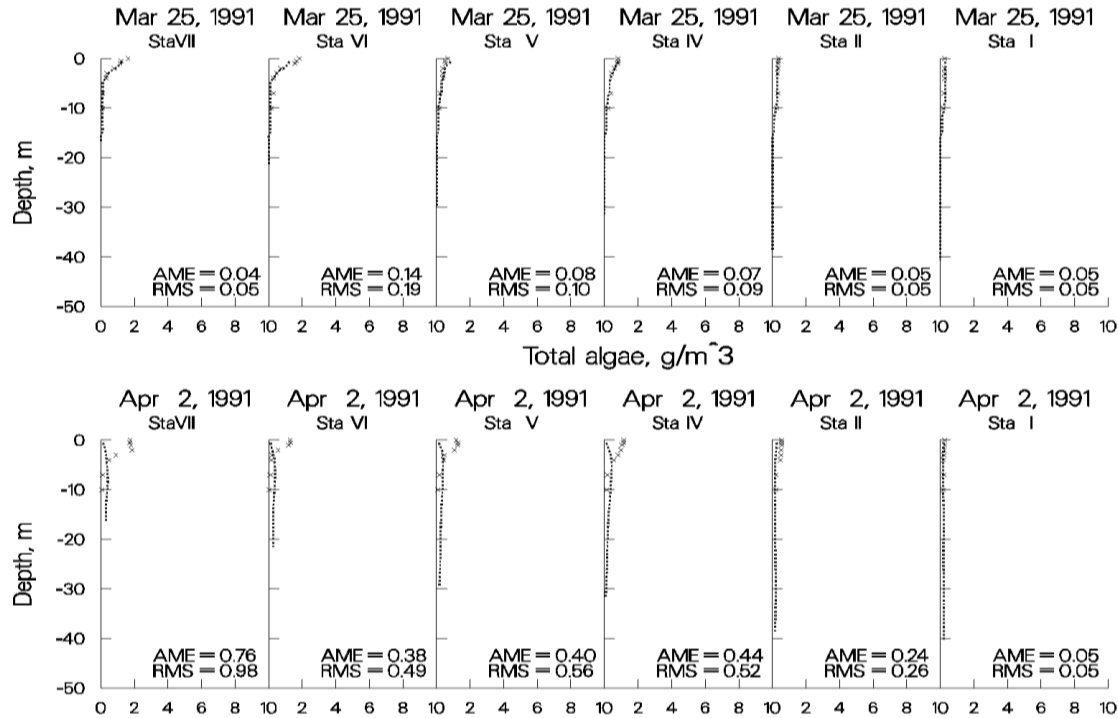


Figure 78. Rimov Reservoir computed vs. observed phytoplankton with no inflowing phytoplankton.

CALIBRATION

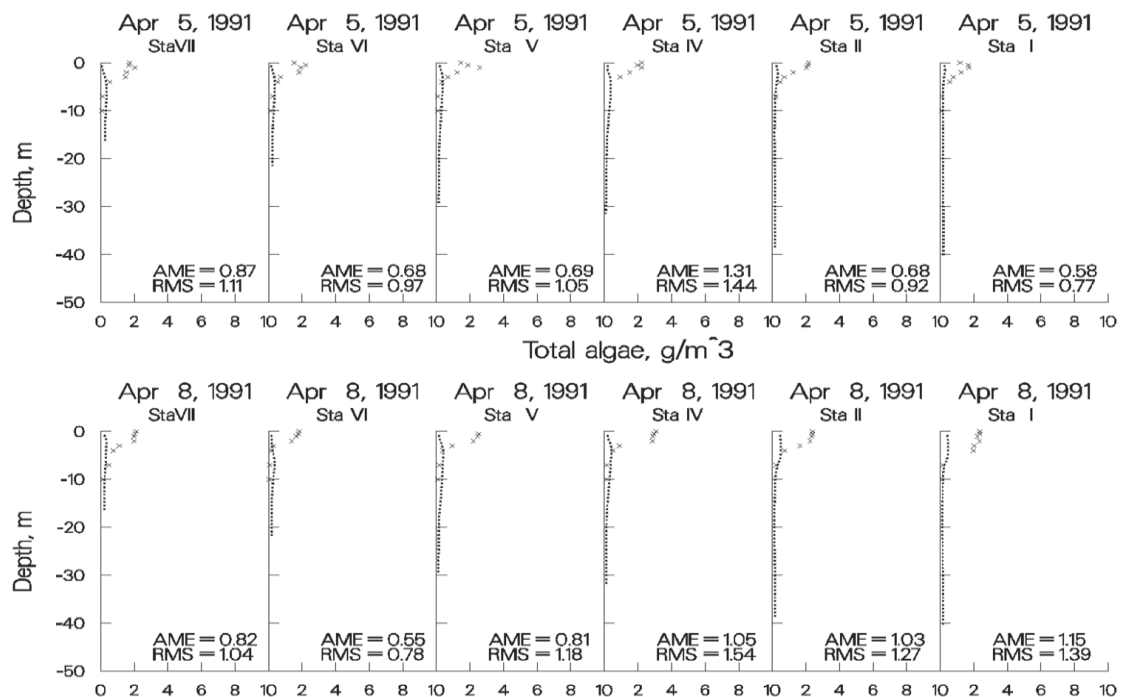


Figure 79. Rimov Reservoir computed vs. observed phytoplankton with no inflowing phytoplankton.

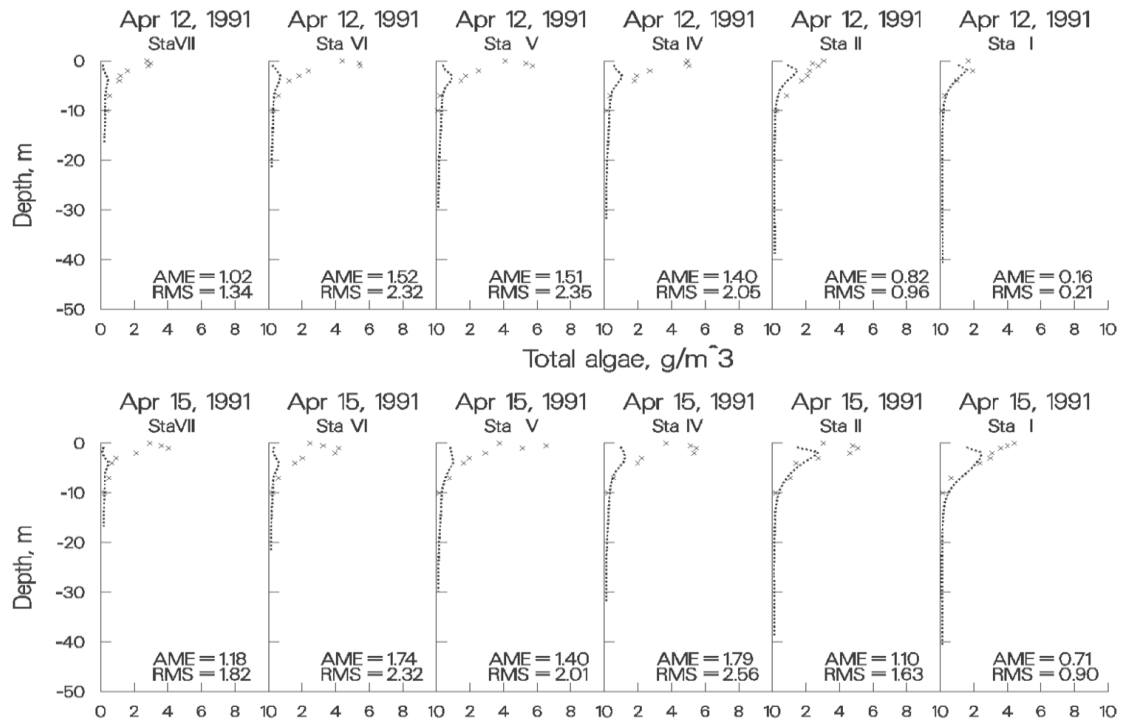


Figure 80. Rimov Reservoir computed vs. observed phytoplankton with no inflowing phytoplankton.

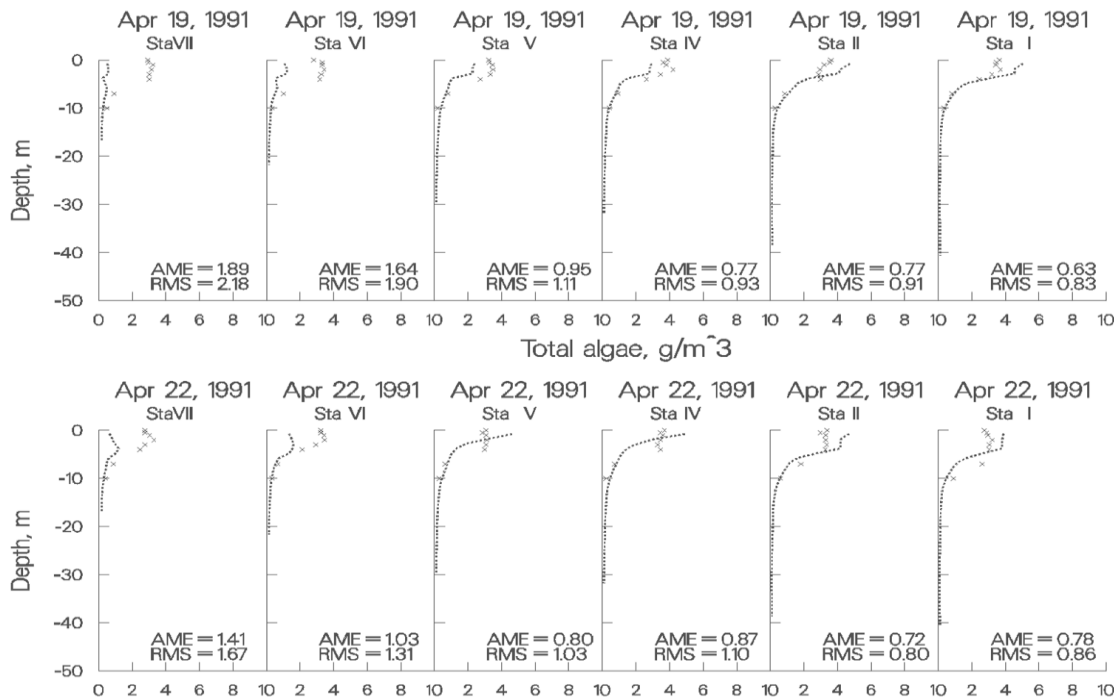


Figure 81. Rimov Reservoir computed vs. observed phytoplankton with no inflowing phytoplankton.

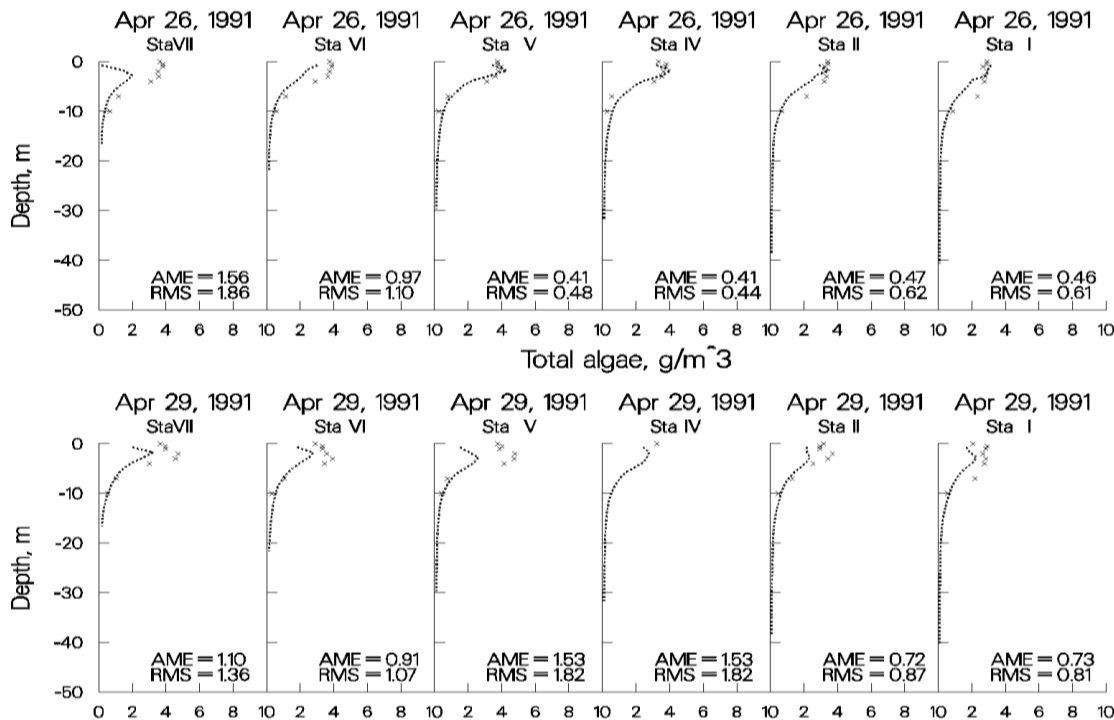


Figure 82. Rimov Reservoir computed vs. observed phytoplankton with no inflowing phytoplankton.

CALIBRATION

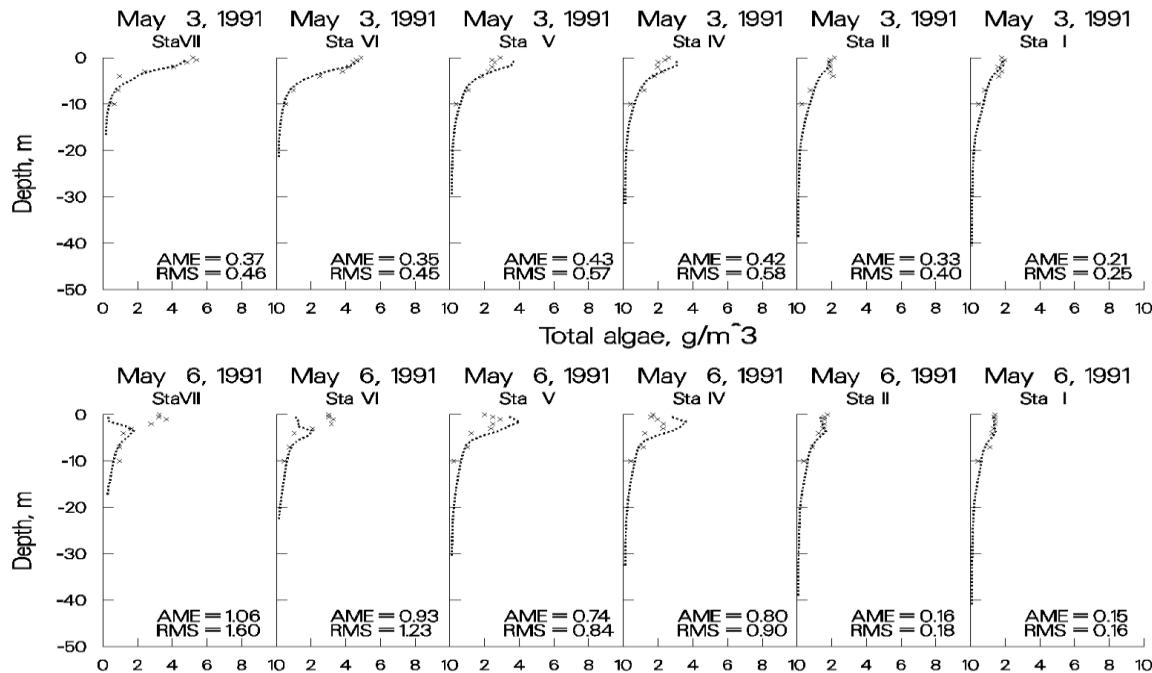


Figure 83. Rimov Reservoir computed vs. observed phytoplankton with no inflowing phytoplankton.

Estuary

Estuarine modeling is similar to reservoir and lake modeling for both bathymetry development and water quality modeling, but there are a few important differences in the hydrodynamic calibration. Salinity is commonly used to assess model hydrodynamic performance. However, as with reservoirs, water quality variables such as dissolved oxygen and phytoplankton can be used to also assess the accuracy of the hydrodynamics. When calibrating salinity, it is common practice to plot predicted versus observed time-series of surface and bottom salinity. While plots such as these are useful, vertical plots of computed versus observed salinity, if available, should always be included as part of the calibration process.

Boundary conditions

Ocean boundary conditions play a critical role in estuarine modeling and the data should be frequent and of high quality. At a minimum, downstream head boundary elevations should be available on an hourly basis. The model can be used to linearly interpolate [HDIC](#) between observed elevations. Alternatively, formulas can be used to compute elevations at any frequency based on various components of the tidal cycle.

Equally important are salinity concentrations specified at the downstream boundary. It is always preferable to set the boundary sufficiently downstream so that there is no vertical variation in salinity and hopefully only small temporal changes. However, the boundary needs to be set where the head elevations are measured, and oftentimes there are significant vertical and temporal variations in salinity at the site. Weekly vertical profiles are usually of insufficient frequency to reproduce the hydrodynamics of the estuary with any accuracy in this case. The same will hold true for temperature and constituents if they exhibit vertical and temporal variations.

Upstream freshwater inflows need to be accurately gaged and evaporation and precipitation should be included in the simulation if possible. Because of the inaccuracies associated with gaged inflows, sensitivity analyses should be run by increasing and decreasing upstream inflows to determine their impacts on hydrodynamics and water quality rather than initially turning to a model “knob” to adjust model results, particularly for vertical salinity distributions in a stratified estuary. Many times the model has provided information as to where forcing functions need to be more accurately measured for a successful model application.

Water surface elevations and flows

In an estuarine system, the first step is to make certain the model correctly replicates tidal elevations and flows at various stations along the length of the system. Usually these stations have continuous data for comparison. Problems in water level and flow calibration can be caused by the following:

1. **Incorrect or inadequate bathymetry.** The user should ensure that the model correctly reproduces cross-sections where these are measured. The model is very sensitive to small changes in the cross-section and more frequent cross-sectional data may be necessary for accurate water level and flow simulations.
2. **Incomplete inflow/outflow data.** A substantial amount of flow can often be unaccounted for as a result of not including tributaries, point sources, precipitation, stormwater, irrigation users, and groundwater. Although precipitation and evaporation will normally be minor sources and sinks, they should be included by turning on the precipitation **[PRC]** and evaporation options **[EVC]**. In an estuary, flow is very dependent on the cross-sectional area at a given location, so grid evaluation should also be part of the calibration process.
3. **Bottom friction.** Bottom friction values **[FRICT]** for an estuary significantly affect the water level. Bottom friction can be used to calibrate the model to observed water levels at gages along the length of the estuary.

In most cases, the initial water level **[WSEL]** in the estuary is specified as flat with a velocity field of zero. The model should be run for several days with steady-state inflows **[QIN]**, inflow temperature **[TIN]**, inflow salinity **[CIN]**, [meteorology](#), and downstream head boundary conditions for temperature **[TDH]** and salinity **[CDH]**. Once the temperature and salinity distributions are no longer changing, the simulation can continue with observed boundary conditions.

The initial water surface elevation should be the same elevation as the external downstream elevation **[EDH]** at the start of the simulation. If there is a large elevation difference between the initial condition water level and the first head boundary condition, the model can quickly become unstable because of large flows generated as a result of the water level differences at the head boundary.

Typically, the user will first plot observed versus computed water surface elevations for the simulation period after all the inflow/outflow data have been collected and the model is running to completion. Distributed tributary flows **[DTRC]** may need to be added or subtracted if the mean flows over a tidal period are not correct. The model user should also check not only instantaneous flow rates, but tidal average rates to make sure the total flow coming into the system at the upstream boundary condition agrees with the net residual flow at different locations downstream. This could point to unaccounted inflows or outflows.

The model user should always take the model segment next to the downstream boundary and compare it to the actual water level data used and the flow rate at the gage, if measured. This checks that the water level in the model is correct and the flow rate predicted by the model agrees with the field data at that

CALIBRATION

location. If the water level matches and the flow does not, this could point to channel bathymetry errors or too high or too low a channel friction near the head boundary condition.

A typical comparison of field data to model predictions of water level are shown in [Figure 84](#) for the Columbia River at Longview, Washington approximately 110 km from the Pacific Ocean. The absolute and root mean square errors were 0.12 m and 0.18 m, respectively, over the period of record with a maximum tidal range of 1.5 m.

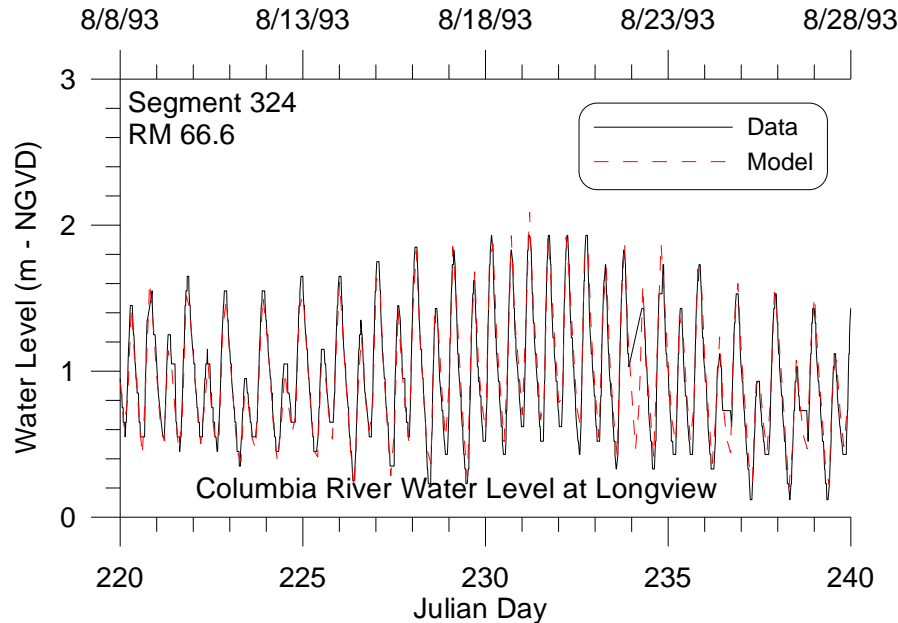


Figure 84. Water level data versus model predictions for Longview, WA during a 20-day period in 1993.

Similarly, a typical comparison of model predictions and field data of flow rate is shown in [Figure 85](#) for the Columbia River approximately 90 km from the Pacific Ocean.

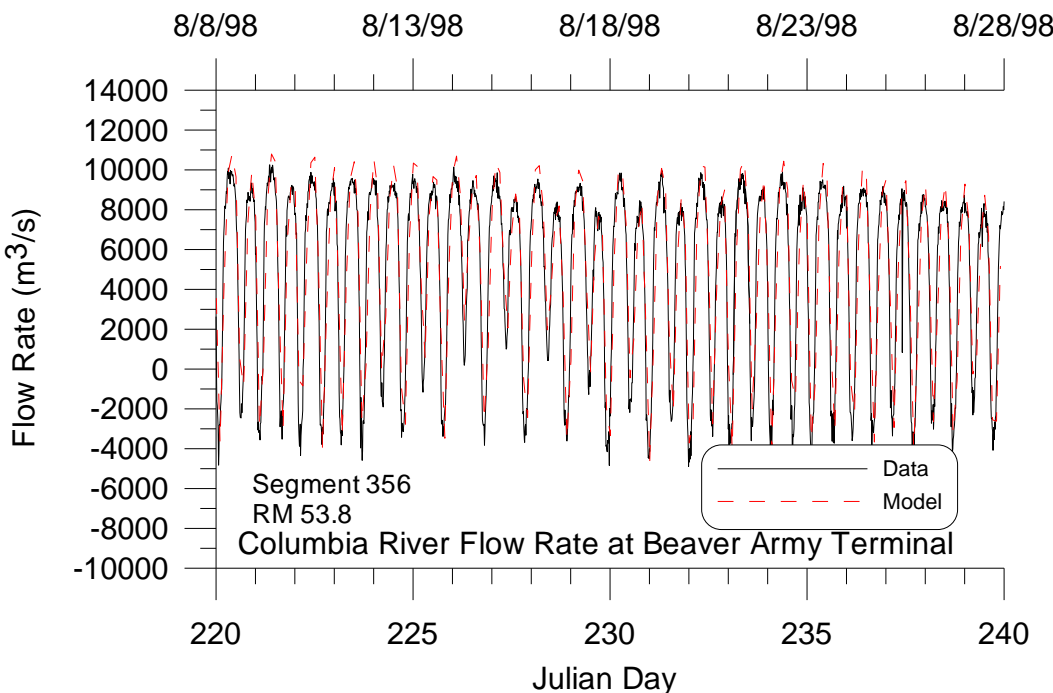


Figure 85. Model flow predictions versus data for a 20-day period during 1998 at Beaver Army Terminal near Quincy, OR.

Time of Travel

If at all possible, the model should be calibrated to a time-of-travel or dye study. This is important to ensure the model represents transport and mixing characteristics of the estuary accurately. Usually, the adjustment of bottom friction is the primary calibration parameter, but in some cases the bathymetry may need revision. The longitudinal eddy viscosity [AX] and diffusivity [DX] can also be adjusted during calibration. Since CE-QUAL-W2 uses a constant value for these coefficients for each waterbody, the user may need to include a longitudinal dispersion algorithm based on theoretical formulae if the constant value is not appropriate.

In many cases a dye release will also vary vertically as a result of stratification. The model internally computes the vertical diffusion coefficient based on the eddy diffusivity using the Reynolds analogy. The model user should ensure that they are using the implicit solution technique for the transport of vertical momentum, **[AZSLC]**=IMP, and that the maximum value of the vertical eddy viscosity **[AZMAX]** is at least $1 \text{ m}^2 \text{ s}^{-1}$ for estuarine systems.

Temperature and Salinity

Calibrating the model for estuarine temperature and salinity includes the same caveats as for reservoirs with, as previously mentioned, the additional need for accurate boundary conditions at the ocean boundary. If the user has developed a good hydrodynamic calibration for water surface elevations and flows, then temperature and salinity calibrations should require a minimal effort. However, keep in mind that water surface elevation, flow, and time of travel calibrations are all affected by the adequacy of the temperature and salinity calibration.

CALIBRATION

[Figure 86](#) and [Figure 87](#) are from an application of CE-QUAL-W2 to the estuarine portion of the Patuxent River that feeds into Chesapeake Bay (Lung and Bai, 2003). They illustrate the model's ability to reproduce vertical profiles of salinity and temperature over time.

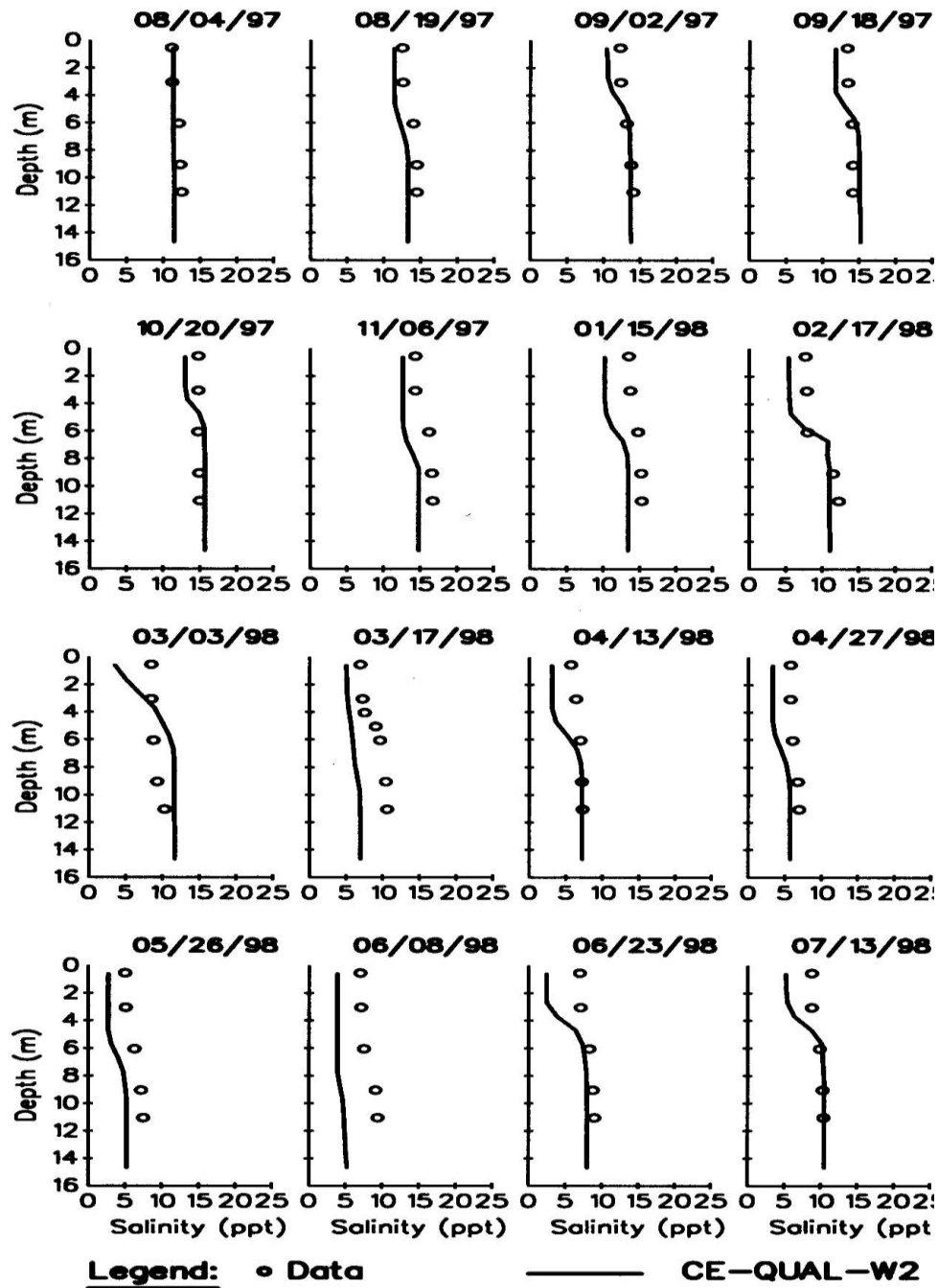


Figure 86. Patuxent River computed versus observed vertical salinity distributions.

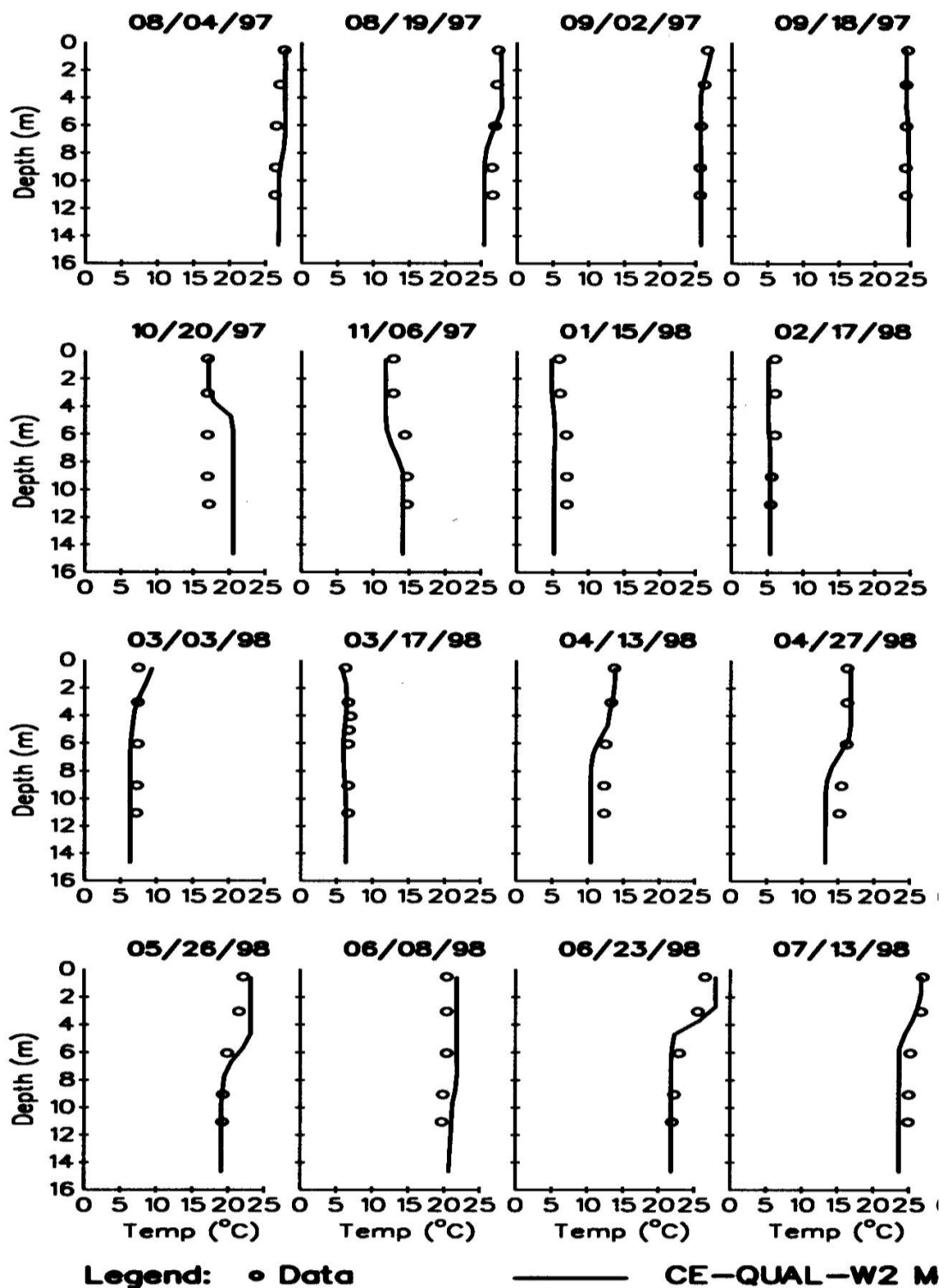


Figure 87. Patuxent River computed versus observed vertical temperature distributions.

CALIBRATION

Water Quality

Water quality calibration for estuaries is again subject to the same caveats as for reservoirs with the additional importance of accurate downstream boundary conditions. Again, if at all possible, the downstream boundary should be located sufficiently downstream where vertical variations in water quality are negligible.

[Figure 88](#) presents results for nutrients, dissolved oxygen, and chl *a* concentrations for Lung and Bai's Patuxent River application of the model.

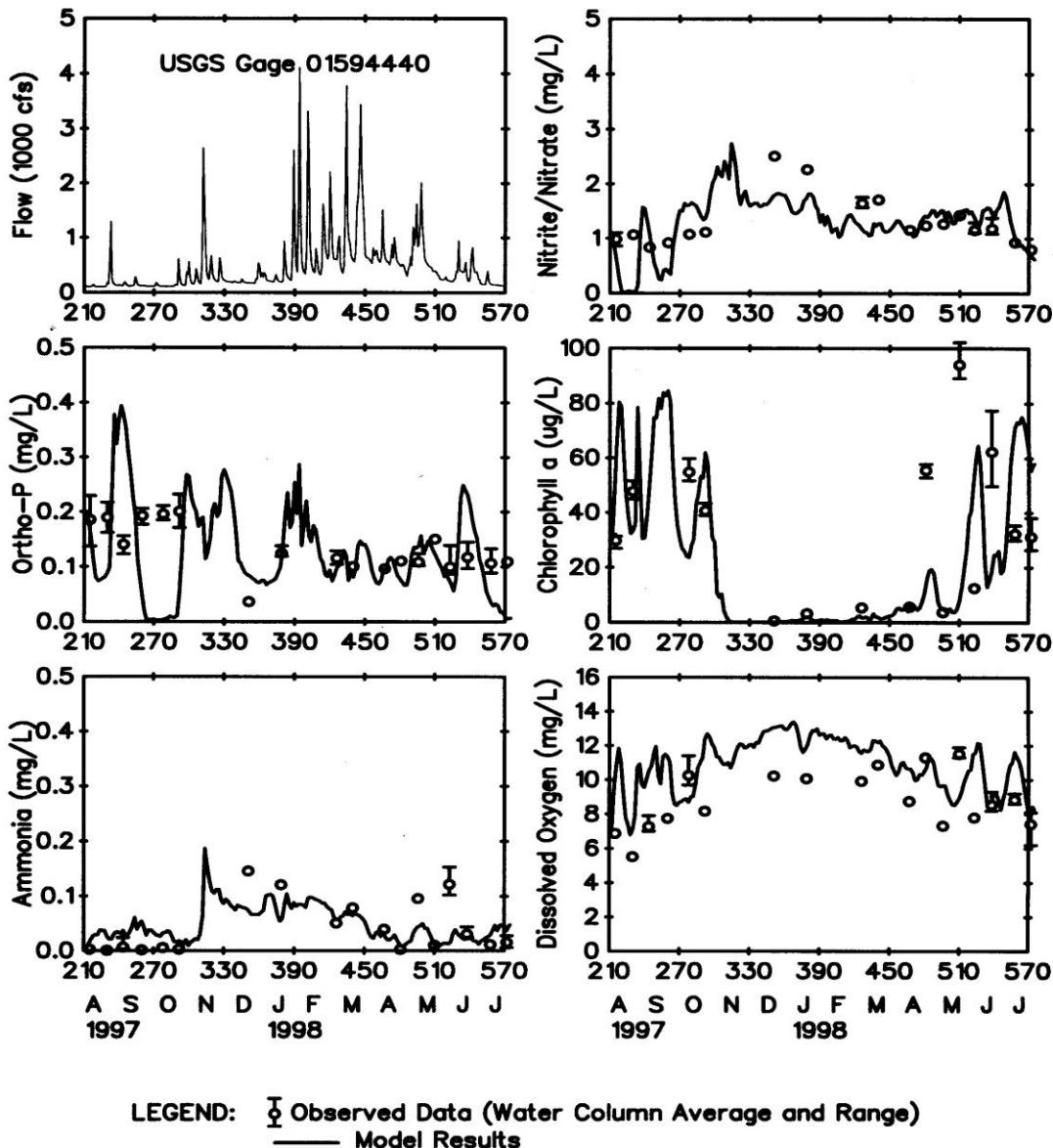


Figure 88. Patuxent River computed versus observed nutrient, dissolved oxygen, and chl *a* time series.

Calibration Problems Modeling an estuarine system requires a tremendous amount of data, expertise, and patience for proper calibration. In previous estuarine applications, calibration consisted mainly of determining whether known inaccuracies in a given forcing function could be responsible for the discrepancies in the model predictions and then describing the forcing function more accurately. This procedure included the following:

1. Ensuring the model reproduces flow and water level at various control points in the model domain and involved detailed evaluation of inflows and outflows, head boundary conditions, channel bathymetry, and channel friction.
3. Adjusting channel friction or longitudinal dispersivity to match time-of-travel data or dye study field data
4. Ensuring accurate vertical profiles for the downstream boundary
5. Ensuring grid refinement does not affect the model results
6. Ensuring accurate meteorological data for the estuary especially if the model domain extends over a large geographical area. Wind variability is extremely important and can be reflected in the wind sheltering coefficient that varies by segment and time.
7. Using an implicit eddy viscosity solution scheme, **[AZSLC]**=IMP, and a maximum vertical eddy viscosity **[AZMAX]** of $1 \text{ m}^2 \text{ s}^{-1}$.

Since the model can be susceptible to accuracy issues using an implicit water surface solution scheme with a large time step, the user should ensure results are not impacted by using a smaller maximum time step **[DLTMAX]**. Again, keep in mind that the more accurately the behavior of the prototype is described, the more accurately the model responds.

River

Dynamic river modeling can be a challenging endeavor because:

1. Velocities are generally high resulting in a lower time step for numerical stability
2. Shear and bottom friction effects are significant requiring a considerable calibration effort
3. Channel slopes accelerate the fluid
4. Changes in river bathymetry can dramatically affect the velocity field
5. Dynamic flow rates at low flows can dry up segments causing the model to stop running

One of the original motivations for development of the capability of modeling sloping rivers was to eliminate vertical accelerations in the fluid since the model does not solve the full vertical momentum equation. Keeping this in mind, the grid slope should be chosen to minimize the vertical fluid acceleration.

Channel Slope

The channel slope is used to compute the gravity force of the channel. This slope should be the slope of the water surface as that is the slope used to accelerate fluid parcels, or the energy grade line, rather than the bottom slope from segment to segment. As an example, consider the slope of a section of the Snake River shown in [Figure 89](#).

CALIBRATION

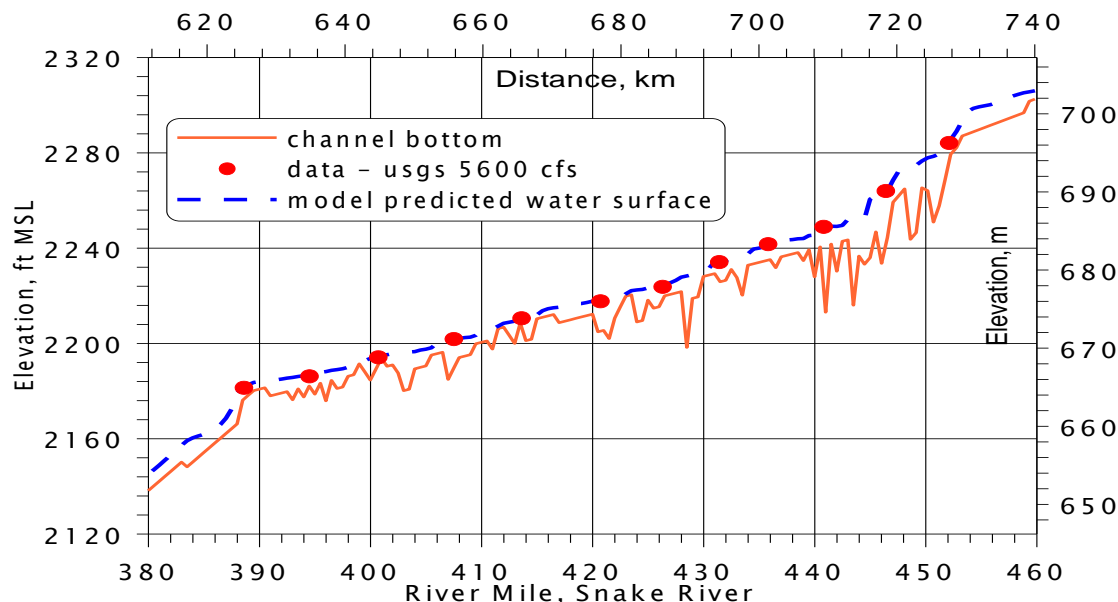


Figure 89. Snake River water level comparison between CE-QUAL-W2 V3 and USGS field data.

The slope of the vertical grid as well as the different branch slopes is shown in [Figure 90](#).

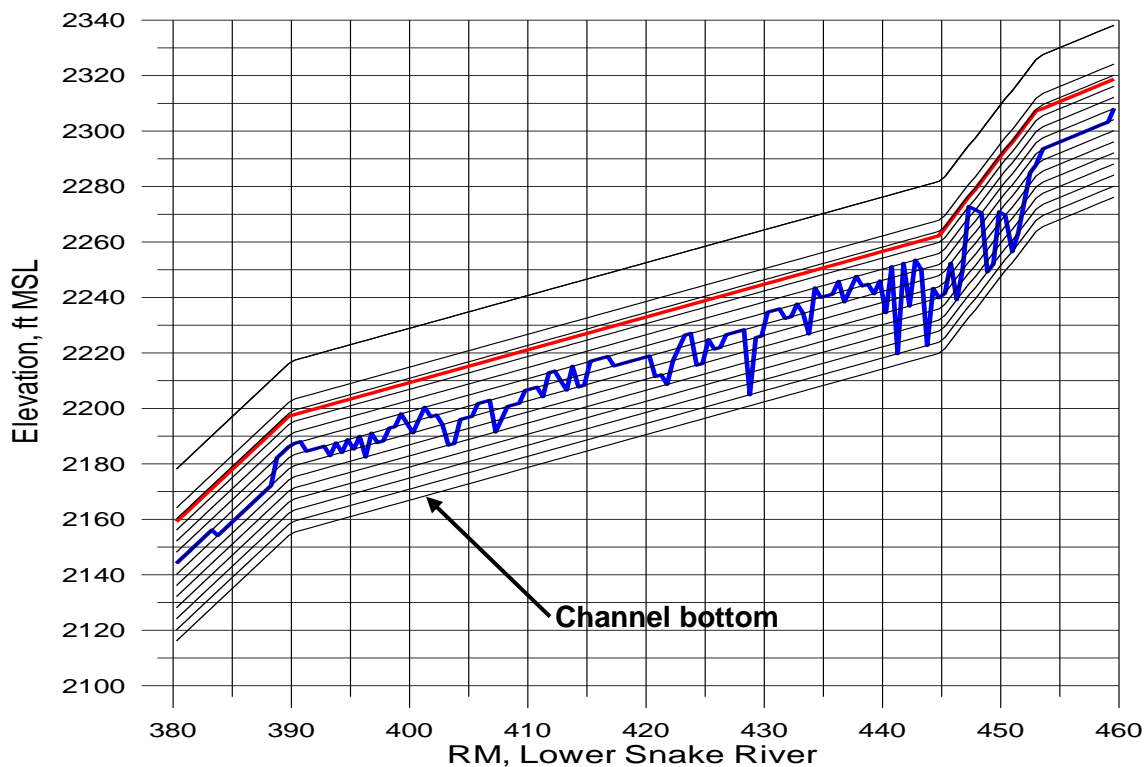


Figure 90. Channel vertical grid where every slope change is a new branch.

Rather than going from segment to segment with varying slopes, a general channel slope is used for a collection of segments with similar water slope. As the variability in water slope changes, so does the grid Model Examples and Applications

slope. How can one obtain this slope? [Figure 91](#) illustrates the use of a regression line to fit the channel slope for the section between RM 390 and 445 for the Snake River.

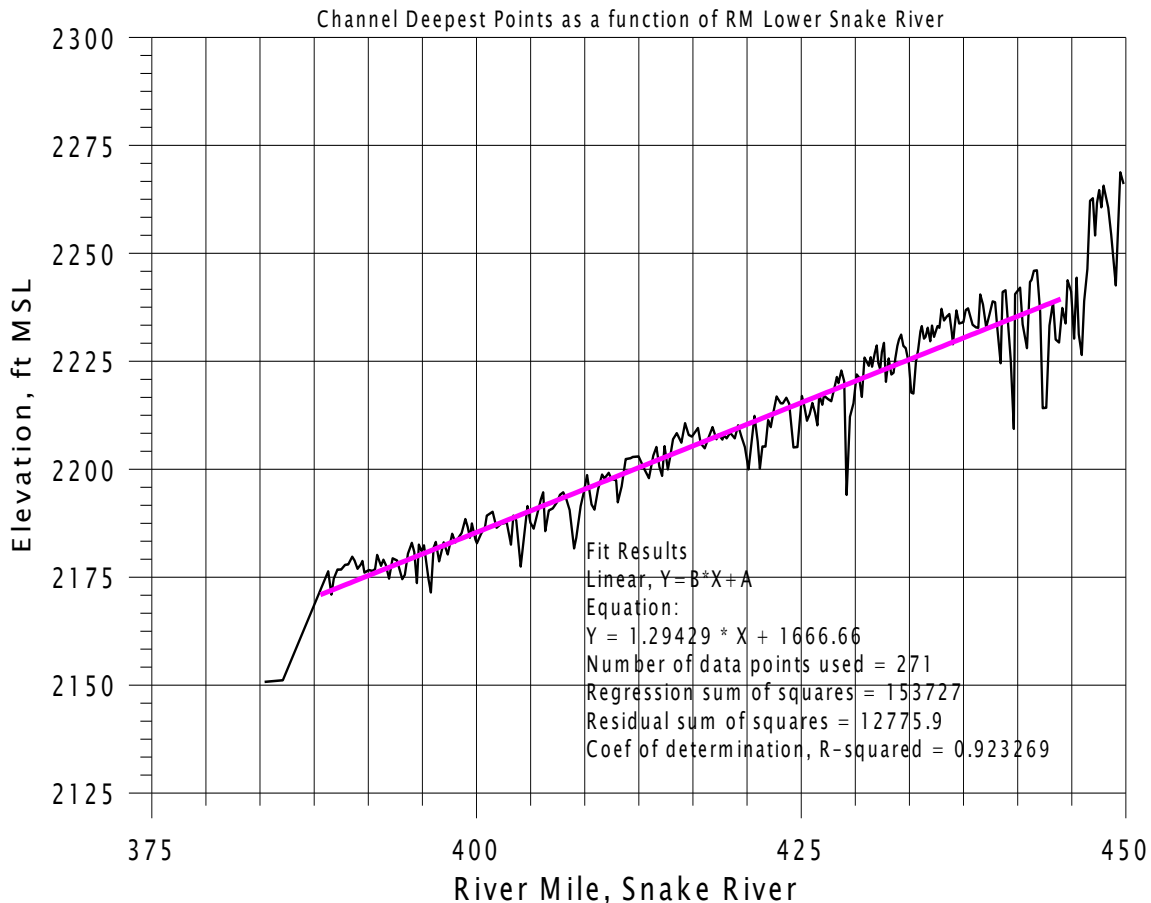


Figure 91. Snake River channel slope determination.

Why does W2 not use a segment-by-segment slope? Consider the “noise” in the cross-sections in [Figure 91](#). Even though the geometry could be set up with a variable channel slope for each segment (in the current application this means creating multiple waterbodies or branches for each slope), setting a general channel grade is often simpler and one still has the noise of the bathymetry represented as shown in [Figure 91](#). Computing the slope from one segment to a deep hole would not be correct since the water is flowing along its energy grade line and not the channel slope. Bottom elevations for many of the channel segments rise or have a negative channel slope following a depression. In using a segment-by-segment slope, these variations become unrealistic when represented using a slope for each segment. Therefore, the proper channel slope should be that of the water surface.

In estuarine flow, one usually uses a channel slope of zero and considers fluid accelerations as a result of water surface elevation changes rather than gravity flow down a slope, at least in the estuary section below the head of tide. This is similar in a reservoir, which may have a sloping channel, but a relatively flat water surface.

In some cases, the average channel slope changes and the user must separate the different sections into separate branches or waterbodies. The model can be set up to have almost continuous changes in channel

CALIBRATION

slope by making branches with two segments and changing the slope where it is required. If the choice is to create separate branches, then the surface layer and grid will be the same for all branches. If the choice is to create separate waterbodies, then each waterbody computes a surface layer independently of the other and there can be different vertical grids between water bodies.

When there are problems keeping water in upstream segments, which is a very common problem, the model takes the lowest water level in a waterbody and subtracts layers such that the lowest water level resides in the surface layer. If the surface layer is below the bottom layer in a segment, the model will subtract that segment and all segments above it from the active computational grid. If this occurs in a shallow location in the middle of a branch, the model will not run since it dries up a segment in the middle of a branch.

How can this be corrected? One way is to decouple one branch from another by splitting them into waterbodies. By splitting the system into more than one waterbody, water can be maintained at various levels throughout the domain since each waterbody has its own separate surface layer.

This is another reason why the model does not use segment-by-segment slopes since the surface layer defines the upper layer for a waterbody and in many cases these need to be broken apart into waterbodies to keep water in all segments. In addition, the translation from one waterbody to another introduces some small error into the solution since concentrations, temperatures, and velocities are interpolated from one 2D grid onto another. If the model were run in 1D mode with only one vertical layer, then this problem would not exist.

Consider another case study, the Bull Run system shown in [Figure 92](#).

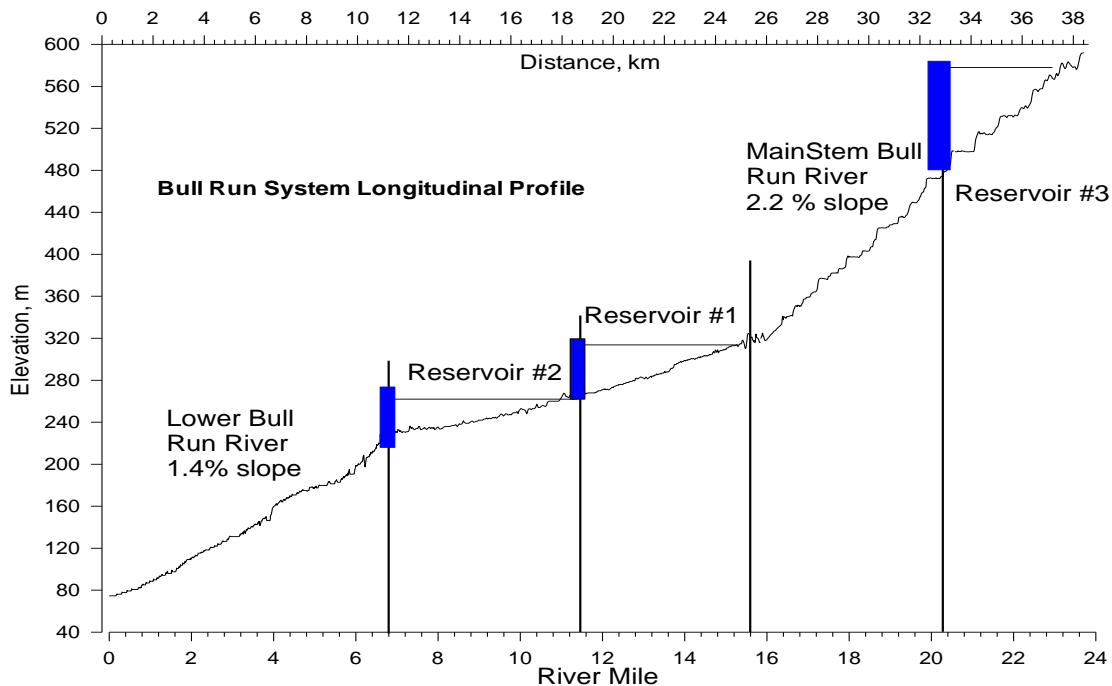


Figure 92. Channel slope for the Bull Run system.

The reservoirs were modeled with a channel slope of zero. Instead of a constant slope of 1.4%, the river is really divided into a large number of small-scale changes including pools and riffles. A section of the river

is shown in Figure 93 with the assumed model grid divided into branches and waterbodies. In most cases, different waterbodies were used between branches of different slope. This allowed the water surface layer determination to be based on the water level in the branch with the given slope. However, the steeply sloping section may not have a slope equal to the grid slope shown. This may occur because if the steeply sloping section were modeled in more detail, it would really be a series of “flat” pools with small water drops (or falls) between the pools. If all the fine scale variability is ignored and the system is modeled on a larger scale, the problem becomes one of trying to estimate the “equivalent” channel slope that represents the channel.

This is similar to modeling a network of pipes and ignoring all the details but inserting pipes of “equivalent” slope and diameter. In this case, the channel slope is used as a calibration tool to match water level or dye study data. If channel friction were used to hold the water back, the values would have to be enormous to reproduce the complicated pool-waterfall system.

In addition, if the grid is broken into different waterbodies, discontinuities in the water surface such as waterfalls can be simulated.

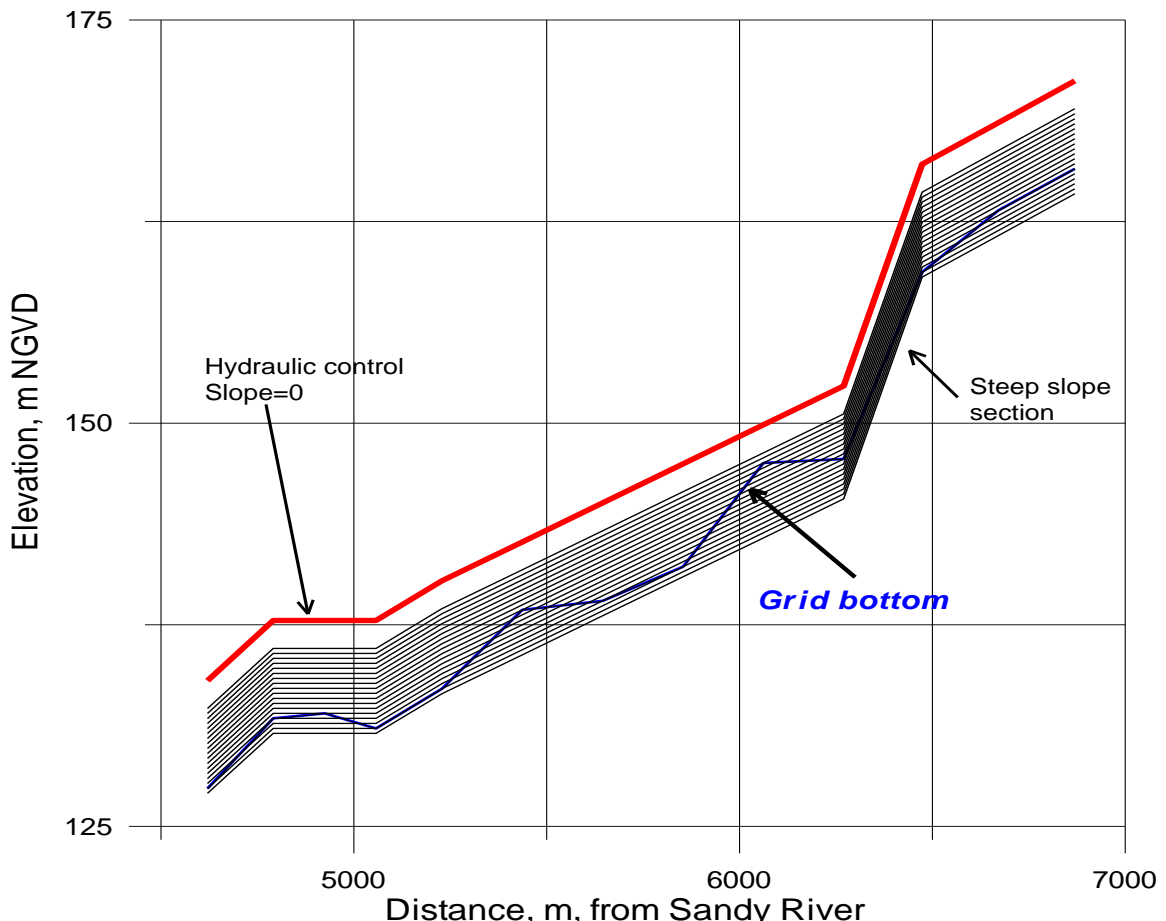


Figure 93. Vertical grid for W2 model of Bull Run Lower River.

Modeling of shallow streams with large slopes is difficult and takes patience. The model drying out at intermediate sections is often the cause of problems and can be remedied by breaking the system into smaller pieces or waterbodies and/or by adding additional computational cells below the bottom layer at a given

CALIBRATION

segment. Matching river data is accomplished by adjusting friction factors, refining the geometry, and in some cases refining the “equivalent” channel slope if detail has been sacrificed in setting up the model. The quality of the model geometry is essential for good model-data reproducibility in a river system, especially one that is highly irregular in slope and channel width.

Developing a river model is also difficult at low flows since the model may become either unstable during the initial time steps or become dry in a segment. The reason for this is that, in the beginning, an initial water surface elevation is set and the river is “frozen” at that elevation until the model is started, at which point the water starts moving downstream. If a conservative high water is set initially in all segments, a wall of water will be sent downstream. If inflows are so small that at the upstream edge of this wave there is too little water, segments can dry out. The model includes a warning [w2.wrn] and error file [w2.err] that contains information for debugging a river model problem.

The following are suggestions for setting up a river model:

1. For the first 0.1 JDAY or so of the simulation, choose a maximum timestep [**DLTMAX**] that is small (10 s or less). This should be done only if the code seems to go unstable soon after starting the model. Alternatively, one can lower the fraction of the timestep [**DLTF**] used as this can provide numerical stability and allow for higher timesteps. The maximum timestep should be lowered if the number of time step violations is greater than 10% for an extended period of time.
2. Start with high flow rates gradually approaching the lower flow regime if model stability is a problem at low flows.
3. In order to keep water in the model, friction factors and geometry are very important considerations. The goal is to have sufficient model friction so that water does not quickly drain out of the system.
4. Add active computational cells at the bottom of the grid using small widths to prevent the section of the river from drying up or subtracting segments unnecessarily because the water surface layer [KT] is below the bottom [KB].
5. For a river that has sloping sections followed by flat sections (slope=0), you may want to set the slope to a non-zero value of 0.000001. This activates in the code the ability of the model for KT to be below KB when the segment is still hydrated.
6. If the water surface elevation becomes unstable as evidenced by a negative surface layer thickness, try reducing the maximum timestep [**DLTMAX**] to 5-10 seconds or less during the unstable time period. Alternatively, the fraction of the timestep [**DLTF**] can be set to 0.5 or less during this period.
7. For the end of the river, often a weir/spillway condition is used. This allows the specification of the stage-discharge relationship for the river. See the Part 2 of the User Manual under Spillways for an example of how to do this.
7. Set AZSLC=IMP and AZMAX=1.0. Do not use ASC=W2; use one of the other formulations.

The following discussion illustrates the model’s ability to accurately simulate river hydrodynamics, temperature, and water quality and includes a synopsis of the model’s application to the Bull Run River, Snake River, and Spokane River

Bull Run River. The Bull Run River is located in Oregon and the two existing reservoirs located on the river provide water for the city of Portland ([Figure 92](#)). A third reservoir upstream of the existing reservoirs is in the planning stage. The two portions of the free flowing river that were modeled had slopes of 1.4% and 2.2%. The model was used to address temperature and suspended solids questions about the system.

Snake River. The Lower Snake River from C.J. Strike to Brownlee Reservoir suffers from eutrophication problems below the city of Boise. Chlorophyll *a* concentrations in the river often exceed $100 \mu\text{g l}^{-1}$ and ultimately can cause severe dissolved oxygen depletion in the upper reaches of Brownlee Reservoir leading to fish kills. The model was used to determine how inflowing algae and nutrients affect chl *a* and dissolved oxygen concentrations in Brownlee Reservoir.

Spokane River. The Spokane River from the Idaho border to Long Lake was modeled as part of a Total Maximum Daily Load allocation study and was conducted by Portland State University, the Washington State Department of Ecology, and the U.S Army Corps of Engineers. Epiphyton were added to the model because of their importance on nutrient and dissolved oxygen dynamics in the River.

The system is complex hydraulically with three run-of-the-river impoundments used for power generation, significant groundwater inflows during low flow periods, a water fall, and Long Lake, a deep storage impoundment. Although Long Lake is a long and fairly deep reservoir, residence times during the summer are relatively short (< 1 month). Therefore, accurate inflow temperatures and constituent concentrations were crucial for accurate simulations of temperature and water quality in Long Lake, which required accurate simulations of over 40 miles of the Spokane River upstream of Long Lake.

The system is also complex with respect to water quality as epiphyton dominate nutrient and dissolved oxygen dynamics in the river and phytoplankton dominate their dynamics in Long Lake. Additionally, there are four point source discharges including the City of Spokane's wastewater effluent.

Hydrodynamics and Temperature

[Figure 94](#) shows results of a dye study conducted as part of the hydrodynamic calibration for the Bull Run River. Results show that the QUICKEST/ULTIMATE transport algorithm does not suffer from excessive numerical dispersion nor does it generate over/undershoots and that the model is capable of accurate river hydrodynamic simulations.

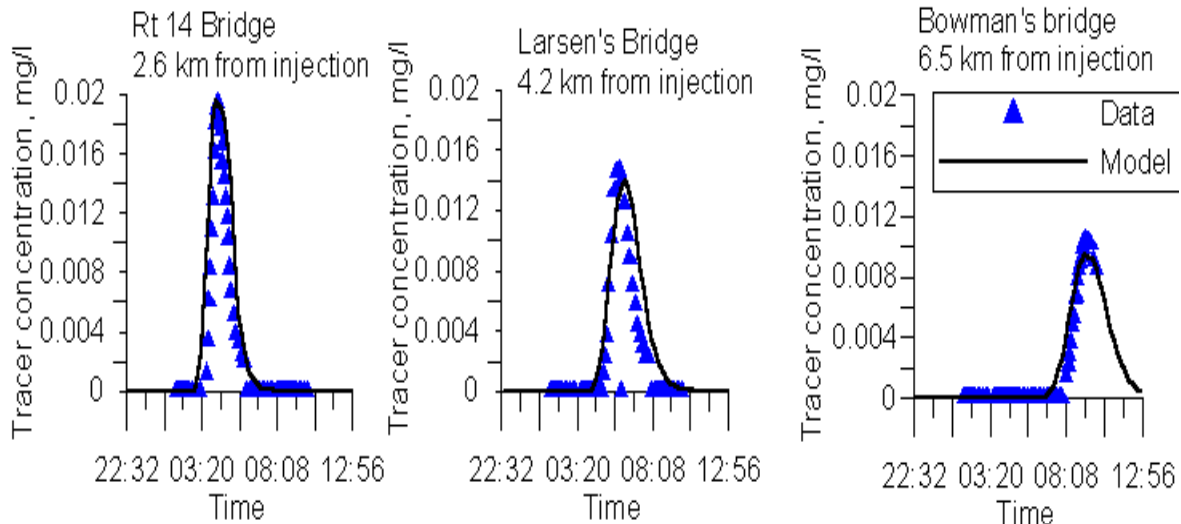


Figure 94. Bull Run River computed versus observed tracer at three stations progressing downstream.

CALIBRATION

[Figure 95](#) illustrates the accuracy of the water balance at the City of Spokane and [Figure 96](#) shows the accuracy of the computed flows at the same location.

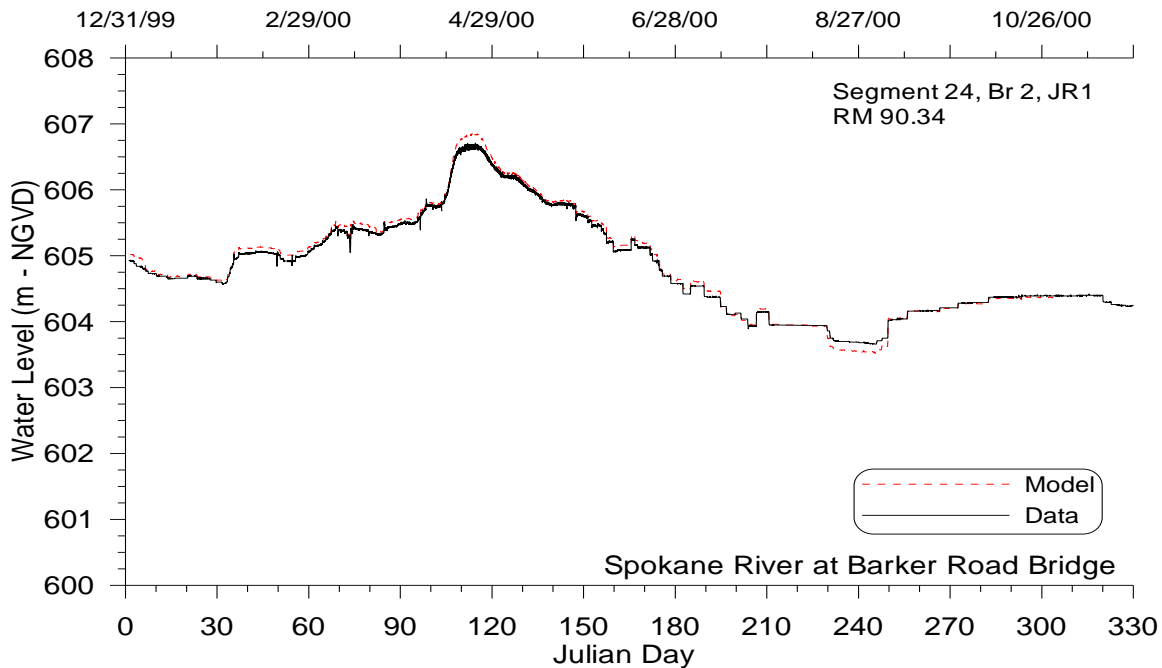


Figure 95. Spokane River computed versus observed water surface elevations at Spokane.

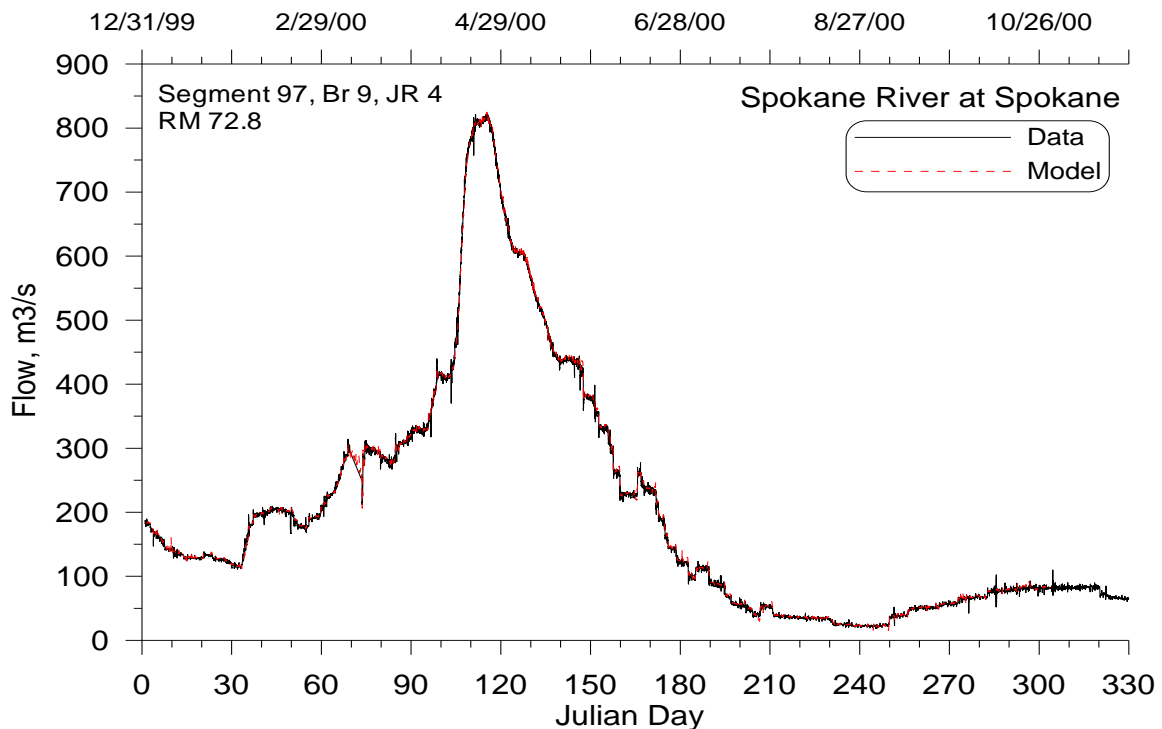


Figure 96. Spokane River computed versus observed flows at the city of Spokane.

Computed versus observed temperatures are shown in [Figure 97](#) and [Figure 98](#) for the Snake and Spokane rivers. As for reservoirs, temperature predictions are in close agreement with observed data.

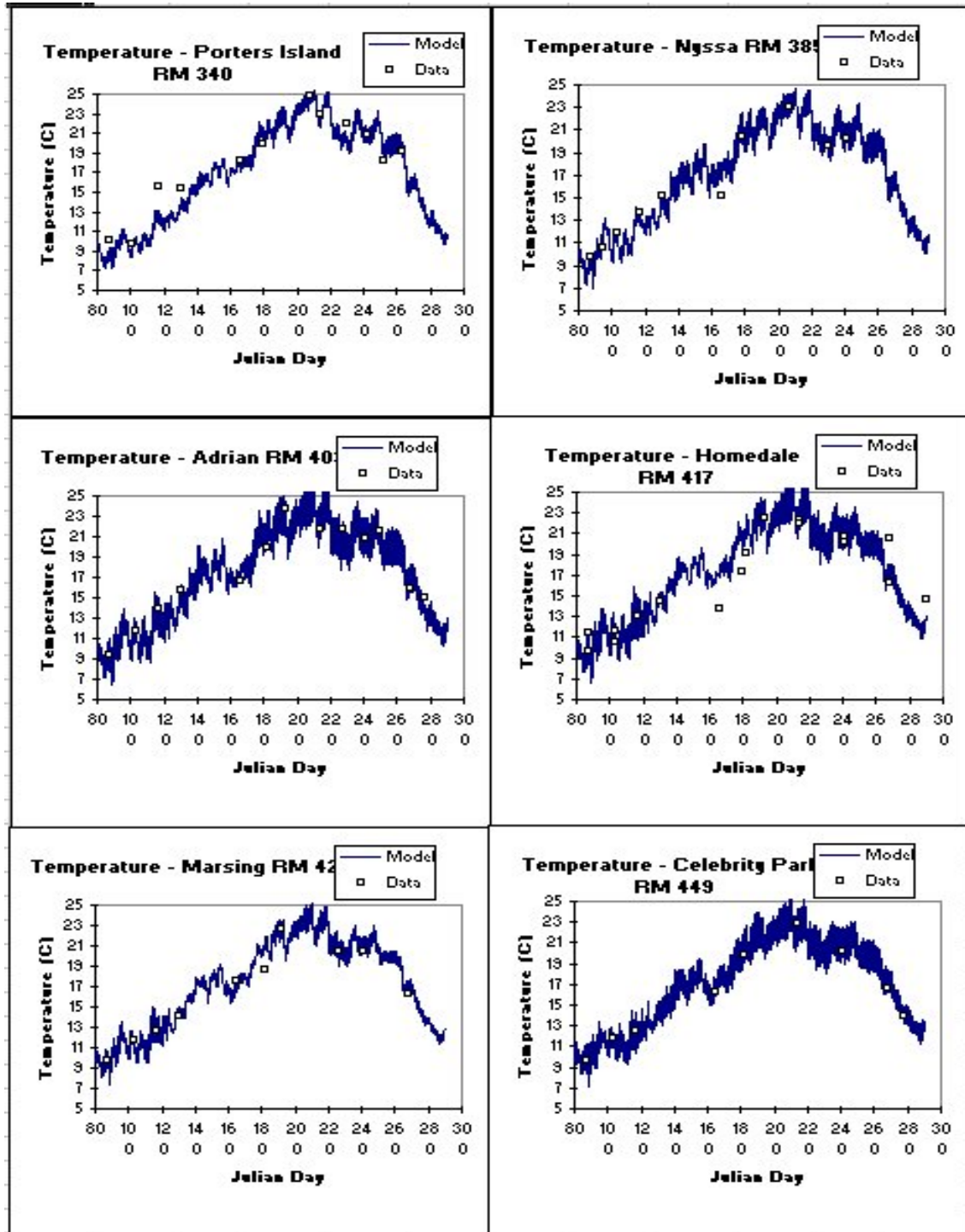


Figure 97. Snake River computed versus observed temperature at six stations.

CALIBRATION

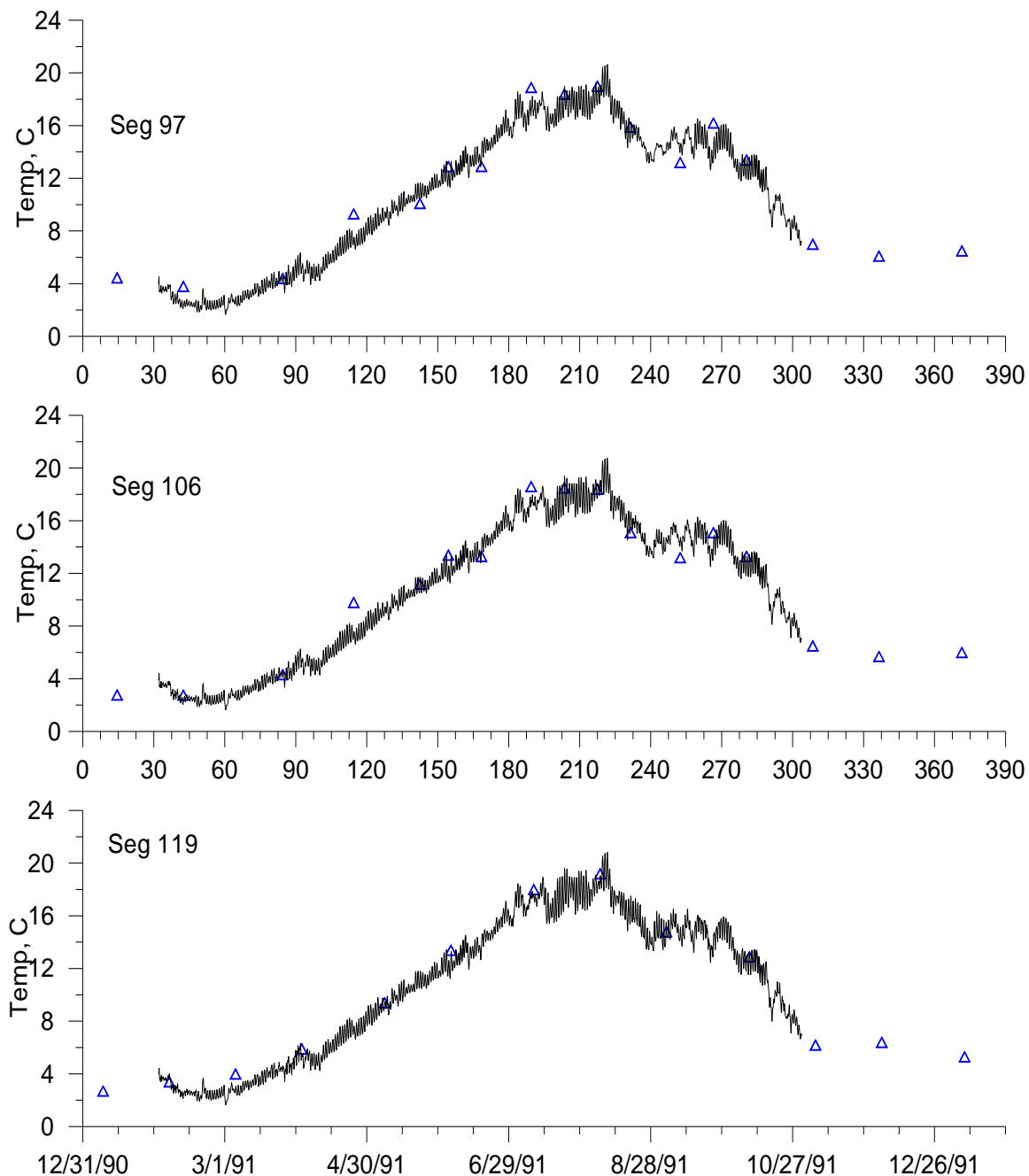


Figure 98. Computed versus observed temperatures for the Spokane River at Stateline Bridge (upstream boundary), City of Spokane, Fort Wright Bridge, and Riverside State Park.

For the Spokane study, conductivity was an important indicator of not only the hydrodynamics but also of the groundwater portion of the water balance. The model is accurately reproducing the temporal variation in conductivity ([Figure 99](#)) and is probably more accurate than any other method for determining groundwater inflows.

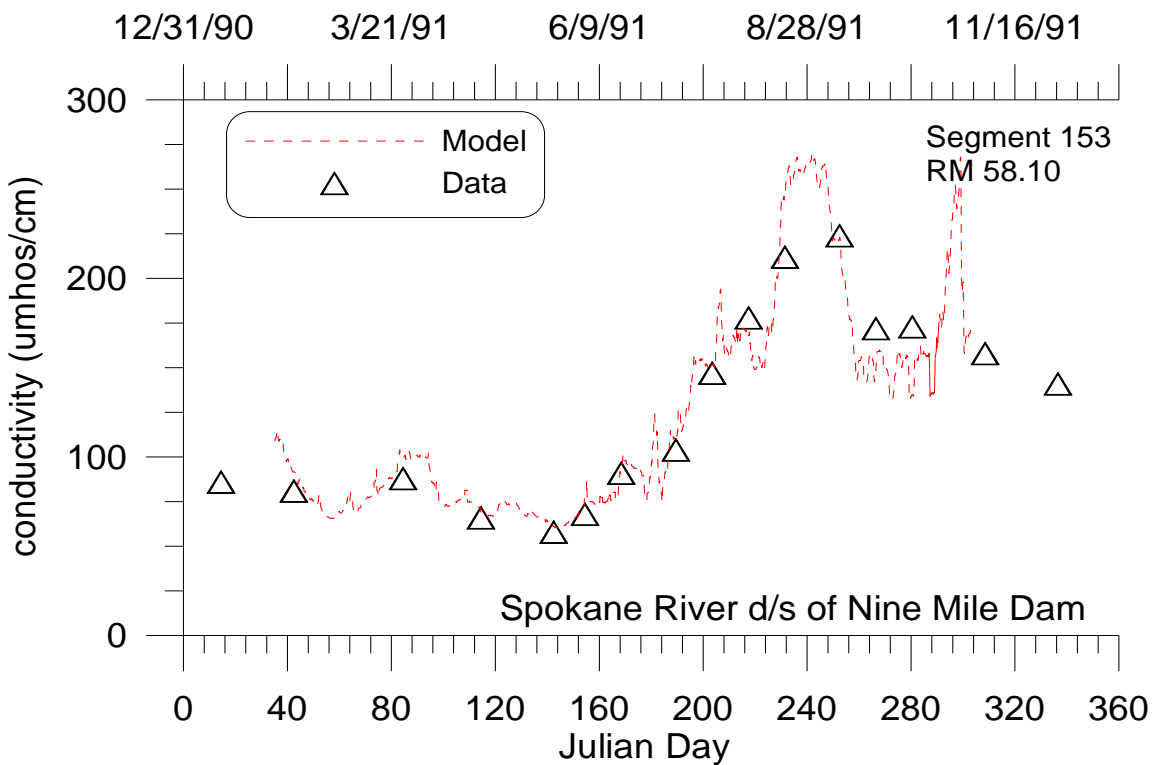


Figure 99. Spokane River computed versus observed conductivity below Nine Mile Dam.

Water Quality

Results for nutrients, dissolved oxygen, and chlorophyll *a* are given in [Figure 100](#)-[Figure 104](#) for the Snake River. The model is capturing much of the spatial and temporal changes in water quality for the river section where, unlike the Spokane River, phytoplankton rather than epiphyton dominate dissolved oxygen and nutrient dynamics.

CALIBRATION

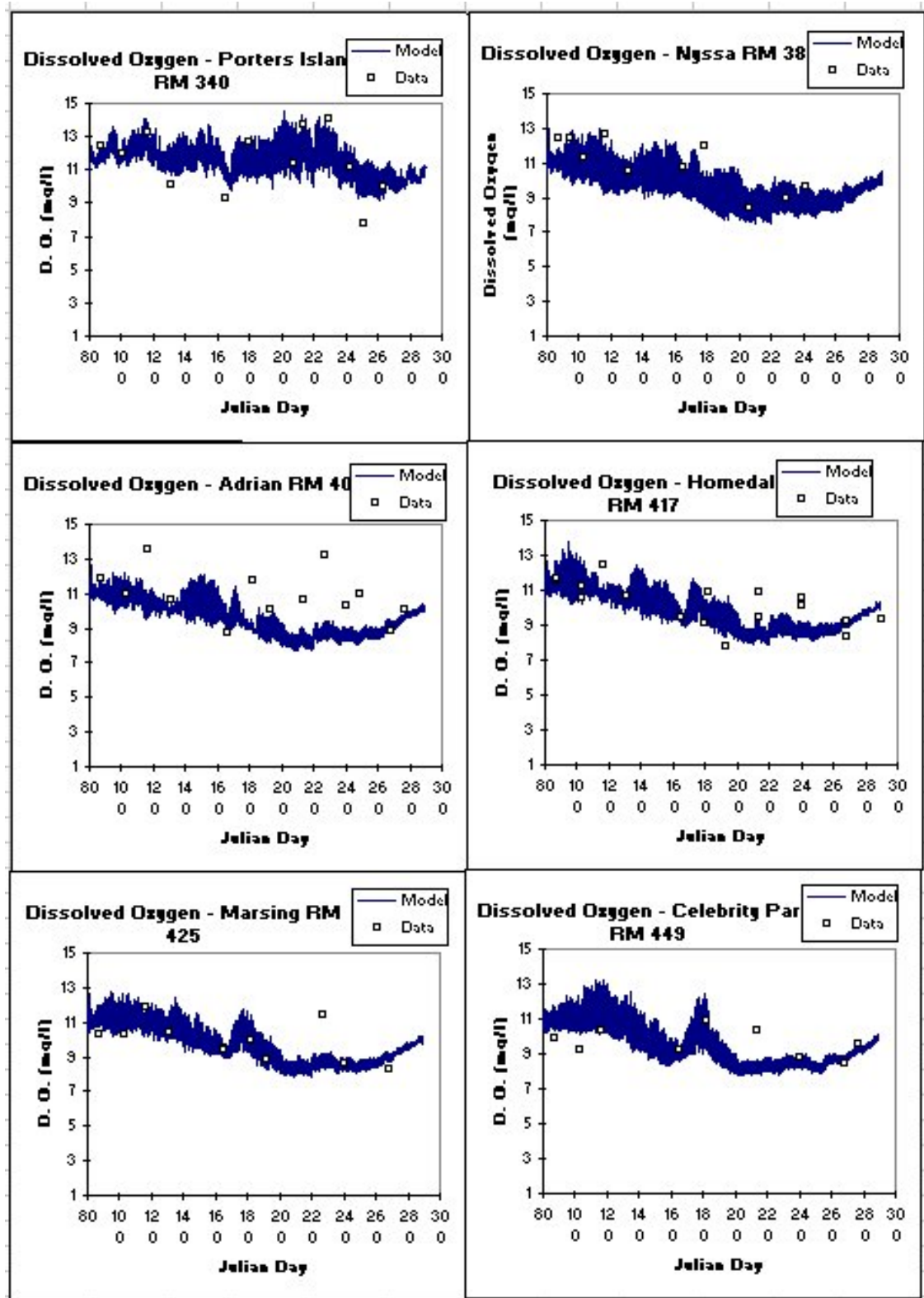


Figure 100. Snake River computed versus observed dissolved oxygen at six stations.

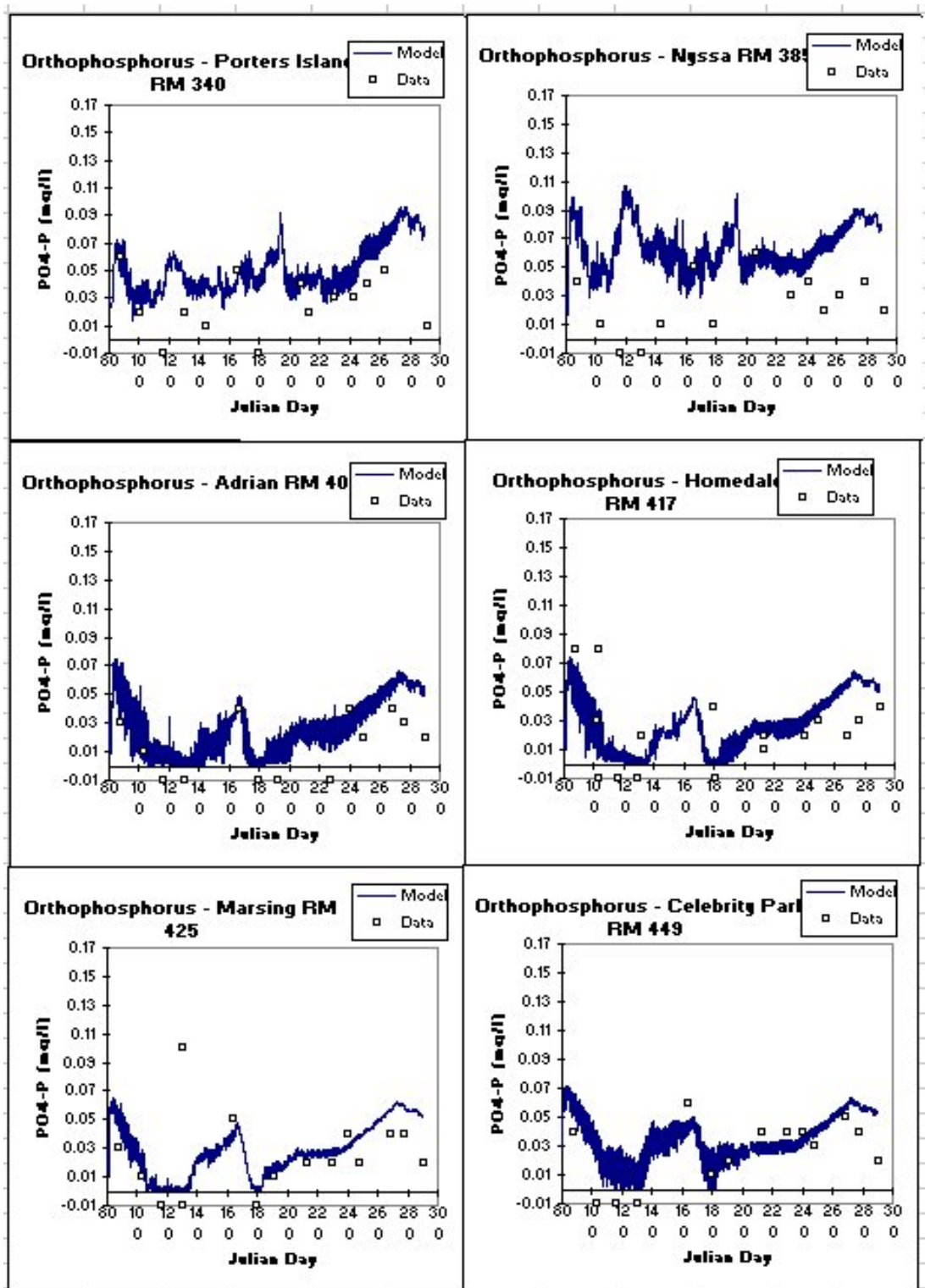


Figure 101. Snake River computed versus observed orthophosphorus at six stations.

CALIBRATION

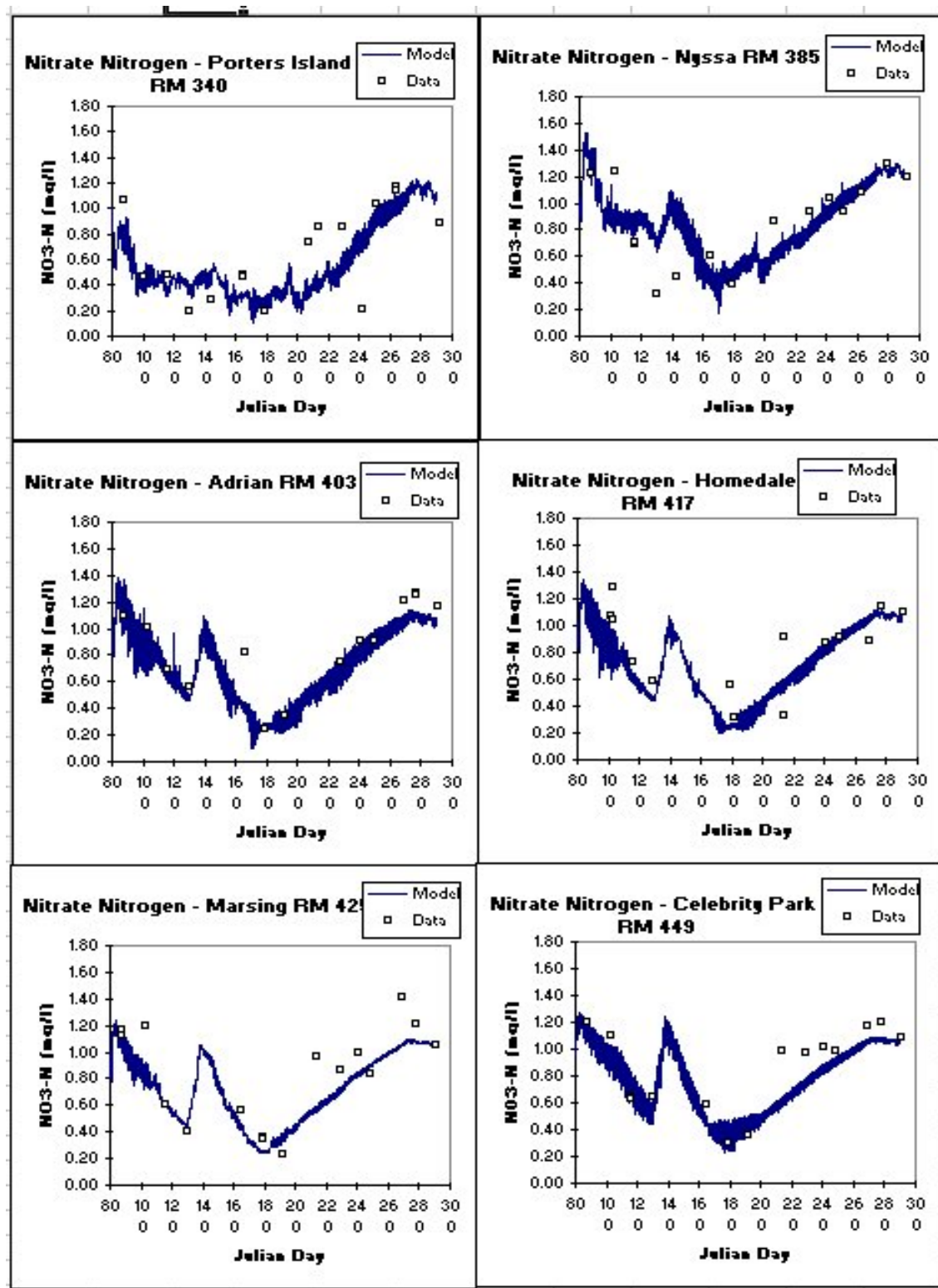


Figure 102. Snake River computed versus observed nitrate-nitrite at six stations.

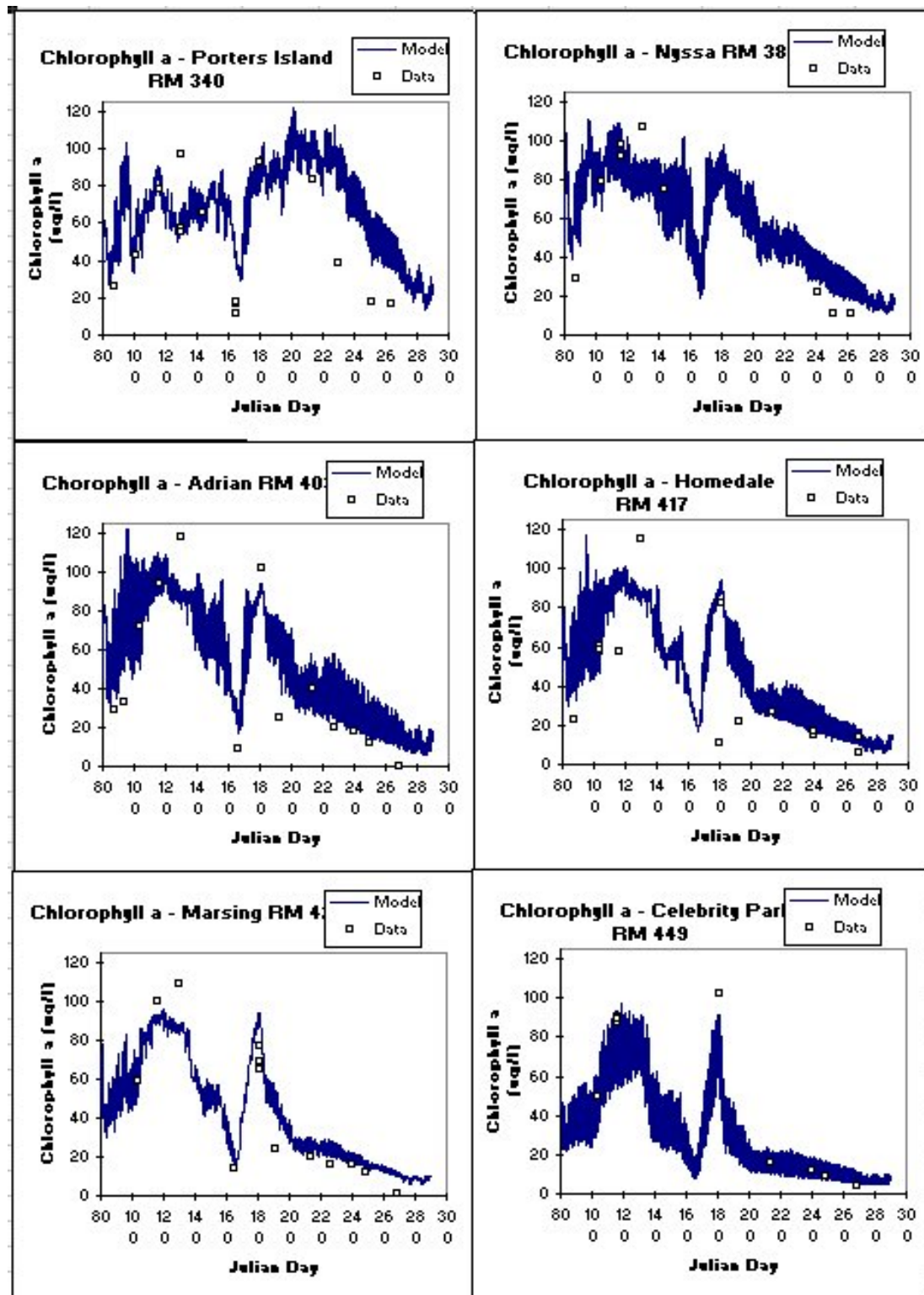


Figure 103. Snake River computed versus observed chlorophyll a at six stations.

CALIBRATION

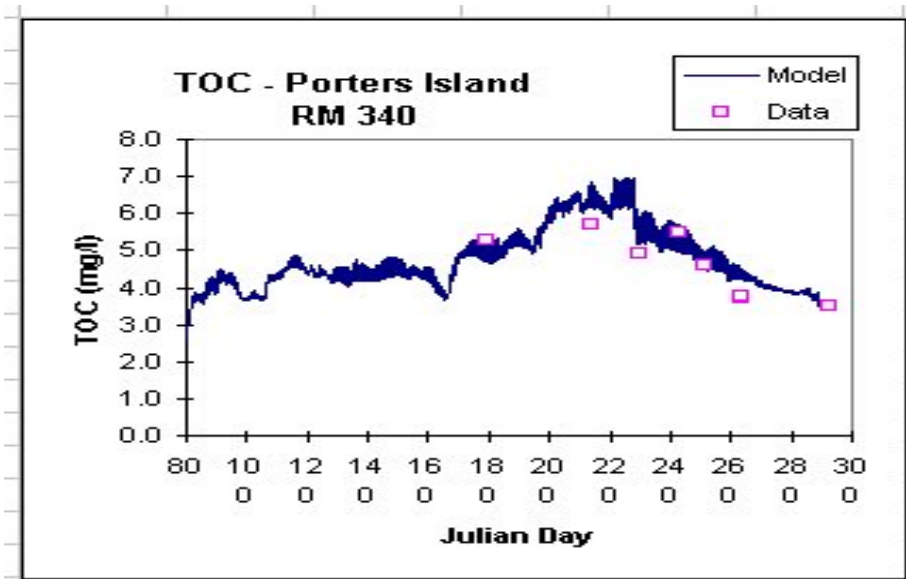


Figure 104. Snake River computed versus total organic carbon.

[Figure 105](#) and [Figure 106](#) illustrate the models ability to reproduce changes in dissolved oxygen over a year and also on a diel basis on the Spokane River. Note how the model has captured not only the diel swings in dissolved oxygen, but also the decrease in the magnitude of the diel variation, which indicates that the model is accurately reproducing epiphyton primary production. This is reinforced in [Figure 107](#) where the model is reproducing diel variations in pH due to epiphyton growth and respiration and the decrease in diel variation over time

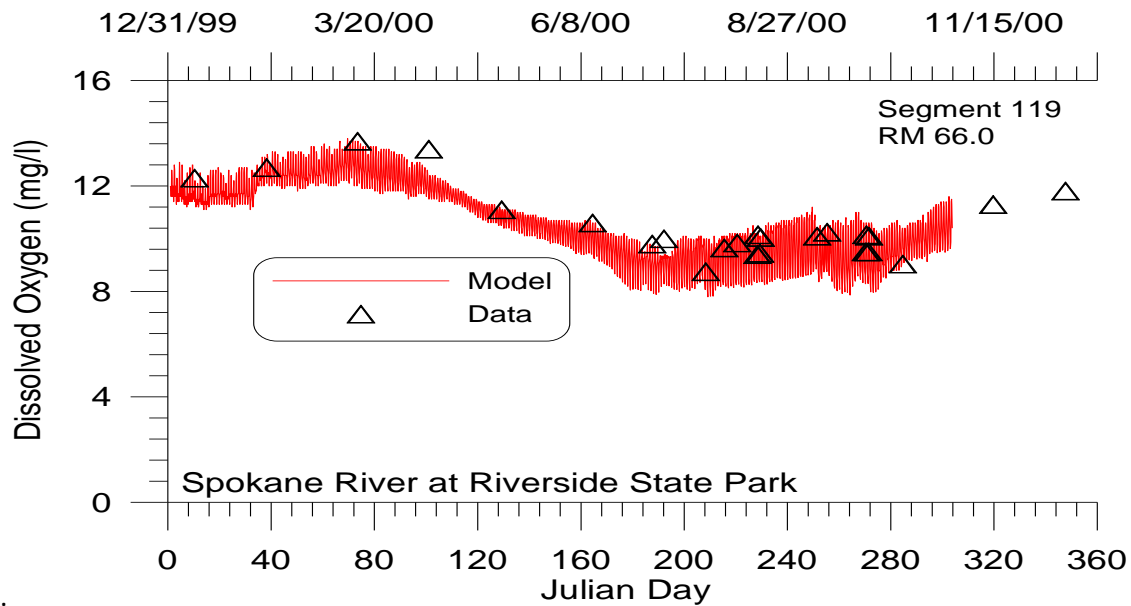


Figure 105. Spokane River computed versus observed dissolved oxygen at Riverside State Park.

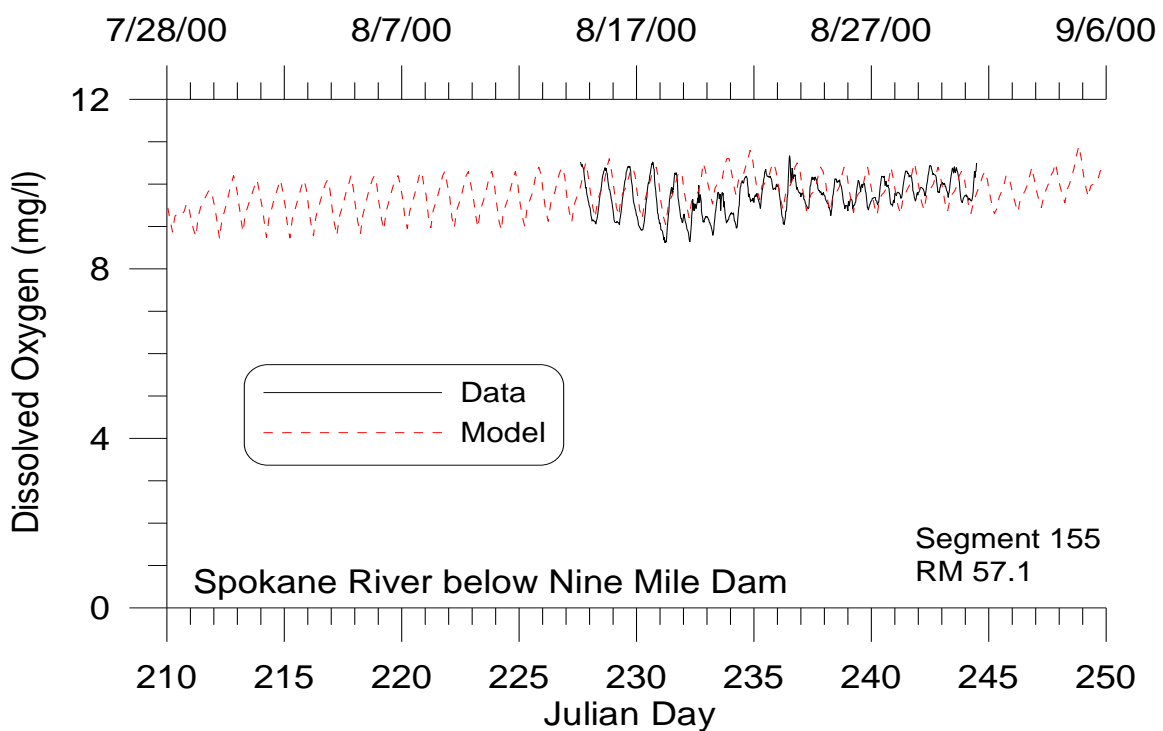


Figure 106. Spokane River computed versus observed dissolved oxygen below Nine Mile Dam.

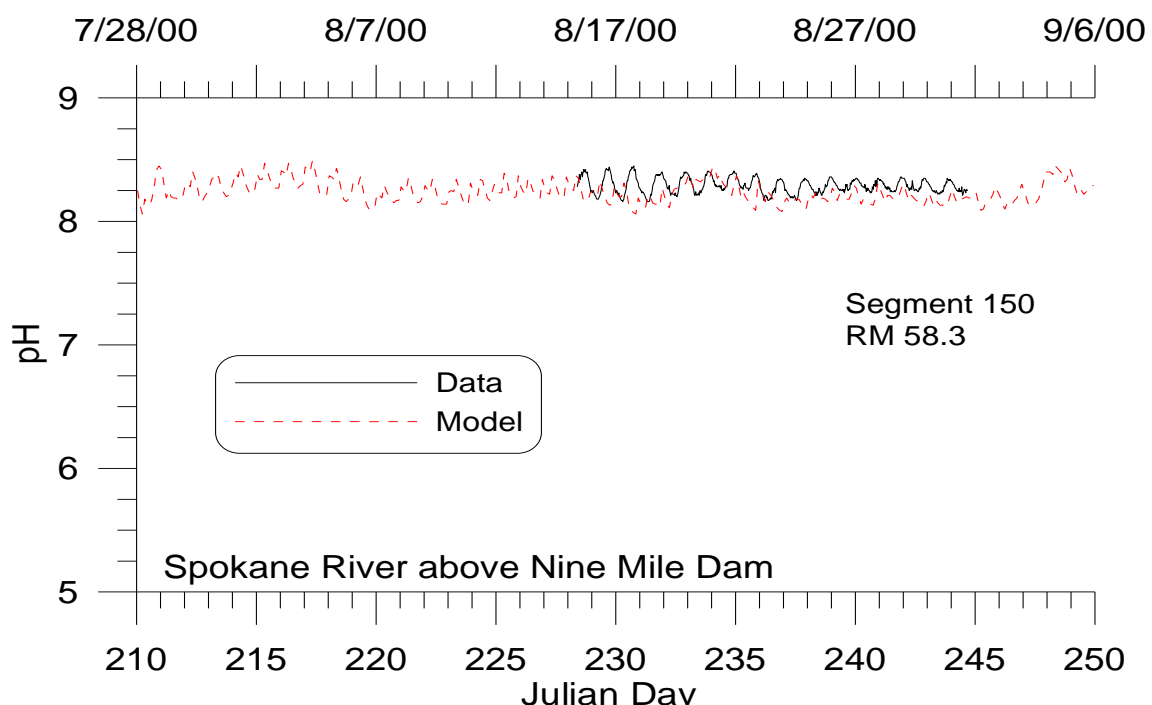


Figure 107. Spokane River computed versus observed pH upstream of Nine Mile Dam.

CALIBRATION

[Figure 108](#)-[Figure 110](#) illustrate the model's ability to reproduce nutrient dynamics that are impacted by upstream inflows, groundwater inflows, point source loadings, and epiphyton interactions.

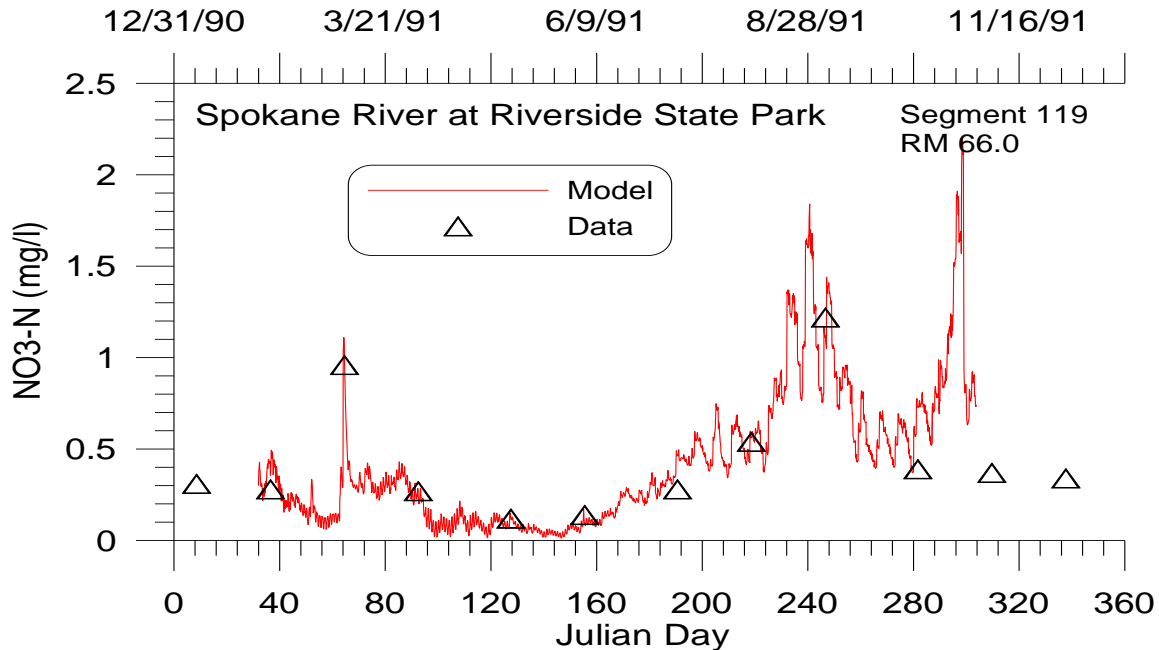


Figure 108. Spokane River computed versus observed nitrate-nitrite at Riverside State Park.

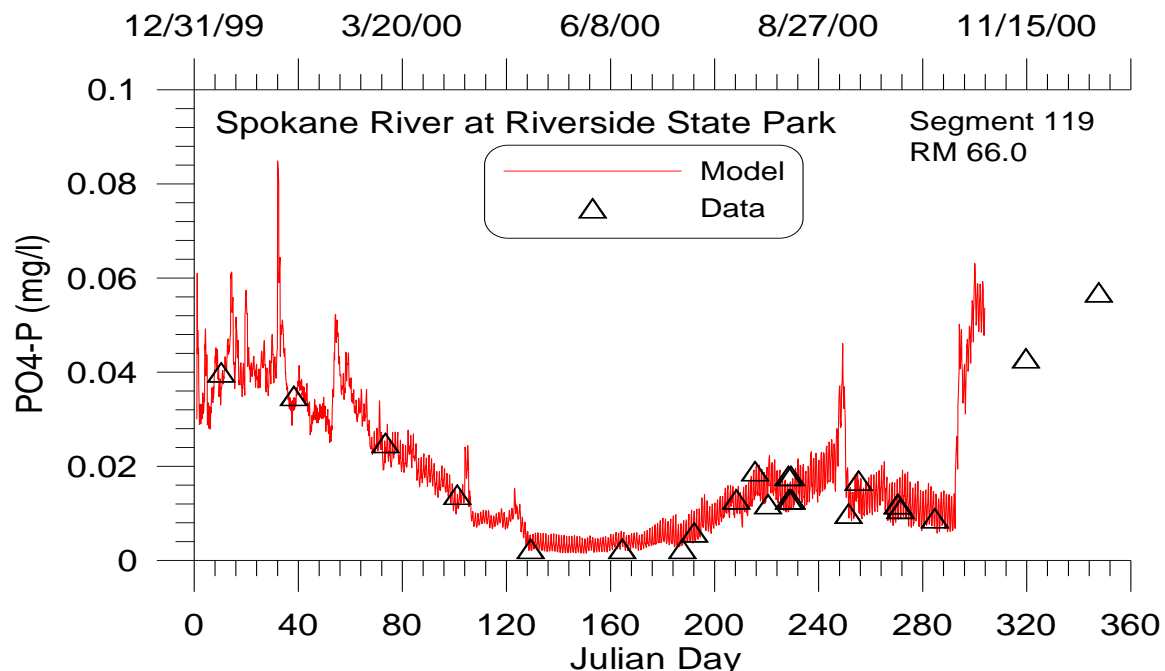


Figure 109. Spokane River computed versus observed soluble reactive phosphorus below Nine Mile Dam.

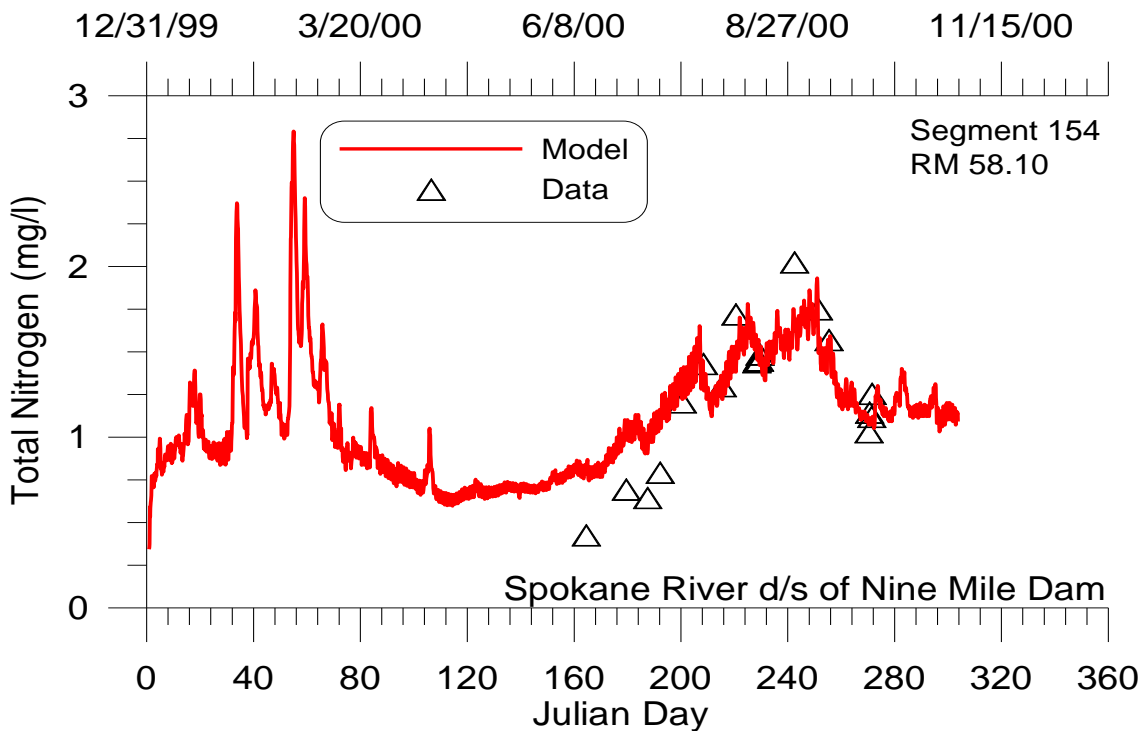


Figure 110. Spokane River computed versus observed total nitrogen below Nine Mile Dam.

Summary

As the preceding figures illustrate, CE-QUAL-W2 is capable of reproducing a wide range of complex hydrodynamics, temperature, dissolved oxygen, nutrient, and phytoplankton and epiphyton regimes in rivers, lakes, reservoirs, and estuaries. If the model is not adequately reproducing prototype behavior, the reason is most likely that the bathymetry or important boundary conditions are not being described with sufficient accuracy. The saying “You cannot make a silk purse out of a sow’s ear” applies equally well to water quality modeling.

A few final words about model calibration. For some applications, no amount of model adjustment or data reconstruction will provide acceptable calibration if data are insufficient to describe the dominant forcing functions in the prototype. For these cases, the model can still be used to provide information about the prototype by pointing out data inadequacies, important mechanisms not included in the model but important in the prototype, or inappropriate assumptions used in the model. In these cases, further fieldwork will be necessary to successfully apply the model.

4. References

Cole, T. and Wells, S. A. 2019. "CE-QUAL-W2: A two-dimensional, laterally averaged, hydrodynamic and water quality model, version 4.1," Department of Civil and Environmental Engineering, Portland State University, Portland, OR.

Lung, W., and Bai, S. 2003. A water quality model for the Patuxent estuary: Current conditions and predictions under changing land-use scenarios. Estuaries, 26:267-279.

Sullivan, A.B., Rounds, S.A., Sobieszczyk, S., and Bragg, H.M., 2007, Modeling hydrodynamics, water temperature, and suspended sediment in Detroit Lake, Oregon: U.S. Geological Survey Scientific Investigations Report 2007-5008, 40 p.

Washington Department of Ecology (WADOE). 2001. Upper Chehalis River Basin Temperature Total Maximum Daily Load. Publication No. 99-52.